Graduate Theses and Dissertations   Graduate School

10-29-2010

Plasma Mediated Molecular Delivery

Richard J. Connolly
University of South Florida

Scholar Commons Citation

Plasma Mediated Molecular Delivery

by

Richard J. Connolly

A dissertation submitted in partial fulfillment
of the requirements for the degree of
Doctor of Philosophy
Department of Chemical and Biomedical Engineering
College of Engineering
University of South Florida

Major Professor: Mark Jaroszeski, Ph.D.
Richard Gilbert, Ph.D.
Richard Heller, Ph.D.
Andrew Hoff, Ph.D.
Anthony Llewellyn, Ph.D.
Karl Muffly, Ph.D.
Kenneth Ugen, Ph.D.

Date of Approval:
October 29, 2010

Keywords: Nonequilibrium Plasma, Ion Delivery, Electroporation, DNA Delivery, Gene
Delivery, Gene Therapy, DNA Vaccines

DEDICATION

I dedicate this thesis in memory of Ian Gammie, who inspired me to always strive for improvement and persevere against all odds.

ACKNOWLEDGEMENTS

TABLE OF CONTENTS

LIST OF TABLES

LIST OF FIGURES

ABSTRACT

Non-viral delivery of plasmid DNA has traditionally relied upon physical forces applied directly to target tissues. These physical methods typically involve contact between an applicator and the target tissue and often cause transient patient discomfort. To overcome the contact-dependent limitations of such delivery methodologies, an atmospheric direct current plasma source was developed to deposit ionized gas molecules onto localized treatment sites. The deposition of charged species onto a treatment site can lead to the establishment of an electric field with strengths similar to those used for traditional electroporation. In vitro experiments proved that this technology could transiently permeabilize cell membranes and that membrane restabilization followed first order kinetics. Optimum delivery of tracer molecules to cell suspensions occurred after 10 minutes of plasma exposure and was attained without adversely effecting cell viability.

In vivo testing of the plasma discharge demonstrated the capability of this system to deliver plasmid DNA to murine skin. Initial experiments involved the injection of plasmid DNA encoding luciferase into the dermis of C57BL/6J mice and then exposing the tissue to plasma discharge for 10 mintues. Delivery by this method resulted in increased luminescence that was as much as 19-fold greater than DNA injection alone. Follow-up optimization experiments demonstrated it was possible to obtain luminescence results that were similar in magnitude to those obtained using electroporation, which under optimum conditions resulted in about a 40-fold increase in peak luminescence. Finally, optimum conditions were used to deliver a plasmid DNA encoding for the 120 kilodalton glycoprotein present on the surface of a macrophage tropic HIV. Results from this vaccination ex-

periment indicated this method was capable of producing antigen specific humoral immune responses at similar levels as when electroporation was utilized as the delivery method.

CHAPTER I: BACKGROUND

1.1   DNA Therapies and Vaccines

Advances in the understanding of disease prevention and treatment have shown the utility of deoxyribonucleic acid (DNA) based therapies and vaccines. Delivery of genetic material to somatic cells results in the production of proteins which induces a biological, biochemical or immunological response. These responses can be used to treat acquired or inherited diseases, as well as prevent disease through vaccination.

1.1.1   Cancer Treatments

Development of cancer treatments account for the majority of research activity in gene therapy. This is likely due to the high fatality rate associated with this disease, which claimed 2.5 million lives in the United States between 1976 and 1996 (Ries et al. 1999). Genetic immunotherapy is a common DNA-based strategy to treat cancer, and frequently involves the transfection of neoplastic cells with cytokine encoding genes. An example of this is the delivery of interleukin-12 (IL-12) to tumor cells. Increased production of IL-12 by these cells activates many immune system components, predominately natural killer cells and cytotoxic T lymphocytes (Caruso et al. 1996, Saudemont et al. 2002). The success of this therapy in animal models is evident by published accounts of complete tumor regression in hepatacellular carcinoma, adenocarcinoma, melanoma, mammary carcinoma and ovarian cancer (Barajas et al. 2001, Wigginton et al. 2001, Lucas et al. 2002, Shi et al. 2002, Zhang

et al. 2003). Immunotherapy has also demonstrated promising preclinical effects in studies targeting melanoma, liver carcinoma, human papillomavirus-induced tumors, human immunodeficiency virus (HIV) and hepatitis C (Weiss et al. 2007, Daud et al. 2008, Morrow and Weiner 2010).

1.1.2 Gene Therapies

Gene therapies have also been evaluated as a treatment strategy for inherited diseases. Typically these strategies are applied against monogenetic disorders, where a single gene has become mutated or deleted. This therapy attempts to repair the function of the cell by inserting a wild type copy of the defective gene (El-Aneed 2004). One disease targeted with this strategy is hemophilia B which is caused by a deficiency in factor IX, a critical component in the blood clotting cascade. Introducing genes encoding for factor IX have proved effective in mice, canines and non-human primates (Herzog et al. 1997, Herzog et al. 1999, Nathwani et al. 2002). Human trials using this approach have been well tolerated by patients and have produced detectable, but sub-therapeutic, levels of circulating factor IX (Emery 2004). Research in this area has focused on increasing the delivery yield of the factor IX gene to provide a potentially effective treatment for this disease. Other diseases targeted for novel gene therapies include X-linked severe combined immunodeficiency disorder, congestive heart failure as well as many circulatory disorders (Aiuti et al. 2009, Dean 2010, Mancini and Farr 2010).

1.1.3 Vaccines

Vaccines are another application of DNA-based drugs and can be used to provide long-term cellular and humoral immunity. Most DNA vaccines target infectious diseases, such as anthrax, HIV, malaria, tuberculosis, influenza and human papillomavirus (Gurunathan

et al. 2000, Best et al. 2009, Livingston et al. 2010, Loudon et al. 2010). Traditional vaccination strategies for these diseases have proved ineffective, and unlike DNA vaccines some of these carry the risk of secondary infection (Boyer et al. 2003). DNA vaccines work by mimicking natural infection and synthesizing foreign proteins. Proteins produced within the cell take the native confirmation, as post-translational modification is performed by the host cell. These proteins are then processed by the major histocompatibility complex (MHC) class I or class II pathways to produce antibody and T cell responses. At the present time DNA vaccines have entered the veterinary market and provide protection for horses to West Nile virus, salmon to hematopoietic necrosis virus and canines to oral melanoma (Morrow and Weiner 2010). Recent approval of this technology for the veterinary market is an indication DNA vaccines might soon be available for humans.

1.2 Delivery Methodologies

These developing treatment strategies show DNA-based therapeutics as a promising technology. However, DNA treatments capable of producing these advantageous effects have yet to enter mainstream clinical use. A factor hindering DNA therapeutics is the relative size of linear and plasmid DNA, which prevents diffusion through cell membranes. This has spurred development of DNA delivery mechanisms broadly classified as viral and non-viral.

1.2.1 Viral Gene Delivery

Viral gene delivery is a very effective and popular means for delivering genetic material to cells. This delivery technique commonly uses an adenovirus, adeno-associated virus, vaccinia virus and retrovirus vectors. Each of these viruses has a different capacity to carry genetic material, different insertion characteristics and a different capacity for the viral particles themselves to evoke an immune response in the host. Adenoviruses have a capacity of 30-38 kbp of double stranded DNA, transiently infect the host genome, and produce strong immune responses. Adeno-associated viruses have a capacity for 4.7 kb of single-stranded DNA, stably infect the host genome, and produce strong immune responses. Vaccinia viruses have the capacity for 190 kbp of double stranded DNA, transiently infect the host genome, and produces a relatively weak immune response. Finally, retroviruses have the capacity for 3.5 kb of single-stranded ribonucleic acid (RNA), stably infect the host genome, and produces weak immune response (Verma and Somia 1997).

While viral delivery methods have been very attractive to perform, there are many drawbacks to its use in vivo. The first problem is strong immune responses have the potential to trigger fever that could potentially harm patients. A related issue involves exposure to

vectors that have previously induced immune responses in a patient either through therapy or other infection. Exposure to a virus that has previously triggered an immune response could induce anaphylaxis (Guo et al. 2008). This makes gene therapy regimens and booster treatments that use the same vector extremely difficult. Another risk is integration into the host genome could result in insertional mutagenesis. This may cause normal gene expression to be interrupted, which could lead the disruption of normal metabolism or induction of cancer (Fischer and Cavazzana-Calvo 2008).

1.2.2 Microinjection

The drawbacks and complexity associated with viral delivery have led many researchers to believe physical methods to insert naked DNA in cells are safer and have the potential to be more effective. One of the oldest physical DNA delivery techniques is microinjection. This technique is the most direct physical method for introducing foreign DNA into cells. It utilizes a microcapillary pipette mounted to a micromanipulator. The micropipette is carefully inserted through the cell membrane using fine adjustments on the manipulator while visually monitoring the pipette position with a microscope. Once inside the cell plasmid DNA is delivered by applying hydrostatic pressure to the solution contained in the microcapillary pipette (Capecchi 1980). Despite being the most efficient physical delivery method, it is very tedious and time consuming, because cells are injected manually one at a time. The need for a microscope and the single cell manipulation approach make this method impractical for in vivo applications.

1.2.3 Hydrodynamic Injection

Hydrodynamic injection is a method that uses mechanical force to deliver plasmid DNA to internal organs. This method utilizes rapid high volume intravenous injections to disrupt

the endothelial barrier. It is hypothesized that the mechanical stress opens pores in cells allowing the uptake of exogenous DNA (Niidome and Huang 2002). This delivery method would presumably cause a degree of discomfort and possibly tearing of the vasculature leading to clotting issues.

1.2.4 Biolistics

Biolistics is another physical method used to introduce plasmid DNA into cells. This method utilizes gold beads with a diameter of 1.0 to $1.5\,\mu$m that have plasmid DNA precipitated onto their surfaces. These doped microbeads are loaded into a chamber above the target tissue and accelerated into the tissue with a rapid discharge of high pressure helium gas. After the ballistic beads have been delivered to the cytoplasm their DNA payload gradually dissociates away from the bead surface (Klein et al. 1987). When applied in vivo this delivery technique is modestly effective assuming the targeted tissue is the epithelium. If deeper tissues are targeted invasive surgery must be performed due to the limited penetration depth of this technology (O'Brien et al. 2001). Also, targeting different tissues requires modifying delivery parameters, such as particle size, doping level and velocity of the microbeads (Matthews et al. 1993). The relevance of biolistics has decreased recently due to the relatively low transfection rate of about 2%, complexity associated with operating the machine and the collateral damage caused to tissues surrounding the treatment site (Karra and Dahm 2010).

1.2.5 Sonoporation

Sonoporation is a physical delivery method that uses high frequency mechanical oscillations to aid in the diffusion of plasmid DNA into cells. This delivery method uses a vibrating probe that is placed in direct contact with the target tissue. Vibrations from the probe

are transmitted through the tissue in the kilohertz to megahertz range to cause acoustic cavitation of microscopic air bubbles surrounding cells. These air bubbles eventually collapse and release energy causing the formation of transient pores in adjacent cells (Greenleaf et al. 1998, Haar 2007, Sboros 2008). The presence of these pores allows DNA to diffuse past the membrane and into the cytosol. A major issue encountered when performing sonoporation is a lack of control over the exposed area. The broad treatment zones associated with this technique lead to poor transfection efficiency and cell death in areas that are over exposed to the field (Hassan et al. 2010).

1.2.6 Electroporation

Electroporation is currently the most developed and successful physical method for gene delivery. This method utilizes electrodes placed in direct contact with tissues to impart high-energy pulses. The electric field generated by these pulses cause ion movement inside the cell that leads to a dielectric breakdown of the lipid bilayer (Weaver and Chizmadzhev 1996). The feasibility of this technology to deliver plasmid DNA in vivo took place almost 20 years ago when plasmids were delivered to cells in the skin and liver of rodent models (Titomirov et al. 1991, Heller et al. 1996). Building on the success of these early works electroporation has been used extensively to deliver plasmid DNA to cartilage, blood, muscle, epithelial and loose connective tissue (Grossin et al. 2003, Weissinger et al. 2003, Kunieda and Kubo 2004, Hirao et al. 2008, Yuan 2008). As well as these basic tissue types, electroporation has also been applied to tumors to enhance the uptake of immunomodulatory genes (Lohr et al. 2001, Yamashita et al. 2001, Li et al. 2002, Lucas et al. 2002). While electroporation is a highly effective method for performing molecular delivery it does have several drawbacks. The most notable being high-energy pulses required to achieve significant delivery often cause tissue damage and patient discomfort (Prausnitz 1996, Denet et al. 2004). This leads to a balance between using electrical conditions severe enough to

deliver an adequate amount of molecules to elicit a biological response and mild enough to avoid destroying the very cells needed to produce the response.

These drawbacks have led many to design new techniques for performing electrically mediated delivery. One way of doing this is by changing the electrodes themselves. This has been done by making electrode arrays that are placed on the surface of a tissue with electrode pairs spaced closer than in previous applicators. This configuration allows lower voltages to be applied to generate fields similar to traditional electroporation, which results in reduced muscle stimulation without any effects on the efficacy of DNA delivery (Heller et al. 2010, Broderick et al. 2010). Another change occurring in the field of electroporation is the monitoring of changes in the electrical properties of tissues during electroporation sequences. This approach would allow just enough energy to be delivered to the tissue to induce membrane destabilization without over exposing the tissue and damaging cell viability (Davalos et al. 2002, Connolly et al. 2009).

1.3 Plasma

It is evident from the literature that all physical delivery methods exhibit some undesirable characteristics, such as patient discomfort, tissue damage, limited control, complex optimization, and tedious operation. Therefore, the research described in this document builds on the success of electroporation which, as previously stated, is currently the most successful physical delivery. The general strategy was to address the source of pain and tissue damage by decoupling the applicator from the treatment site. This was accomplished through deposition of ionized gases, or plasma, onto a treatment site. Ion deposition on a targeted tissue will lead to the accumulation of a steady state charge, causing an electric potential to be established. It is speculated that achieving a high potential would lead to the formation of pores, similar to electroporation, without the deleterious effects caused by electrodes.

Plasma refers to any gas that has been energized to the point of ionization. This unique phase is composed of electrically charged particles with abundant energy. As such, this gas-like phase is heavily influenced by electromagnetic fields and can act as a conductor. Interestingly over 99% of the known universe is composed of plasma, but interaction with this phase on Earth is relatively uncommon.

1.3.1 Types

Generally plasmas can be subdivided into two major categories based on their operating temperature. The first type is a local thermodynamic equilibrium (LTE) plasma, which are plasmas with equivalent electron and ion temperatures. These plasmas operate with temperatures in the thousands of kelvin. The other type of plasma is a non-LTE, or cold, plasma. Electron temperatures in non-LTE discharges are typically on the order of thousands of kelvin, while ion temperatures remain in the hundreds of kelvin. Another dis-

9

tinction between non-LTE and LTE plasmas is the extent of ionization within the plasma volume. Normally LTE plasma volumes are composed entirely of ionized gases, while non-LTE plasma volumes contain less than 5% of ionized species. This gives non-LTE discharge volumes a much lower operating temperature; thus, they are referred to as cold plasmas.

1.3.2 Generation

Generating a plasma requires a transfer of energy to the atoms or molecules to be ionized. The amount of energy required to remove one electron from an atom or molecule is called the first ionization energy. This energy follows a periodic trend, where alkali elements require the least amount of energy to remove an electron and noble gases require the most. Common methods employed in the ionization of gases are heating, bombarding the gas with photons, or exposure to high electric fields.

Most plasmas classified as non-LTE are created by exposure to electric fields. These fields are established between a pair of electrodes, where one is set to a high potential and the other set at a low potential. The electric field, $\vec{E}$, established between a pair of electrodes can be determined by knowing the difference in the electrode potentials, V, and the geometry of the generator.

$$\vec{E} = -\nabla V \tag{1.1}$$

Plasmas produced by this method require the created electric field be strong enough to pull electrons or ions from the surrounding atmosphere towards its opposing polarity electrode. The vectoral force, $\vec{F_e}$, placed on charged atmospheric species can be determined if the electric field, $\vec{E}$, and the charge of the species, q, are known.

$$\vec{F_e} = q\vec{E} \tag{1.2}$$

As these species are accelerated towards the electrodes they undergo inelastic collisions with other atoms or compounds in the gas phase causing further ionizations (Conrads and Schmidt 2000). These types of plasma have been employed in biology to treat both prokaryotic and eukaryotic cells.

1.3.3 Applications

Plasma discharges used on prokaryotes typically aim to destroy these organisms. A promising application of these discharges is the decontamination of bacteria laden surfaces (Laroussi 2000, Vleugels et al. 2005). It is thought this technique works in a similar fashion to electroporation, where the microorganism's membrane is compromised by exposure to ionized gases (Moreau et al. 2008). Membrane defects result from exposure to oxidizing components in the plasma and not from dielectric breakdown as with electroporation. Stable pores formed in the organism's membrane prevent normal metabolic functions from occurring, which results in cell death.

Plasmas have more recently been applied to eukaryotic cells for augmenting molecular delivery. A study by Chalberg et al. used a microarray plasma generator surgically implanted in a bolus of plasmid rich solution that was injected into the retina of a rabbit. This study utilized microsecond biphasic electrical pulses to generate a plasma capable of vaporizing the conductive media surrounding the electrode array. It was speculated that rapid vaporization of the media around the electrode causes the transmission of a mechanical shock wave through the retina resulting in the delivery of DNA (Chalberg et al. 2006). Another study published by Ogawa et al. showed that plasmas generated with radio frequencies are capable of delivering plasmid DNA to primary cell cultures. In this study, neuronal cells were exposed to a discharge source marketed for polymer surface modification for one second (Ogawa et al. 2005). Disappointingly, the authors failed to mention many of the operating parameters used such as frequency, current, voltage and discharge

temperature. A more recent study by Ramachandran et al. utilized a stationary array of needles positioned several millimeters above a treatment site to generate corona ions for molecular delivery. Corona ions result from the ionization of atmospheric constituents. This study proved corona ions are capable of driving molecular delivery for drugs and genes in vitro and in vivo (Ramachandran et al. 2008).

Electroporation is the most developed physical delivery method, but has significant drawbacks that lead to the investigation of methods that rely on electric fields without intimate contact between an applicator and cells or tissues. Plasma provides a means of performing this treatment without directly contacting the targeted tissue. Proof of this delivery method has been performed in vitro to deliver both drugs and genes. Corona discharges have been used in vivo, but require the generator to operate in close proximity to the target tissue. Being close to the treatment site increases the risk of creating arcs, which can decrease cell viability and cause transient pain. In order to avoid this and still invistigate charge-based mechanisms for molecular delivery a generator that created a flowing stream of ionized gas was designed and developed. The focus of this study was to characterize the delivery capability of this noninvasive charge-based system. To accomplish this, the plasma generator was first characterized in vitro. After characterization the system was tested in vivo to determine the delivery capacity in animals. Finally, the system was used to deliver a DNA vaccine, and the results of this delivery were compared to electroporation. This dissertation discusses the results obtained from these studies.

CHAPTER II: HYPOTHESIS AND RESEARCH AIMS

2.1 Hypothesis

It is evident from the literature that naked DNA therapies and vaccines will soon serve a significant role in medicine. Generating therapeutic quantities of protein in humans from DNA-based drugs will require their delivery be coupled with a forcing function. Current physical forcing functions have features that make them undesirable for clinical applications. Electroporation is the most developed of these physical functions, but can cause temporary pain and tissue damage. This served as the motivation to create a noninvasive charge-based system for molecular delivery.

This research focused on the creation of a tool that used a stream of ionized gas to drive molecular delivery. This stream was used to create a non-LTE discharge as it causes no rise in the temperature of the treatment site, creates no painful sensations and can be deposited to establish an electric field. Therefore, this research was designed to test the hypothesis of whether direct current plasma discharges could be used to augment plasmid DNA uptake in vivo without causing tissue damage.

2.2   Research Aims

In order to investigate the utility of plasmas for molecular delivery it was necessary to first design and construct a plasma generator. Then, the generator was tested in vitro to determine the extent of delivery attainable and viability effects caused by exposing mammalian cells to plasma. Following this, the ability of the system to deliver plasmid DNA in vivo was evaluated. After obtaining proof of concept, the plasmid dose and plasma exposure time were optimized to give the maximum expression of a luciferase encoding plasmid. Once optimized these conditions were evaluated with a biologically relevant plasmid to determine the feasibility of using the discharge for DNA vaccine applications. Finally, an electrostatic finite element model of the discharge was created to provide evidence of a plausible delivery mechanism. Each of these items was addressed as a key research goal in this investigation.

2.2.1   Aim 1: Creating a Plasma Discharge for In Vivo Use

An atmospheric plasma generator was designed and constructed to enable the application of discharges to cells and tissues. The electrical characteristics of the discharge were determined by a series of heuristic experiments where the applied voltage and generator height were modulated while current values were recorded. Ultraviolet and visual light spectroscopy were performed to determine the excited constituents in the plasma volume.

2.2.2   Aim 2: In Vitro Experimentation

Once a working generator was constructed and characterized, a series of in vitro experiments was performed to determine the effects of plasma exposure on eukaryotic cells. This experimental work examined the delivery efficacy, viability impact and kinetics of

membrane restabilization following plasma exposure. These in vitro experiments were performed with B16F10 and HaCaT cells.

2.2.3 Aim 3: Delivery of Plasmid DNA to Murine Skin In Vivo

Obtaining successful delivery in vitro allowed the investigation to move forward to in vivo experiments. This work examined the ability of the plasma discharge to deliver plasmid DNA to skin. To determine this, plasmid DNA encoding for luciferase was injected into the dermis of mouse flank skin. Following injection, the skin was exposed to the noncontact charge-based delivery system.

2.2.4 Aim 4: Optimization of Plasma Delivery In Vivo

Proof that the system could deliver not only small molecules in vitro, but plasmid DNA in vivo enabled a more rigorous set of experiments to be performed. The aim of these experiments was to optimize delivery to produce the maximum expression of luciferase. In these experiments plasmid dose and treatment time were both analyzed to determine the conditions that resulted in maximum expression.

2.2.5 Aim 5: Delivery of a DNA Vaccine In Vivo

At this point the conditions that resulted in the maximum expression of plasmid DNA were known and were tested with a more biologically relevant protein. These experiments focused on delivering plasmid DNA encoding for the 120 kilodalton envelope glycoprotein present on the surface of a macrophage tropic HIV. Immune responses generated were quantified by antibody levels in mouse serum.

2.2.6 Aim 6: Transdermal Electric Field Simulation

After having shown the efficacy of the plasma system to deliver plasmid DNA in vivo, an electrostatic model was created to determine the electric field strengths present during treatment. This was performed by producing a two dimensional model of an ordinary mouse during treatment. Electric potential measurements obtained from mouse skin during exposure to positive and negative polarity plasma was curve fit and used as a boundary condition in the model. After inputting the epidermal surface potential and other boundary conditions, the model was solved to obtain the electric field intensity present in the skin during treatment.

CHAPTER III: MATERIALS AND METHODS

This chapter describes the equipment and techniques used to test the hypothesis. Each section within this chapter corresponds to a research aim, previously mentioned in Chapter II. The overall goal of this research was to construct a plasma generating device, characterize the effects of plasma exposure on cells in culture and evaluate the capability of this novel device to deliver plasmid DNA in vivo. After having performed these tasks the system was tested with a more biologically relevant plasmid and simulated using a finite element model. The results obtained for each of these sections can be found in the following chapter.

3.1   Creating a Plasma Discharge for In Vivo Use

3.1.1   Plasma Generator

The first plasma generator prototype fabricated was made from a 15 cm long Teflon dowel. This dowel was hollowed to create a tube having a 1 cm inner diameter and wall thickness of 2 mm. Two electrodes were positioned at either end of the 15 cm long tube. A steel hose barb attached to ground potential was positioned on one end of the tube to serve as a ground reference electrode and interface with a gas inlet stream. A flat annular stainless steel electrode with a 3.5 mm internal diameter occupied the opposite end of the Teflon tube. This electrode was connected to a high voltage direct current power supply (Spellman Model CZE2000, New York, NY). A plasma discharge was created by applying a
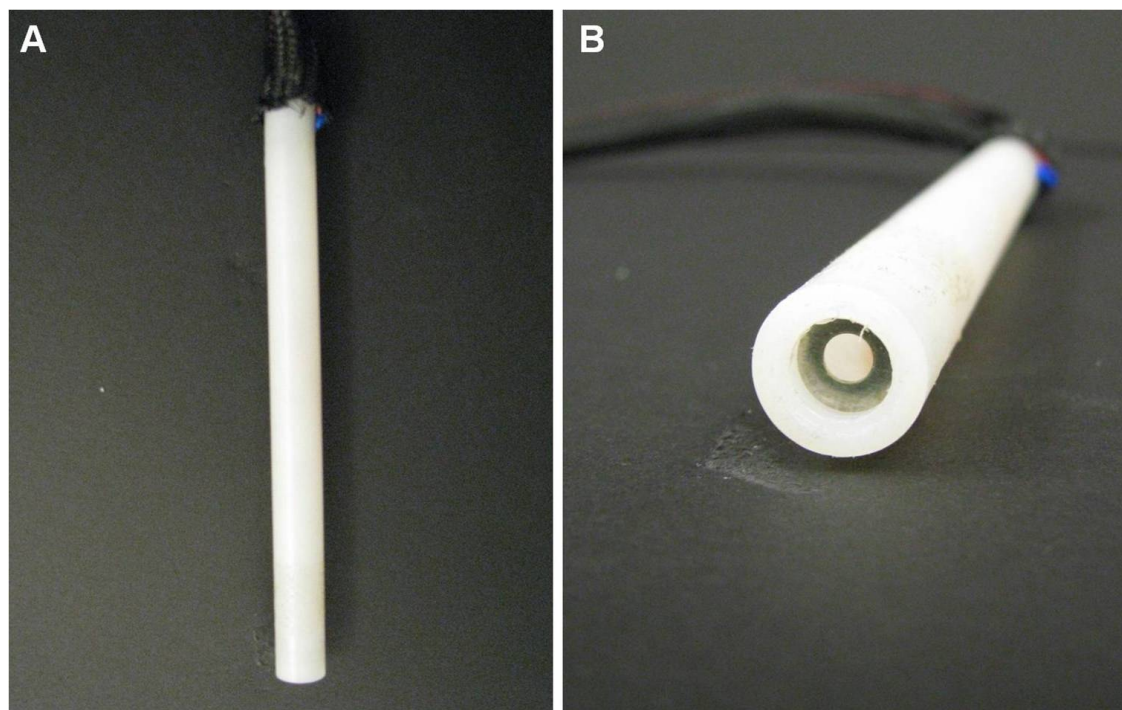
Figure 3.1: First generation plasma generator.

potential greater than 4 kV to the annular electrode while a stream of ultra high purity helium (AirGas, Tampa, FL) was passed through the tube at a rate of $15\,^1\!/_{\text{min}}$. Figure 3.1 shows this plasma generator.

A software interface platform (National Instruments LabVIEW, Austin, TX) was used to control the high voltage power supply and allowed the voltage, maximum current and exposure time to be set prior to treatment. A current limit was set to $100\,\mu A$ as a safeguard to prevent sparking. Figure 3.2 and Figure 3.3 show the graphical user interface and source code for the first generation plasma system.

3.1.2 Electrical Parameters

Current measurements were performed to determine the operating height and potential that would be applied to the high voltage electrode to generate the optimum discharge. The first step in these experiments was to position the bottom of the generator 1, 2, 3, 4 or 5
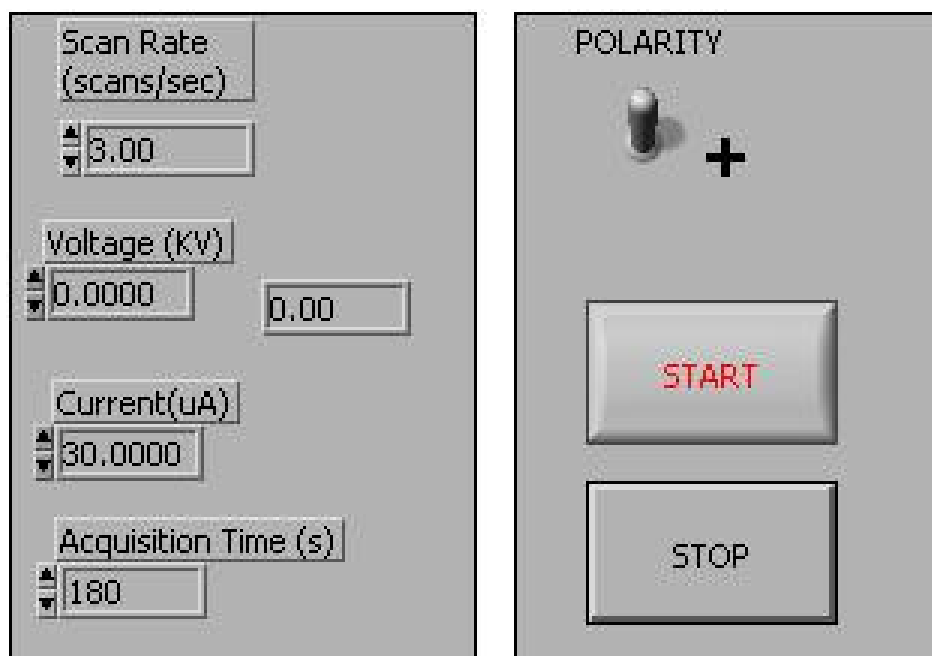
Figure 3.2: Graphical user interface for the first generation plasma system.

cm above a $4\,\text{cm}^2$ stainless steel plate that was connected to ground potential through an electrometer (Keithely Model 6517A, Cleveland, OH). Then the high voltage electrode was swept from -10 kV to 10 kV at 1 kV intervals. At each potential the current delivered to the grounded steel plate was recorded.

3.1.3 Optical Emission Spectroscopy

Ultraviolet and visual light spectroscopy was performed to determine the excited constituents in the discharge plume. Spectra were collected by placing a fiber optic probe (Ocean Optics QP230-1-XSR, Dunedin, FL) 0.5 cm perpendicularly from the plasma discharge. This probe was connected to a spectrometer (Ocean Optics USB2000) with a dispersion range of 200 to 1100 nm. Spectral information was recorded with a 5 second integration time and uploaded to a computer as a data matrix of wavelengths and intensities utilizing the manufacture's software package (Ocean Optics SpectraSuite). This matrix was then analyzed in Matlab (The MathWorks, Natick, MA) with a peak detection algo-

19
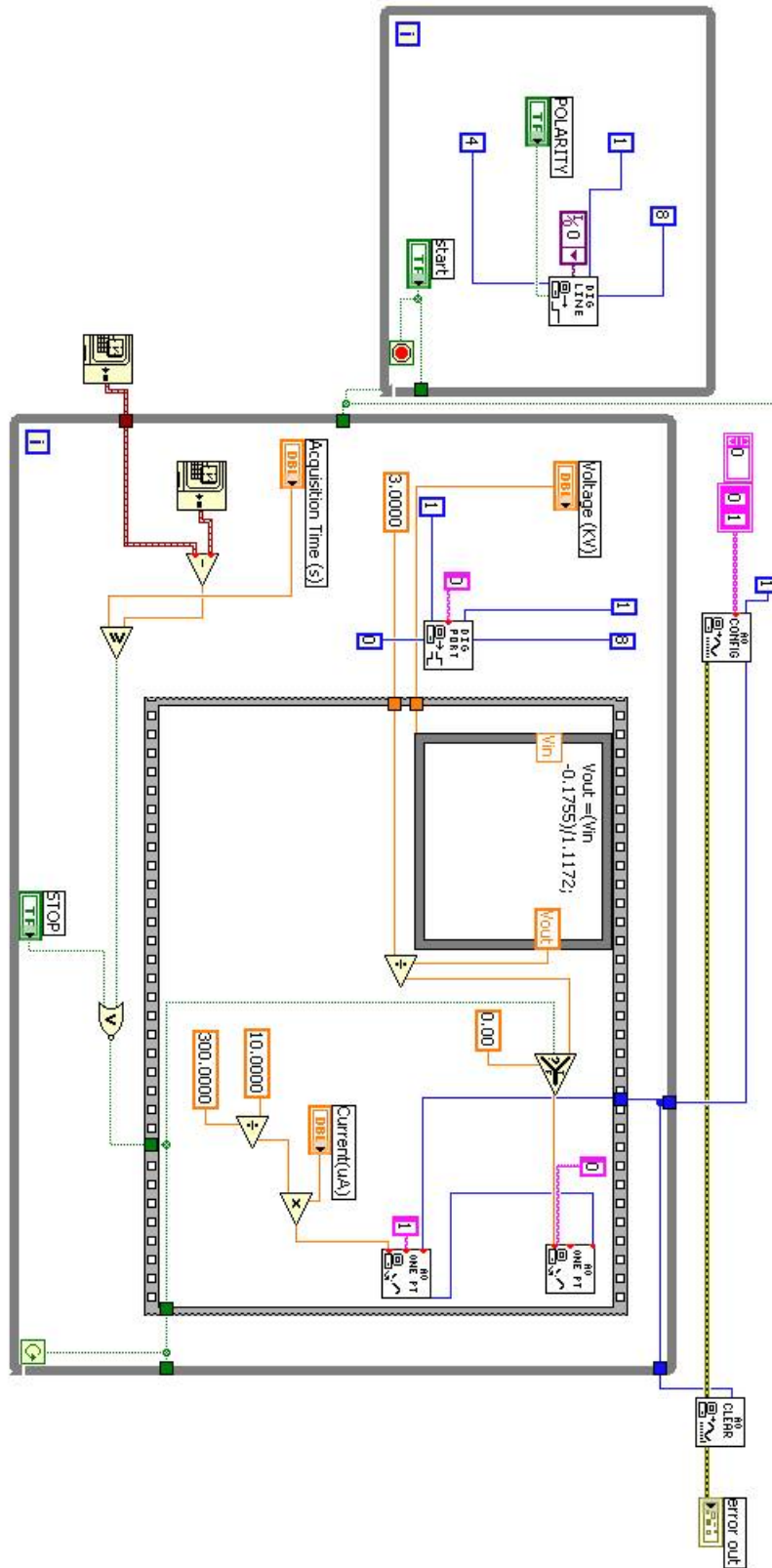
Figure 3.3: Source code for the first generation plasma system.

rithm. Peaks found with the program were then compared to those listed on the National Institute of Standards and Technology (NIST) Atomic Spectra Database. The intensity of emissions in the ultraviolet range were quantified with a low illumination light meter (Sper Scientific, Scottsdale, AZ).

3.2 In Vitro Experimentation

3.2.1 Plasma Generator

The first generation plasma generator, described in Section 3.1.1, was used for this investigation. During these treatments, the high voltage electrode was held at 8 kV while a stream of ultra high purity helium (AirGas, Tampa, FL) was passed through the tube at 15 $^l/_{min}$. A maximum current limit of $100\,\mu$A was set as a safety mechanism during treatment. The generator utilized $10\,\mu$A of current at 8 kV while operating. At these conditions it produced a visible glow discharge that measured 3.0 cm in length.

3.2.2 Cell Culture

A portion of these in vitro experiments were performed using B16F10 (ATCC CRL-6475) melanoma cells derived from C57BL/6J mice. These cells were propagated in McCoy's 5A media (MediaTech, Herndon, VA) supplemented with 10% ($^v/_v$) fetal bovine serum (MediaTech) and $50\,^{\mu g}/_{ml}$ gentamicin sulfate (MediaTech). Cultures were incubated at $37\,^{\circ}$C in a 5% CO_2 atmosphere. Once cells were confluent on the culture surface they were subcultured at a 1:12 ratio.

The remainder of these experiments were performed with immortalized human keratinocyte cells, HaCaT (Cell Line Services, Eppelheim, Germany). These cells were propagated in Dulbecco's Modified Eagle Media (MediaTech) supplemented with 10% ($^v/_v$) fetal bovine serum and $50\,^{\mu g}/_{ml}$ gentamicin sulfate. These cells were also incubated at $37\,^{\circ}$C in a 5% CO_2 atmosphere. Cells were subcultured at 90% confluency at a ratio of 1:6.

3.2.3 Molecular Delivery

Experiments performed to determine the delivery capability of the plasma discharge were carried out with B16F10 and HaCaT cell lines. Dual chambered tissue culture dishes (Becton Dickinson Falcon, Franklin Lakes, NJ) having an inner diameter of 15 mm and outer diameter of 60 mm were used to perform these experiments. Prior to treatment the inner chamber was loaded with 1×10^6 cells suspended in $500\,\mu$l of phosphate buffered saline (PBS). The outer chamber was filled with 2 ml of PBS and contained a 22 gauge tinned copper wire connected to ground through a $1.5\,$GΩ resistor. This ring prevented the plasma plume from being affected by air currents, which can change the nature of the discharge during treatments. The height of the generator was set at 3 cm, which was determined to allow the tip of the visible discharge plume to touch the cell solution in the inner well. Exposure times of 0, 2, 5 and 10 minutes were performed. After plasma exposure was complete $500\,\mu$l of $2\,\mu$M Sytox Green (Molecular Probes, Eugene, OR) was added to the cell suspension in each dish. Sytox Green is a fluorescent tracer molecule that is only able to enter cells having a compromised membrane. Once inside the cell this tracer molecule binds with nucleic acids which increases its fluorescence by >500 fold (Gaforio et al. 2002). After adding the nucleic acid probe, cells were incubated at $37\,^{\circ}$C and 5% CO_2 for 45 minutes. Following incubation, cells were resuspended by pipetting and three representative samples of $150\,\mu$l were transferred to a black 96-well spectroscopy plate (Corning, Lowell, MA). Fluorescence levels were quantified with a fluorescent plate reader (BioTek Instruments FLx800, Winooski, VT) using a 485 nm excitation filter and 528 nm emission filter. Each treatment condition was performed a total of 3 times per experiment and each experiment was repeated 3 times in order to increase the statistical power.

3.2.4 Viability Impact

Treatments performed to determine cell viability following plasma treatment were also carried out with both B16F10 and HaCaT cell lines. Dual chambered tissue culture dishes, as described above, were also used for this study. Before treatment the inner chamber of the dual dish was loaded with a suspension of 1×10^6 cells suspended in $500\,\mu$l of supplemented growth media. The outer chamber of the dish contained the 22 gauge wire immersed in 2 ml of PBS which was connected to ground through a $1.5\,\text{G}\Omega$ resistor. An operating generator height of 3 cm was used with exposure times of 2, 5 and 10 minutes. Following exposure, the cell suspensions were incubated at $37\,^{\circ}$C and 5% CO_2 for 4 hours. After incubation $50\,\mu$l of trypan blue (MP Biomedicals, Solon, OH) was added to the cell suspension. This suspension was then pipetted into a dual chambered hemocytometer (Hausser Scientific, Horsham, PA), and a dye exclusion viability assay was performed by light microscopy. This procedure was repeated a total of three times per treated sample. Each treatment condition was performed a total of 3 times per experiment and each experiment was repeated 3 times.

3.2.5 Membrane Stabilization

Kinetic experiments were performed to determine the time after plasma treatment when tracer molecules were no longer able to enter the cell. These experiments were carried out by adding 1×10^6 B16F10 or HaCaT cells suspended in $500\,\mu$l of unsupplemented media to a dual chambered tissue culture dish. As described above, the outer chamber of the dish contained a 22 gauge wire, immersed in 2 ml of PBS, that ran through a $1.5\,\text{G}\Omega$ resistance to ground. The generator was set 3.0 cm above the fluid level and cells were exposed to plasma for a total of 10 minutes. After exposure $500\,\mu$l of $2\,\mu$M Sytox Green was added to the cell suspension. The suspension with the tracer molecule was mixed by pipetting and

three representative samples of $150\,\mu$l were transferred into a 96-well spectroscopy plate. Fluorescence levels were obtained at 60 second intervals for a total of 20 minutes with a fluorescent plate reader using a 485 nm excitation and 528 nm emission filter set. Due to processing time the first readings occurred 120 seconds after the dye was added to each well. Each treatment was performed a total of 3 times per experiment and each experiment was repeated 3 times in order to increase the statistical power.

3.2.6 Statistical Analysis

After gathering data from delivery, viability, and resealing experiments the mean and standard error were calculated for each identically treated group. Using the obtained information a series of Student's t-tests were performed with a confidence level of 95%. This allowed relative comparisons to be made concerning the implications of each treatment time.

3.3 Delivery of Plasmid DNA to Murine Skin In Vivo

3.3.1 Plasma Generator

The first generation plasma generator was also used in this study. During these treatments the high voltage electrode was held at either $-8\,\mathrm{kV}$ or $8\,\mathrm{kV}$ while a stream of ultra high purity helium was passed through the tube at $15\,^{l}/_{min}$. A current limit of $100\,\mu\mathrm{A}$ was maintained as a safety mechanism during treatment. While operating the generator provided $10\,\mu\mathrm{A}$ of current flow at $8\,\mathrm{kV}$ to the annular electrode and produced a visible glow discharge that measured $3.0\,\mathrm{cm}$ in length. Similarly, $-10\,\mu\mathrm{A}$ was measured when the generator was run at $-8\,\mathrm{kV}$ which produced a glow discharge that measured $2.0\,\mathrm{cm}$.

3.3.2 High Impedance Ring

A high impedance ring was used in combination with plasma treatment for some treatment conditions. This ring was made of a loop of 22 gauge tinned copper wire and had a diameter of $2\,\mathrm{cm}$. The wire ring was placed symmetrically around the bolus created by the injection of DNA into the murine skin. It was affixed to the tissue surface with two butterfly closure bandages (Dynarex, Orangeburg, NY) placed on opposing sides of the ring. The other end of the wire was connected to ground potential through a $1.5\,\mathrm{G}\Omega$ resistive load. This resistive value was chosen as it allowed for a limited amount of current flow, about $2\,\mu\mathrm{A}$, without disrupting the glow discharge characteristics.

3.3.3 Animal Model

Female C57BL/6J mice (National Institutes of Health, Bethesda, MD) were used for this study. Treatments started when these animals were 6-7 weeks of age. All animals were

humanely euthanized at the conclusion of the study in accordance with an approved Institutional Animal Care and Use Committee protocol.

3.3.4 Anesthesia

Prior to treatment mice were placed in a plexiglass induction chamber and anesthetized with a constant supply of 2% isoflurane in oxygen (Caliper Life Sciences, Hopkinton, MA). After the mice had been anesthetized, treatments were carried out while a constant supply of 2% isoflurane in oxygen was delivered by a nose cone to maintain a level anesthesia plane. Animals were placed on a $32\,^{\circ}$C warming pad (Gaymar Industries, Orchard Park, NY) to prevent heat loss caused by the disruption of thermoregulatory mechanisms associated with the anesthesia.

3.3.5 Treatments

This study consisted of six different treatment groups with luciferase encoding plasmid and helium plasma to examine the ability of the charge deposition system to enhance DNA delivery. All plasmid injections were performed using a 1 cc syringe with a 30 gauge needle (Becton Dickinson). A $50\,\mu$l volume containing $100\,\mu$g gWIZ luciferase plasmid in saline (Aldevron, Fargo, ND) was injected intradermally for all animals that received DNA. For each experiment, 4 animal groups were treated with each of the following methods: 1) No treatment, not injected with plasmid and not exposed to plasma. 2) Luciferase plasmid injection with no exposure to helium plasma. 3) Plasmid injection and exposure to positive plasma for 10 minutes. 4) Plasmid injection and exposure to negative plasma for 10 minutes. 5) Plasmid injection and exposure to positive plasma for 10 minutes with a high impedance ground ring encircling the treatment area. And, 6) plasmid injection followed by exposure to negative plasma for 10 minutes with a high impedance ground ring encir-

cling the treatment area. In total, 12 animals were treated in each of the 6 conditions over three independent experiments. These treatments are summarized in Table 3.1.

Table 3.1: Summary of treatments performed in the initial in vivo experiment.

Treatment Performed
No Treatment
$100\,\mu\mathrm{g}$ luciferase plasmid only
$100\,\mu\mathrm{g}$ luciferase plasmid with 10 min positive plasma
$100\,\mu\mathrm{g}$ luciferase plasmid with 10 min negative plasma
$100\,\mu\mathrm{g}$ luciferase plasmid with 10 min positive plasma and high impedance ring
$100\,\mu\mathrm{g}$ luciferase plasmid with 10 min negative plasma and high impedance ring

3.3.6 Luminescence Quantification

Luciferase expression was determined by injecting 150 mg of D-luciferin (Caliper Life Sciences) per kg of body weight intraperitoneally in anesthetized mice 15 minutes before measurement of luminescence. After injection a light producing reaction occurs from the oxidation of luciferin, which is facilitated by the presence of the luciferase enzyme. Light emission caused by this reaction was captured by placing the anesthetized animals into a Xenogen IVIS 200 series imaging system (Caliper Life Sciences). The photon flux ($\mathrm{photons}/\mathrm{s-cm^2}$) from each animal was calculated using Living Image software (Caliper Life Sciences). This procedure was repeated and luminescence data were gathered at days 0, 2, 4, 6, 8, 10, 18 and 26 following the experiment.

3.3.7 Statistical Analysis

After all data was gathered the mean response and standard error of photon flux was calculated for identically treated groups on each of the follow-up days from 0 to 26. With these data, a two-sided Student's t-test was performed with a 95% confidence level between the 6 treatment groups for each day that data was collected. This allowed consideration of dif-

ferences between groups of the amounts of expressed luciferase, indicated by photon flux quantity, produced by each treatment.

3.3.8 Histological Analysis

To study the effects of plasma exposure on the skin a concomitant experiment was performed that involved the injection of $100\,\mu$g gWIZ luciferase plasmid followed by exposure to plasma. All plasmid injections were performed using a 1 cc syringe with a 30 gauge needle. This experiment was composed of the following groups: 1) No treatment, not injected with plasmid and not exposed to plasma. 2) Plasmid injection with no exposure to plasma. 3) Plasmid injection and exposure to positive plasma for 10 minutes. 4) Plasmid injection and exposure to negative plasma for 10 minutes. In total seven animals were treated with each of the four conditions.

Full thickness skin biopsies of the treatment sites were harvested from animals on days 0, 1, 2, 5, 7, 14 and 21. Harvested sections were immediately placed in 10% neutral buffered formalin (Protocol, Pittsburgh, PA). Skin samples were sectioned at $5\,\mu$m, stained with hematoxylin and eosin and mounted on glass slides.

3.4   Optimization of Plasma Delivery In Vivo

3.4.1   Plasma Generator

A new plasma generator was fabricated for this study which was also made from a 15 cm long Teflon dowel. Similar to the first generation system, this dowel was hollowed to create a tube having a 1 cm inner diameter and wall thickness of 2 mm. Two electrodes were positioned at either end of the 15 cm long tube. A brass encased 5 mW red laser pointer (Instapark, Santa Fe Springs, CA) was positioned on one end of the tube and connected to ground potential. This not only served as the reference ground in the system, but also allowed for more accurate targeting of the treatment site. A flat annular stainless steel electrode with a 3.5 mm internal diameter occupied the opposite end of the Teflon tube. This electrode was connected to a high voltage direct current power supply. The gas stream was plumbed into the tube with a polypropylene hose barb that was placed just below the laser pointer. Figure 3.4 shows the second generation plasma system.

A software interface platform was used to control the high voltage power supply and allowed the voltage, maximum current and exposure time to be set prior to treatment. This platform also allowed monitoring and logging of the current and potential leaving to the high voltage electrode and current returning to ground through the high impedance ring. A current limit of $100 \mu A$ was set as a safeguard measure during treatment. Under operational conditions the generator provided a reading of $17.7 \mu A$ at $8 kV$ to the annular electrode and produced a visible glow discharge that measured 3.0 cm in length. When the generator was operated at $-8 kV$ a reading of $-15.1 \mu A$ was obtained, and the visible discharge measured 2.0 cm in length. Figure 3.5 and Figure 3.6 show the user interface and source code for the second generation system.
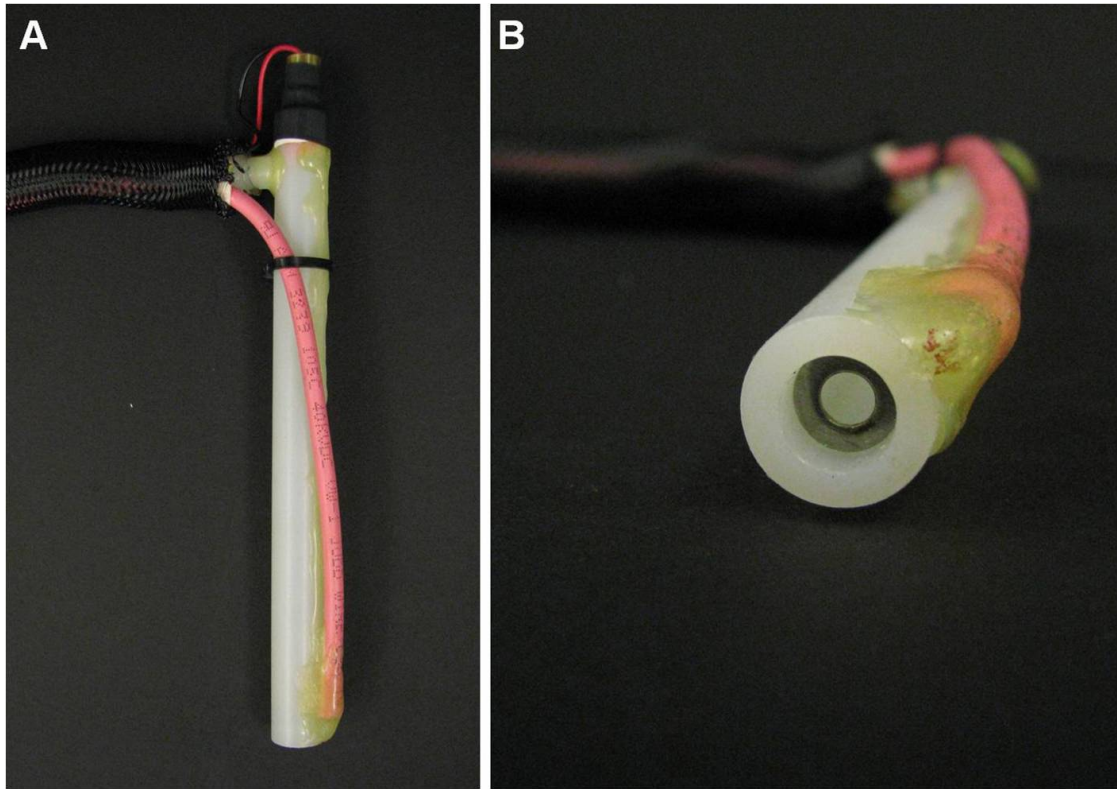
Figure 3.4: Second generation plasma generator.

3.4.2 Animal Model

Female C57BL/6J mice 6-7 weeks of age were used for this study. All animals were humanely euthanized at the conclusion of the study in accordance with an approved Institutional Animal Care and Use Committee protocol.

3.4.3 Anesthesia

Before treatment mice were placed in a plexiglass induction chamber and anesthetized with a constant supply of 2% isoflurane in oxygen. After the mice had been anesthetized, treatments were carried out at a constant plane of isoflurane in oxygen delivered by a nose cone. During treatments animals were placed on a $32\,^{\circ}\text{C}$ warming pad to prevent heat loss.
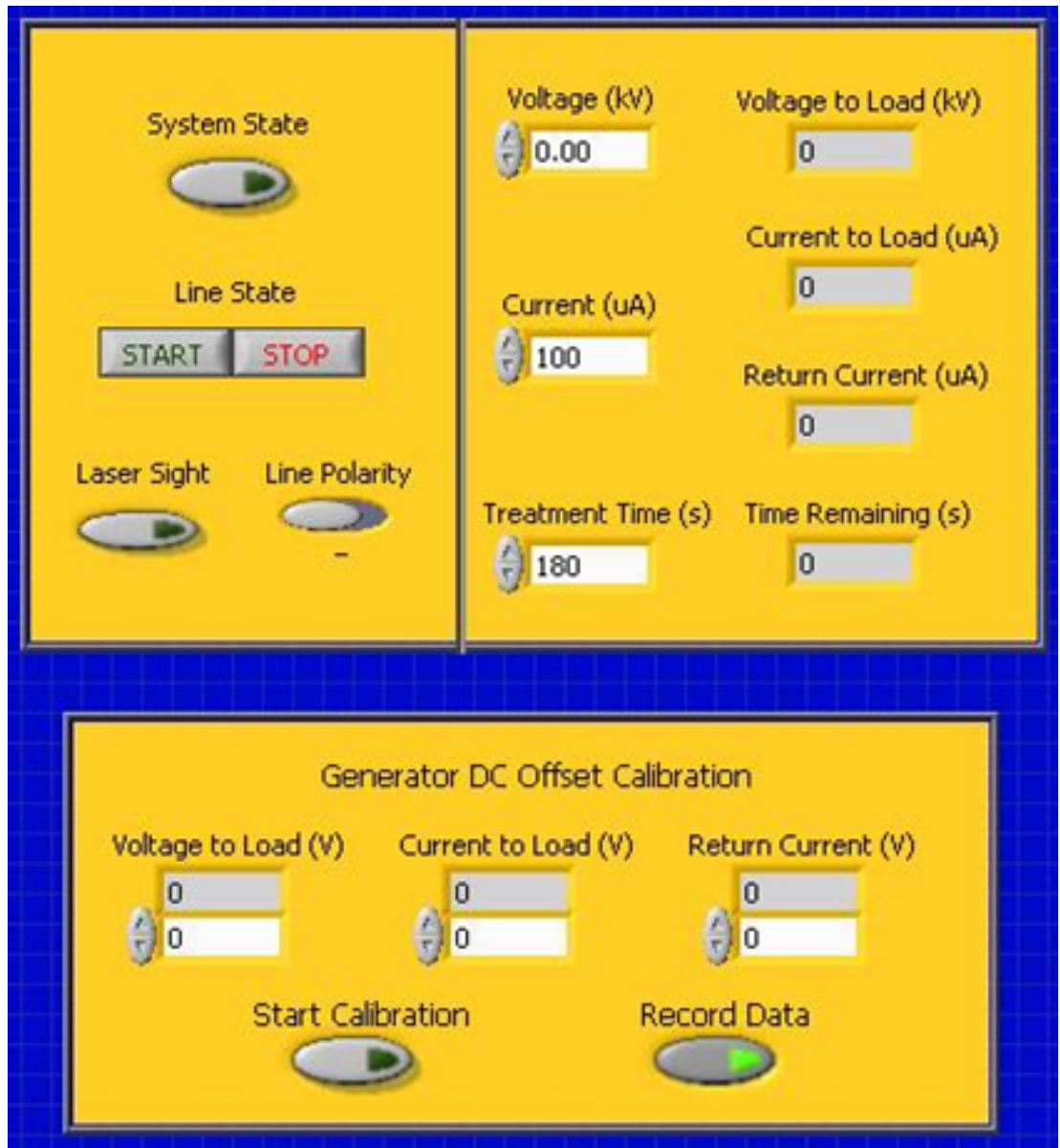
Figure 3.5: Graphical user interface for the second generation plasma system.
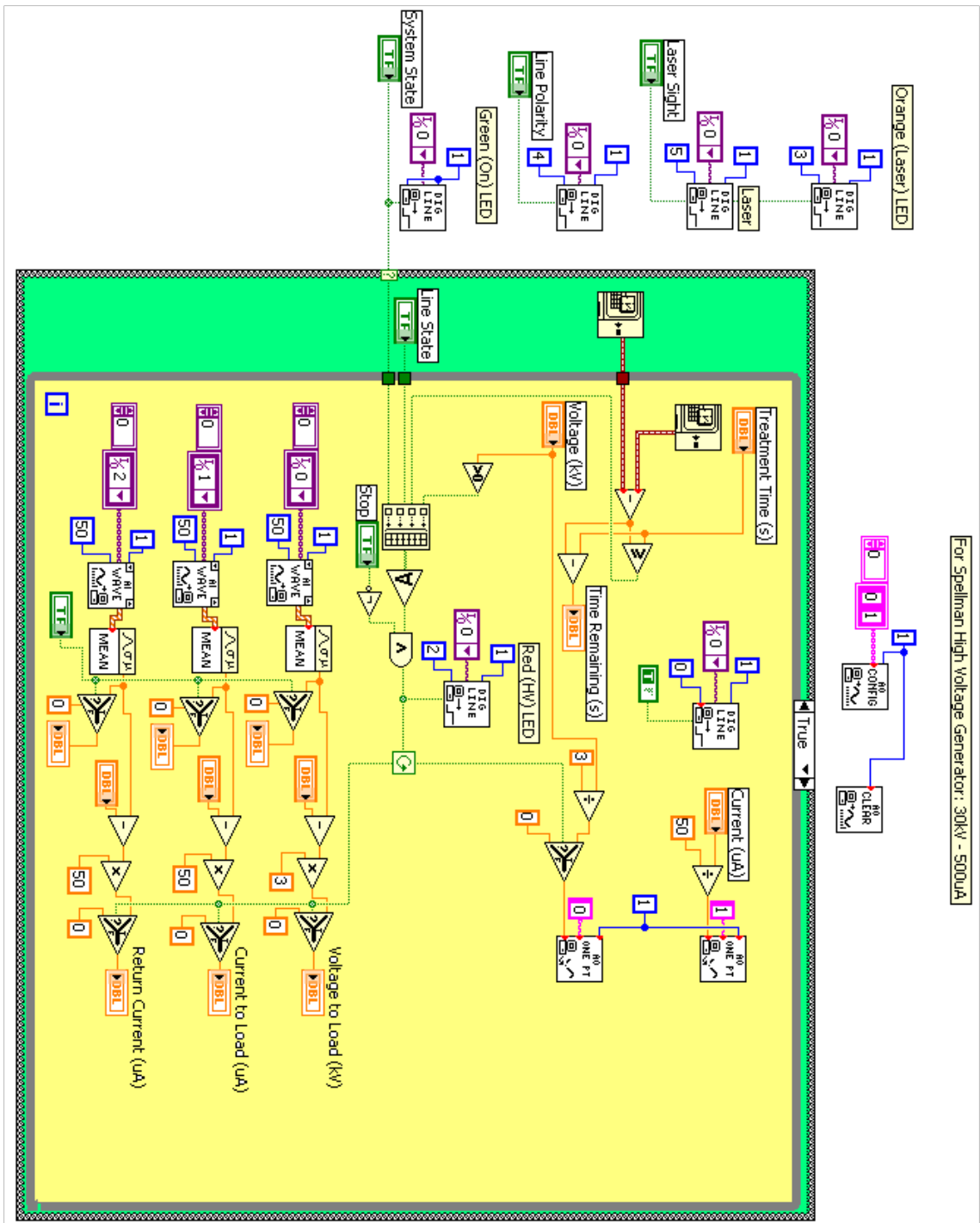
Figure 3.6: Source code for the second generation plasma system.

Table 3.2: Summary of plasma dose response experiments.

Treatment Performed
No Treatment
$100\,\mu$g luciferase plasmid only
$100\,\mu$g luciferase plasmid with 2 min positive plasma
$100\,\mu$g luciferase plasmid with 2 min negative plasma
$100\,\mu$g luciferase plasmid with 5 min positive plasma
$100\,\mu$g luciferase plasmid with 5 min negative plasma
$100\,\mu$g luciferase plasmid with 10 min positive plasma
$100\,\mu$g luciferase plasmid with 10 min negative plasma
$100\,\mu$g luciferase plasmid with 20 min positive plasma
$100\,\mu$g luciferase plasmid with 20 min negative plasma

3.4.4 Plasma Dose Response Treatments

This study consisted of 10 different treatment conditions that involved the injection of luciferase encoding plasmid and treatment with either negative or positive polarity helium plasma. All plasmid injections were performed using a 1 cc syringe with a 30 gauge needle. A $50\,\mu$l volume containing $100\,\mu$g gWIZ luciferase plasmid in saline was injected intradermally for all animals that received DNA. For each experiment, 4 animals were treated with each of the following methods: 1) No treatment, not injected with plasmid and not exposed to plasma; 2) Luciferase plasmid injection with no exposure to helium plasma; 3) Plasmid injection and exposure to positive plasma for 2 minutes; 4) Plasmid injection and exposure to negative plasma for 2 minutes; 5) Plasmid injection and exposure to positive plasma for 5 minutes; 6) Plasmid injection and exposure to negative plasma for 5 minutes; 7) Plasmid injection and exposure to positive plasma for 10 minutes; 8) Plasmid injection and exposure to negative plasma for 10 minutes; 9) Plasmid injection and exposure to positive plasma for 20 minutes; 10) Plasmid injection and exposure to negative plasma for 20 minutes. Table 3.2 summarizes these treatments. In total, 12 animals were treated with each of the 10 conditions over three independent experiments.

3.4.5 Plasmid Dose Response Treatments

The second set of experiments conducted, modulated the plasmid dose while keeping the plasma dose fixed. In these experiments injections of $50\,\mu$g, $100\,\mu$g and $200\,\mu$g of gWIZ luciferase were made to determine the effect increasing plasmid concentration would have on plasma mediated molecular delivery. Injection volumes remained at $50\,\mu$l while gWIZ luciferase concentrations used were $1\,\mathrm{mg/ml}$, $2\,\mathrm{mg/ml}$ and $4\,\mathrm{mg/ml}$ prepared in saline. Animals were treated in groups of 4 with each of the following methods: 1) No treatment, not injected with plasmid and not exposed to plasma; 2) A $50\,\mu$g injection of luciferase plasmid with no exposure to helium plasma; 3) A $50\,\mu$g injection of luciferase plasmid and exposure to positive plasma for 10 minutes; 4) A $50\,\mu$g injection of luciferase plasmid and exposure to negative plasma for 10 minutes; 5) A $100\,\mu$g injection of luciferase plasmid with no exposure to helium plasma; 6) A $100\,\mu$g injection of luciferase plasmid and exposure to positive plasma for 10 minutes; 7) A $100\,\mu$g injection of luciferase plasmid and exposure to negative plasma for 10 minutes; 8) A $200\,\mu$g injection of luciferase plasmid with no exposure to helium plasma; 9) A $200\,\mu$g injection of luciferase plasmid and exposure to positive plasma for 10 minutes; 10) A $200\,\mu$g injection of luciferase plasmid and exposure to negative plasma for 10 minutes. All plasma treatments were performed with a high impedance ring encircling the treatment area. In total, 12 animals were treated with each of the 10 conditions over three independent experiments.

Animals were also treated with electroporation at each of the plasmid concentrations listed above to serve as a comparison. Electroporation pulses were applied with a four plate electrode, shown in Figure 3.7. A total of eight pulses were delivered after the $50\,\mu$l injection was made in the dermis. These pulses had a field strength of $100\,\mathrm{V/cm}$, duration of $150\,\mathrm{ms}$ and a $1\,\mathrm{s}$ duty cycle. To ensure electrical contact was made with the tissue the electrode surfaces were coated with conductive gel (Parker Laboratories Spectra 360 Electrode Gel, Hellendoorn, Netherlands) prior to treatment. In total 3 groups of 4 animals per group

35

Figure 3.7: Four plate electroporation applicator.

were exposed to electroporation. The groups for this section of the experiment were: 1) A $50\,\mu$g injection of luciferase plasmid with electroporation; 2) A $100\,\mu$g injection of luciferase plasmid with electroporation; 3) A $200\,\mu$g injection of luciferase plasmid with electroporation. As with the plasma treatments, 12 animals were treated with each of the 3 electroporation conditions over three independent experiments. Table 3.3 summarizes the plasma and electroporation treatments performed in this experiment.

3.4.6 Luminescence Quantification

Luciferase expression was determined by injecting 150 mg of D-luciferin per kg of body weight intraperitoneally in anesthetized mice 15 minutes before measurement of luminescence. Light emission created by the reaction of luciferase with luciferin were captured by placing the anesthetized animals into a Xenogen IVIS 200 series imaging system. The photon flux ($photons/s-cm^2$) from each animal was calculated using Living Image software.

36

Table 3.3:   Summary of plasmid dose response experiments.

Treatment Performed
No Treatment
$50\,\mu$g luciferase plasmid only
$100\,\mu$g luciferase plasmid only
$200\,\mu$g luciferase plasmid only
$50\,\mu$g luciferase plasmid with electroporation
$100\,\mu$g luciferase plasmid with electroporation
$200\,\mu$g luciferase plasmid with electroporation
$50\,\mu$g luciferase plasmid with 10 min positive plasma
$50\,\mu$g luciferase plasmid with 10 min negative plasma
$100\,\mu$g luciferase plasmid with 10 min positive plasma
$100\,\mu$g luciferase plasmid with 10 min negative plasma
$200\,\mu$g luciferase plasmid with 10 min positive plasma
$200\,\mu$g luciferase plasmid with 10 min negative plasma

This procedure was repeated and luminescence data was gathered at days 0, 2, 4, 7, 10, 14, 21 and 30 following the experiment.

3.4.7   Statistical Analysis

After all data was gathered the mean photon flux and standard error was calculated for identically treated groups on each of the follow-up days from 0 to 30. With these data, a two-sided Student's t-test was performed with a 95% confidence level between all the treatment groups for each day that data was collected. This allowed consideration of differences between groups of the amounts of expressed luciferase, indicated by photon flux quantity, produced by each treatment.

3.5   Delivery of a DNA Vaccine In Vivo

3.5.1   Plasma Generator

The second generation plasma generator was also used in this study. During treatments the high voltage electrode was held at either $-8\,\mathrm{kV}$ or $8\,\mathrm{kV}$ while a stream of ultra high purity helium was passed through the generator body at $15\,{}^{\mathrm{l}}/\mathrm{min}$. A current limit of $100\,\mu\mathrm{A}$ was kept as a safety mechanism during treatment. While operating at these conditions the generator provided $18.1\,\mu\mathrm{A}$ of current at $8\,\mathrm{kV}$ to the annular electrode and produced a visible glow discharge that measured $3.0\,\mathrm{cm}$ in length. Similarly, $-14.8\,\mu\mathrm{A}$ of current was measured when the generator was run at $-8\,\mathrm{kV}$ which produced a glow discharge $2.0\,\mathrm{cm}$ in length.

3.5.2   Animal Model

Female BALB/c mice (National Institutes of Health) 6 weeks of age were used for this study. All animals were humanely euthanized at the conclusion of the study in accordance with an approved Institutional Animal Care and Use Committee protocol.

3.5.3   Anesthesia

Prior to vaccination, animals were anesthetized in an induction chamber with 2% isoflurane mixed with oxygen. After induction, the mice were maintained in an anesthetized state by delivering 2% isoflurane through a nose cone. To prevent excessive heat loss due to anesthesia exposure mice were placed on a $32\,{}^{\circ}\mathrm{C}$ heating pad during vaccination.

Table 3.4: Summary of vaccination conditions.

Treatment Performed
No Treatment
$100\,\mu$g pVAX backbone only
$100\,\mu$g JRFLgp120 plasmid only
$100\,\mu$g pVAX backbone with electroporation
$100\,\mu$g JRFLgp120 plasmid with electroporation
$100\,\mu$g pVAX backbone with 10 mins positive plasma
$100\,\mu$g pVAX backbone with 10 mins negative plasma
$100\,\mu$g JRFLgp120 plasmid with 10 mins positive plasma
$100\,\mu$g JRFLgp120 plasmid with 10 mins negative plasma

3.5.4   Vaccination

Plasmid injections were performed with a 1 ml syringe and a 30-gauge needle. Injections were delivered into the dermis and contained $100\,\mu$g pJRFLgp120 suspended in $50\,\mu$l of saline. Plasma exposure times of 10 minutes were selected based on previous evidence showing high levels of expression with this treatment time. Each of the vaccination conditions were performed on groups of mice containing four animals. The following vaccination groups were evaluated in this study: 1) No treatment, not injected with plasmid nor exposed to plasma; 2) Injection with $100\,\mu$g pVAX plasmid backbone only; 3) Injection with $100\,\mu$g pVAX backbone with 10 minutes of positive plasma exposure; 4) Injection with $100\,\mu$g pVAX backbone delivered with 10 minutes of negative plasma exposure; 5) Injection with $100\,\mu$g pVAX backbone followed by 8 electroporation pulses at $100\,\mathrm{V/cm}$ and 150 ms in duration; 6) Injection with $100\,\mu$g pJRFLgp120 only; 7) Injection with $100\,\mu$g pJRFLgp120 with 10 minutes positive plasma exposure; 8) Injection with $100\,\mu$g pJRFLgp120 with 10 minutes negative plasma exposure and 9) Injection with $100\,\mu$g pJRFLgp120 followed by 8 electroporation pulses at $100\,\mathrm{V/cm}$ and 150 ms in duration. Table 3.4 outlines these treatments. This protocol involved an initial treatment on day 0, followed by three booster vaccinations on days 14, 28 and 130.
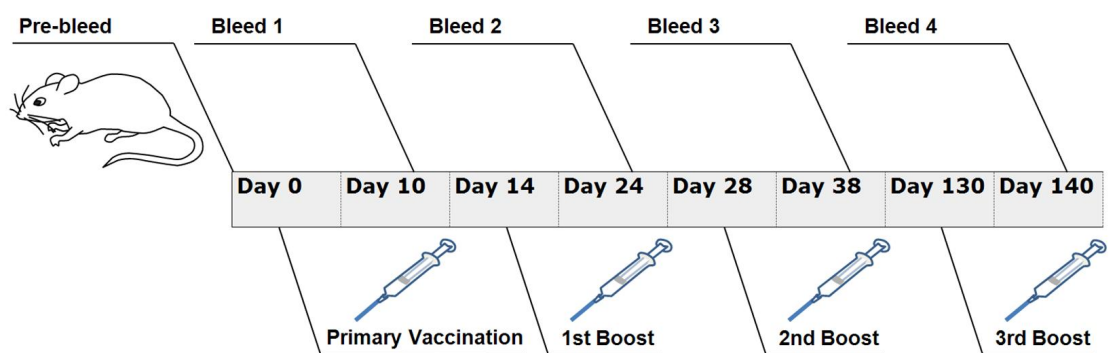
Figure 3.8: Vaccination time line for the JRFLgp120 study.

3.5.5 Serum Collection

Submandibular bleeds were performed 10 days after each vaccination to collect the blood necessary to detect antibody responses. Samples containing approximately $200\,\mu$l were collected in serum separation tubes (Becton Dickinson Micro-Fine Tubes). After collection, the samples were separated by centrifugation at 10,000 rpm for 5 minutes. Once separated the serum was aspirated from the tubes and transferred to micro PCR tubes (Becton Dickinson), which were stored at $-20\,°$C. Figure 3.8 indicates the time line for vaccination and sample collection for the study.

3.5.6 Antibody Quantification

To analyze serum samples for anti-gp120 antibodies an indirect ELISA assay was performed. The antigen used in this assay was ADA gp120, which shares 87.3% amino acid homology with the JRFLgp120 envelope protein. ELISA micro titer plates (Immulon Microtiter 96-Well Plates, Waltham, MA) were coated with this antigen by adding $50\,\mu$l of a $2\,\mu\mathrm{g/ml}$ solution of ADA gp120 (ImmunoDiagnostics, Woburn, MA) to every well and incubating 24 hours at $4\,°$C. After incubation nonspecific sites were blocked by adding $100\,\mu$l of a 2% bovine serum albumin solution prepared in PBS, commonly known as blocking buffer. This solution was also incubated 24 hours at $4\,°$C. Sera dilutions were made in

blocking buffer and ranged from 1:64 to 1:131,072, which was added to the ADA gp120 coated plates in duplicate and incubated for 24 hours at $4\,^{\circ}$C. Plates were then incubated with goat anti-mouse horseradish peroxidase conjugated IgG (Promega, Madison, WI) at $37\,^{\circ}$C for 4 hours. These plates were then developed in a $0.05\,$M phosphate-citrate buffer containing tetramethylbenzidine (Sigma-Aldrich, St. Louis, MO) at $37\,^{\circ}$C for 30 minutes. Finally, development of the plates was stopped by adding $25\,\mu$l of $2\,$M sulfuric acid to each well. Optical densities were determined at 450 nm (BioTek ELx800). This indirect ELISA methodology follows protocols that have been previously published (MacGregor et al. 1998, Ugen et al. 1992).

3.5.7 Statistical Analysis

Statistical differences between endpoint geometric mean antibody titers for the various groups was determined by a nonparametric Kruskal-Wallis analysis of variance test. Results found to contain significant differences were further investigated by the Student's t-test to ensure significance. Each of these tests was performed with a 95% confidence level.

3.6 Transdermal Electric Field Simulation

3.6.1 Surface Potential

To determine the electrical potentials along the surface of the mouse, plasma treatments were performed following normal protocols. Once the plasma discharge was treating the animal skin, potential measurements were made by contacting the epidermal surface with a high voltage probe (Fluke 80K-40, Everett, WA) interfaced with an ammeter. This procedure was carried out with positive and negative polarity plasmas. Data gathered from these experiments was fit with a exponential function, and used as a boundary condition in the model.

3.6.2 Finite Element Model

To model the electric field present in skin a generalized electrostatics model was used in a finite element software package (COMSOL Multiphysics, Burlington, MA). Laplace's equation,

$$-\nabla \bullet (\sigma \nabla V) = 0, \qquad (3.1)$$

was used to calculate the electrical characteristics present in the specified geometry. In this model σ represents the conductivity and V represents the electric potential.

3.6.3 Geometric Objects

This two dimensional simulation contained geometric elements consistent with measurements obtained from an animal during treatment. A vertical cross section of a mouse during treatment was created from two concentric ellipses having a major and minor axis with a 1.5 mm difference. A skin layer was created by the outer ellipse which had a thickness
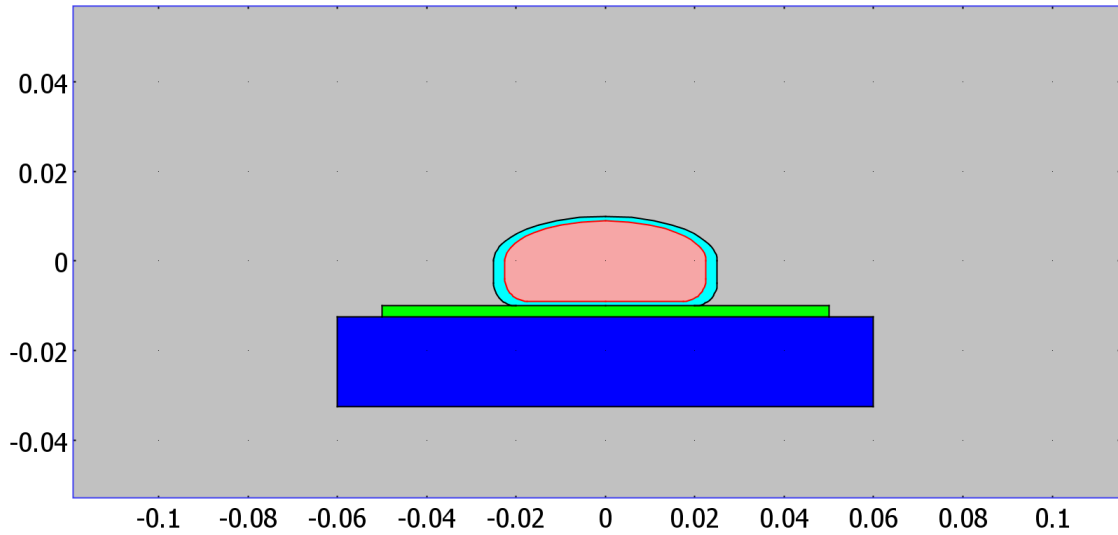
Figure 3.9: Geometric elements created for the finite element model.

of 1.5 mm, electrical conductivity of 0.0002 S/m and relative permittivity of 40. The inner ellipse was 4 cm wide by 1.8 cm tall, had an electrical conductivity of 0.82211 S/m and relative permittivity of 80. Beneath the animal was an insulating heating pad with a height 2.5 cm and 10 cm width. This pad had an electrical conductivity of 1×10^{-12} S/m and relative permittivity of 7. At the bottom of this stack was a grounded stainless steel table with a height of 2 cm and width of 12 cm. The electrical characteristics of this table were set to a conductivity of 4.032×10^{6} S/m with a relative permittivity of 1. Figure 3.9 shows the geometric elements used in this model.

3.6.4 Boundary Conditions

To solve this model the appropriate boundary conditions were added for each of the geometry elements. First the operating table was set as the relative ground in the simulation,

$$V = 0. \tag{3.2}$$

The next boundary condition was to place the electrical potential on the epidermal surface of the animal skin,

$$V = A \exp(-Bx) + C. \tag{3.3}$$

This equation allowed the electrical potential to take values that were experimentally discovered and fit with an exponential function to determine the value of A, B, and C. All other elements in the model took on the continuity boundary condition,

$$\vec{n} \bullet \left(\vec{J_1} - \vec{J_2} \right) = 0. \tag{3.4}$$

This condition specifies the normal component of the current density is continuous across the boundary.

CHAPTER IV: RESULTS

4.1   Creating a Plasma Discharge for In Vivo Use

4.1.1   Construction

To investigate the utility of ionized gases for molecular delivery a plasma generator first had to be constructed. The first generation system consisted of a 15 cm long Teflon dowel. This dowel was hollowed to create a tube having a 1 cm inner diameter and wall thickness of 2 mm. Two electrodes were positioned at either end of the tube. A steel hose barb attached to ground potential was positioned on one end of the tube to serve as a ground reference electrode and interface the tube with a gas inlet stream. A flat annular stainless steel electrode with a 3.5 mm internal diameter occupied the opposite end of the Teflon tube. This electrode was connected to a high voltage direct current power supply. A software interface platform was used to control the high voltage power supply and allowed the voltage, maximum current and exposure time to be set prior to treatment. As a safeguard the maximum current was set at $100\,\mu$A. Figure 4.1 shows the first generation plasma generator.

Figure 4.1: CAD rendering of the first generation plasma generator.

Due to the desire to treat biological samples and cause a minimal effect to viability, helium was chosen as the medium. Helium was selected as it is known for its ability to create a stable plasma volume when operating in air, and its high ionization energy acts as a safeguard to prevent arcing (Kang et al. 2002, Laroussi 2000, Laroussi and Lu 2005). Also, the excitation of helium in air at standard temperature and pressure creates a non-LTE discharge, or cold plasma, which should reduce the thermal impact on treated samples.

4.1.2   Electrical Parameters

To generate a consistent plasma a series of experiments were performed to determine the operating height of the generator and potential that would be applied to the high voltage electrode. To perform these experiments the generator was placed 1, 2, 3, 4 or 5 cm above a 4 cm^2 stainless steel plate. This plate was connected to ground potential through an elec-

trometer. Current measurements were taken as the high voltage electrode was swept from $-10\,\mathrm{kV}$ to $10\,\mathrm{kV}$. Figure 4.2 shows the obtained current data.

The electrical data gathered indicated that as the potential increased or the height decreased the current increased. Operating at a height of $1\,\mathrm{cm}$ or $2\,\mathrm{cm}$ with a positive potential appeared to be too close to the plate as the maximum current from the generator was being supplied well before $10\,\mathrm{kV}$ was reached. Operating at $3\,\mathrm{cm}$ allowed the full range of currents to be generated, while further distances used less than half of the current capacity of the power supply. When a negative potential was applied a spacing of $1\,\mathrm{cm}$ allowed the full current range to be utilized. Heights more than this decreased the maximum currents to 80% or less.

Due to the positive plasma generating the full current range of 0 to $100\,\mu\mathrm{A}$ without arcing at a spacing of $3\,\mathrm{cm}$ this was chosen as the operating distance. Due to the desire to avoid the possibility of developing an arc or spark a value of half that of the maximum current value, $50\,\mu\mathrm{A}$, was selected as the optimum current. This correlated to an operating voltage of 8 kV. As these were selected based on the positive data, -8 kV was chosen as the operating voltage for negative polarity treatments. A similar current of $-47\,\mu\mathrm{A}$ was generated at -8 kV when a height of 2 cm was used, so this was selected as the height that would be used during treatment.

4.1.3 Physical Characterization

Operating at these conditions produced a visible glow discharge emanating from the annular electrode that was $3.0\,\mathrm{cm}$ in length for positive polarity and $2.0\,\mathrm{cm}$ in length for negative polarity. Therefore, operating at the chosen potential and distances would allow the tip of the plasma to touch the treatment site throughout exposure. Temperature measurements made with an infrared thermometer (Fluke Model 62) throughout the plasma volume
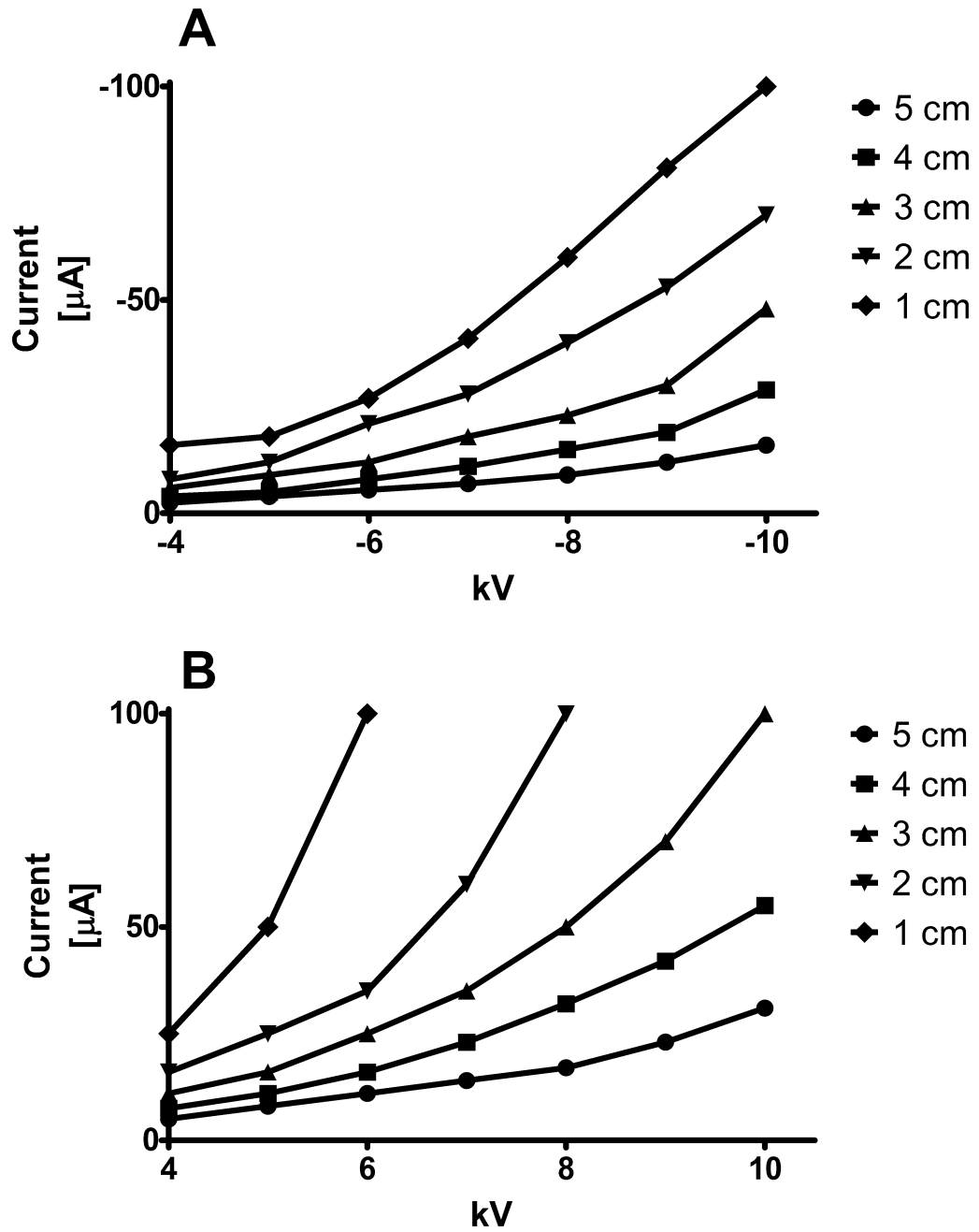
Figure 4.2: Current measurements obtained by modulating the voltage and distance between the generator and ground plate. A represents data collected at negative polarity and B represents data collected at positive polarity.

showed no deviation in temperature from that of gas alone. Figure 4.3 shows the plasma discharge operating at atmospheric conditions.

4.1.4 Optical Emission Spectroscopy

Ultraviolet and visual light spectroscopy was performed to determine the reactive constituents produced by the plasma generator. Figure 4.4 shows spectra collected from the discharge at the opening of the generator. These spectral emissions are dominated by nitrogen and nitrogen ions. Emission lines in the range of 300-400 nm correspond to OH, N_2 and N_2^+; 400-600 nm to N_2 and N_2^+; and 600-900 nm to O and He (Laroussi and Lu 2005, *NIST atomic spectra database [electronic resource]* 1995). The prevalent helium excitation line in the spectroscopic data occurs at 706.5 nm corresponding to the 1s2p–1s3s atomic configuration (Kang et al. 2002). Peaks from species other than helium are suggested to result from the transfer of energy to molecules in the ambient atmosphere at the opening, plasma region, of the generator. The majority of emission lines prevalent in these spectra occur in the ultraviolet range and have an irradiance of $28\,\mu\text{W}/\text{cm}^2$ for negative polarity and $30\,\mu\text{W}/\text{cm}^2$ for positive polarity.

4.1.5 Conclusions

Creating the plasma generator and performing initial testing allowed treatment protocols to be established for this system. It was determined all treatments would be carried out at a potential of $8\,\text{kV}$, irrespective of the polarity. To generate similar currents at this potential a treatment height of $3.0\,\text{cm}$ was selected for positive polarity and $2.0\,\text{cm}$ for negative.

Operating at these conditions creates a stable discharge that is non-thermal in nature. The excited species produced by the generator appear to be mostly a consequence of energy

49
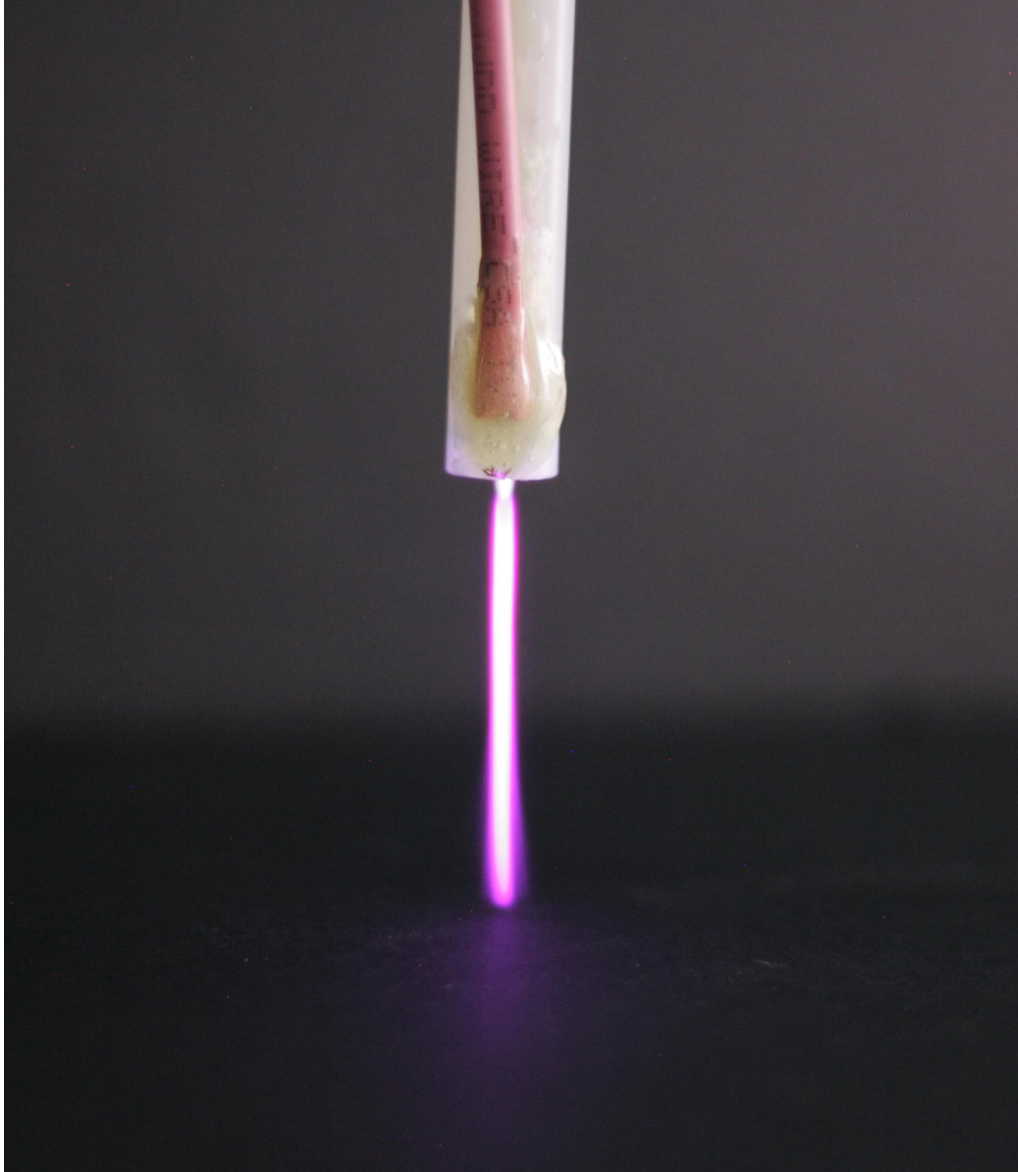
Figure 4.3: First generation plasma generator producing an atmospheric glow discharge. Image was captured with a 15 second exposure.
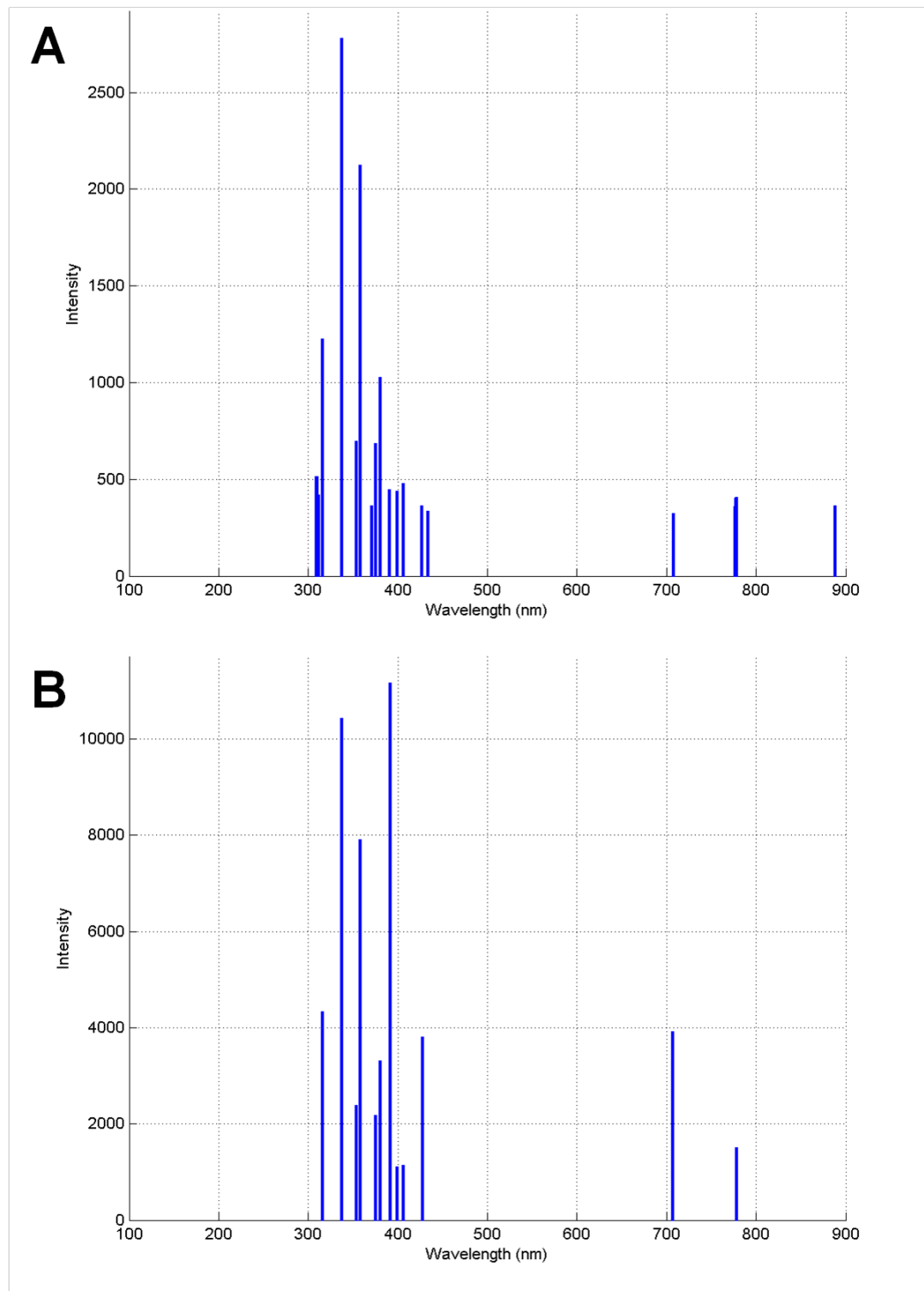
Figure 4.4: Ultraviolet and visual light spectra collected from the glow discharge. The reference point of the spectrometer was the opening of the generator and spectra were collected with a 5 second integration time. Plot A shows spectral peaks collected with negative polarity plasma and plot B shows peaks from positive polarity plasma.

transfer from metastable helium to ambient air, as the majority of spectral peaks are characteristic for nitrogen. Many of the spectral peaks observed reside in the ultraviolet region of the spectra, but have an overall irradiance of less than $30\,\mu W/cm^2$. This level of irradiance is comparable to the background emissions from a standard fluorescent light. Having performed initial characterization of the discharge allowed it to be used in vitro and in vivo.

4.2   In Vitro Experimentation

4.2.1   Introduction

In order to gain insight into the mechanism and establish feasibility of plasma for molecular delivery a series of in vitro experiments were performed.   This work examined the delivery efficacy, viability impact and restabilization kinetics following plasma exposure.

4.2.2   Plasma Characterization

The plasma generator fabricated for this study created a stable discharge and was capable of operating in a reproducible manner.   This generator was operated at a potential of $8\,kV$ on the high voltage annular electrode with a helium flow rate of $15\,l/min$.   Operating under these conditions the generator supplied an average current of $10\,\mu A$ to the high voltage electrode, which corresponded to a maximum power consumption of $80\,mW$ by the plasma discharge.   The visible plume created by this discharge measured approximately $3\,cm$ in length.   Infrared temperature measurements made at $0.5\,cm$ intervals throughout the visible discharge showed no thermal variations from that of the flowing gas alone.   Figure 4.5 shows the plasma generator operating $3\,cm$ above a tissue culture dish.
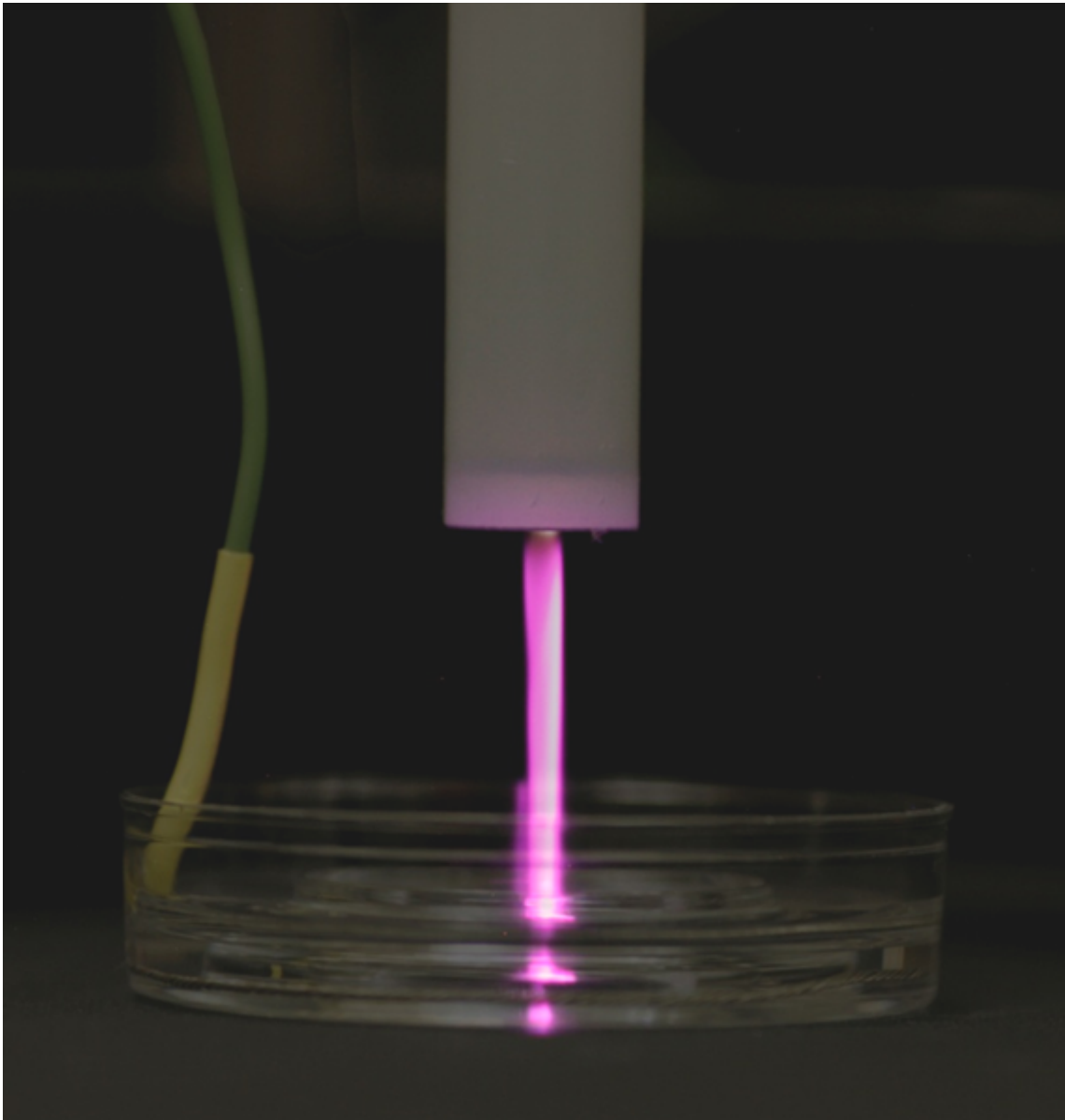
Figure 4.5: Positive polarity plasma treating the inner well of a tissue culture dish. In this image the generator was positioned 3 cm above the inner chamber of a tissue culture dish. The outer chamber of dish contains a 22 gauge wire connected to ground through a $1.5\,\text{G}\Omega$ resistor.

4.2.3 Molecular Delivery

Molecular delivery experiments were performed with HaCaT and B16F10 cells to determine the ability of plasma to enhance the uptake of small molecules in vitro. These ex-

periments were performed using the setup discussed in the Molecular Delivery section of the Materials and Methods chapter. Cell suspensions were treated with the plasma discharge for 2, 5 and 10 minutes. After exposure a fluorescent nucleic acid stain was mixed with the cell suspension to quantify the extent of delivery attainable at each treatment time. Figure 4.6 shows cells stained with the nucleic acid probe Sytox Green. Fluorescent values of HaCaT cells following delivery had a mean rise of 13% for 2 minutes, 41% for 5 minutes and 62% for 10 minutes relative to untreated control samples. Similar increases of 7%, 21% and 55% were obtained when B16F10 cells were plasma treated for 2, 5 and 10 minutes respectively. Figure 4.7 displays fluorescence quotient data for B16F10 and HaCaT cells, which was obtained by dividing the fluorescence value of the treated sample (F) by the respective control value fluorescence (F_0). Statistical analysis performed on these data conclude at the 95% confidence level that HaCaT and B16F10 cells exposed to 5 and 10 minutes had a mean fluorescence higher than that of their respective control groups.
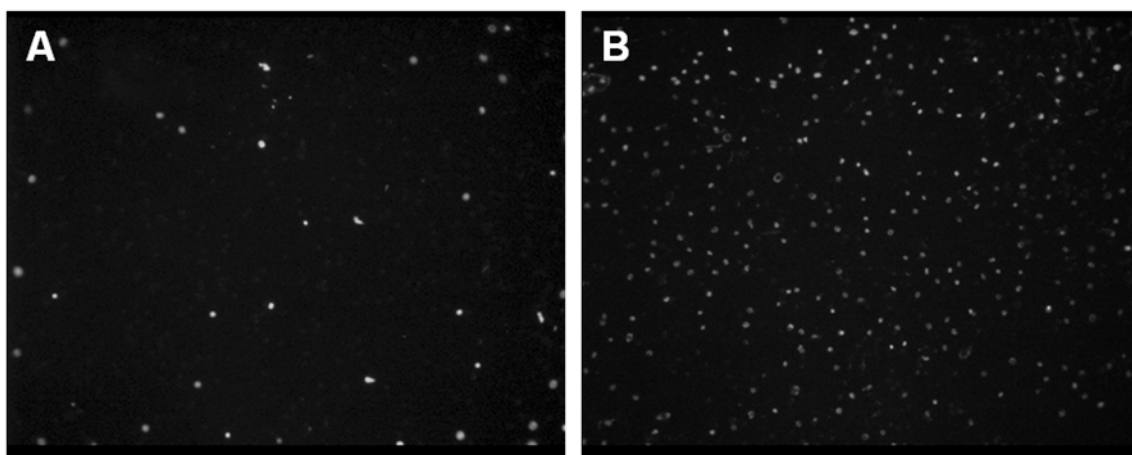
Figure 4.6: Fluorescent images of cells obtained after treatment with 10 minutes of positive polarity plasma and incubation with Sytox Green. A 45 minutes incubation was performed with the nucleic acid probe at 37°C and 5% CO_2. (A) No exposure to plasma prior to incubation. (B) Plasma exposure for 10 minutes prior to incubation.
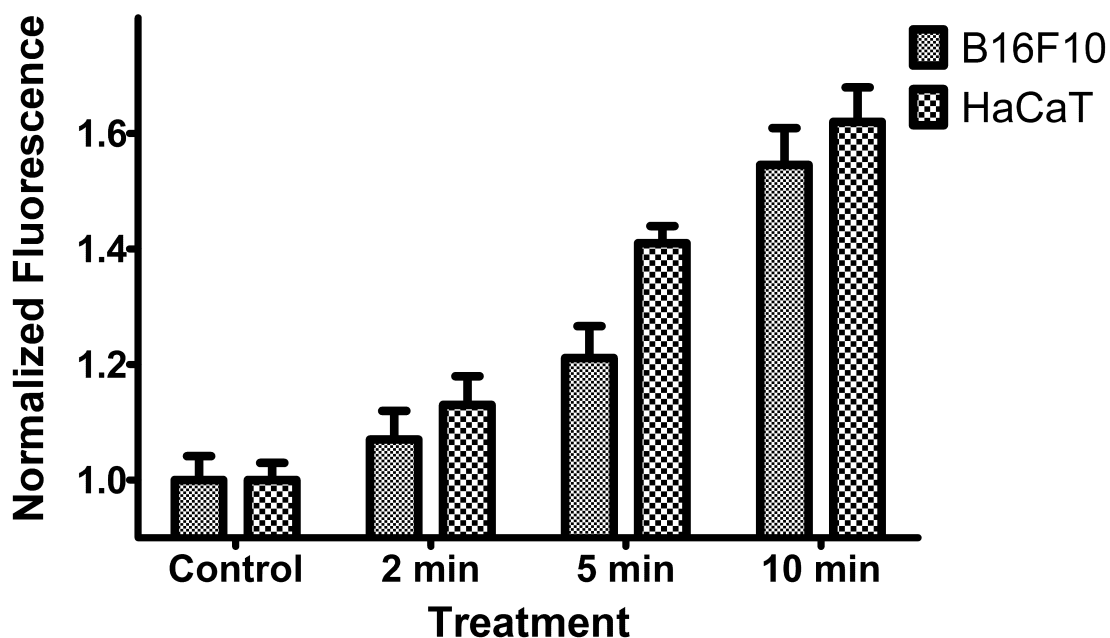
Figure 4.7: Fluorescence quotient of cells after plasma mediated delivery of the nonpermeant nucleic acid stain Sytox Green. Fluorescence values have been divided by their respective controls (F/F_0) to show a relative increase in delivery. Error bars indicate standard error of the mean.

4.2.4 Viability Impact

The next set of experiments ascertained the effect plasma treatment had on cell viability. In these experiments HaCaT and B16F10 suspensions were again exposed to the plasma plume for 2, 5 and 10 minutes. Immediately following treatment the cell suspensions were incubated at 37°C and 5% CO_2 for four hours. Trypan blue assays were then performed to determine cell survival following plasma exposure. Initial HaCaT cell viability was 96.5%, which decreased in the control sample to 92.7% after processing the cells for treatment and incubation. Cells from the treatment groups had a viability of 90.5% for 2 minutes of plasma exposure, 93.0% for 5 minutes and 90.8% for 10 minutes. B16F10 cells had an initial viability of 96.0%, which decreased to 90.2% in the control group four hours later. Treatment group viability was found to be 88.9% for 2 minutes, 87.9% for

56
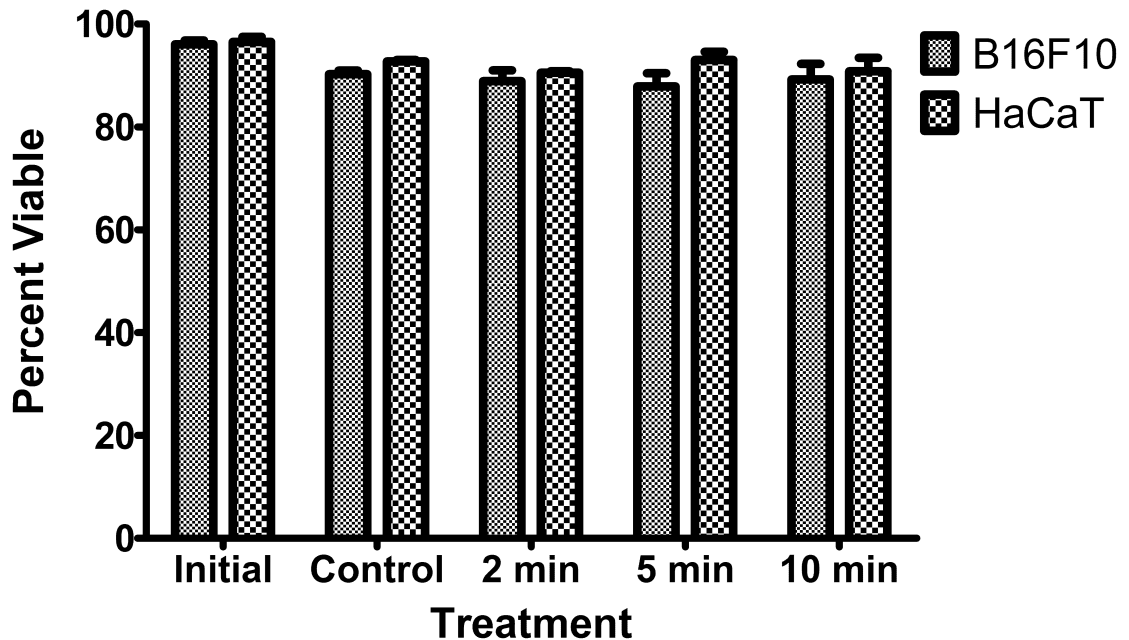
Figure 4.8: Effects of plasma exposure on cell viability 4 hours after treatment. Trypan blue assays were performed to quantify cell viability. Error bars indicate the standard error of the mean.

5 minutes and 89.2% for 10 minutes. Results are summarized in Figure 4.8. Analysis of these data conclude at the 95% confidence level that HaCaT and B16F10 cells exposed to ions generated at the tested conditions do not significantly alter cell viability.

4.2.5 Membrane Stabilization

A final set of experiments were performed to elucidate the duration of membrane defects in both B16F10 and HaCaT cells. These experiments exposed suspended cells to plasma for 10 minutes and followed the uptake of a nucleic acid probe by fluorescence measurements taken at one minute intervals. It was expected that membrane permeabilization would enable the uptake of molecules by the cells causing an increase in fluorescence. The rate of fluorescence increase should slow and eventually cease with time corresponding to cells re-
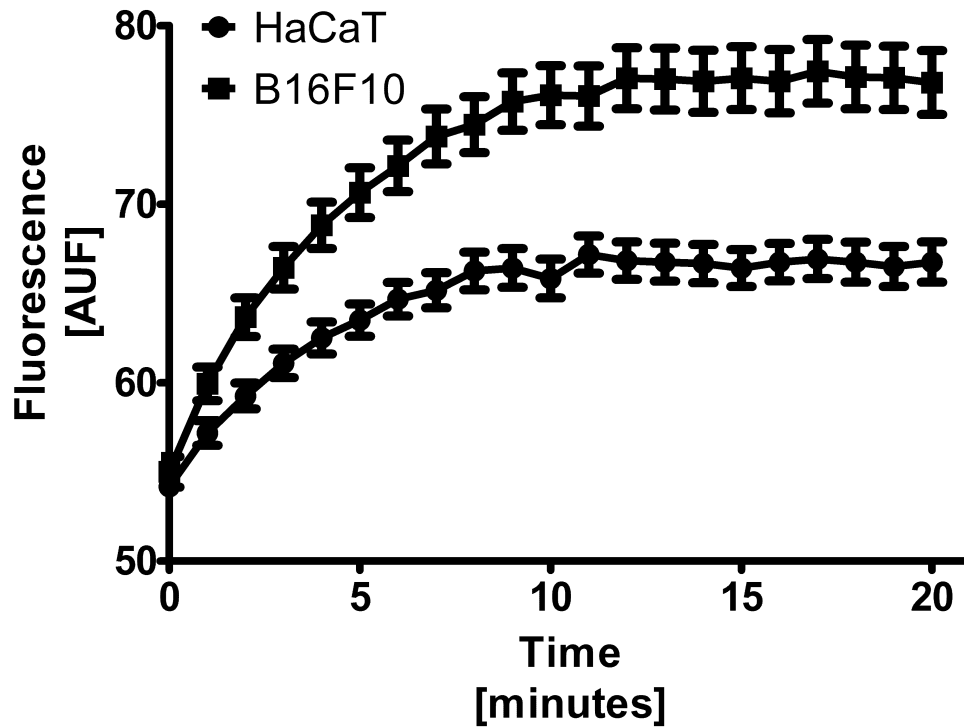
Figure 4.9: Kinetic fluorescence measurements of Sytox Green uptake following 10 minutes of plasma exposure. Mean fluorescence, in arbitrary units (AUF), are plotted at one minute intervals along with the standard error of the mean.

gaining their membrane integrity. Figure 4.9 below shows raw fluorescence measurements obtained over a 20 minute acquisition period for plasma treated B16F10 and HaCaT cells.

As expected, the rate of Sytox Green influx slowed with time in both cases and changes in the fluorescence levels became statistically insignificant at six minutes for B16F10 cells and five minutes for HaCaT cells. This observation was due to the permeability of the membrane decreasing with time. Differentiating the fluorescence, represented by the symbol F, with respect to time allowed the data to be curve fit to determine the rate constant associated with dye exclusion from the cell, which was then correlated to a re-stabilizing cell membrane. The integrated rate law for a first order reaction,

$$Y = Y_0 e^{-kt},$$ (4.1)

58

provided an excellent fit for the differentiated data. In this equation Y represents the change in fluorescence with respect to time, Y_0 is the initial change in fluorescence, k is the rate constant and t corresponds to time. The r-squared values for the fit of the experimental data were over 0.99 for both HaCaT and B16F10 cells. Figure 4.10 displays the differentiated fluorescence data (dF/dt) at each observation for B16F10 and HaCaT cells and its associated curve fit. The rate constant, k, found in the HaCaT fit of membrane restabilization was $0.28 \, \text{minutes}^{-1}$ and the constant for B16F10 membrane restabilization was $0.25 \, \text{minutes}^{-1}$. This shows that cells treated with ions to enhance molecular delivery respond similarly to cells that have been electroporated (Rols and Teissie 1990, Neumann et al. 1998).
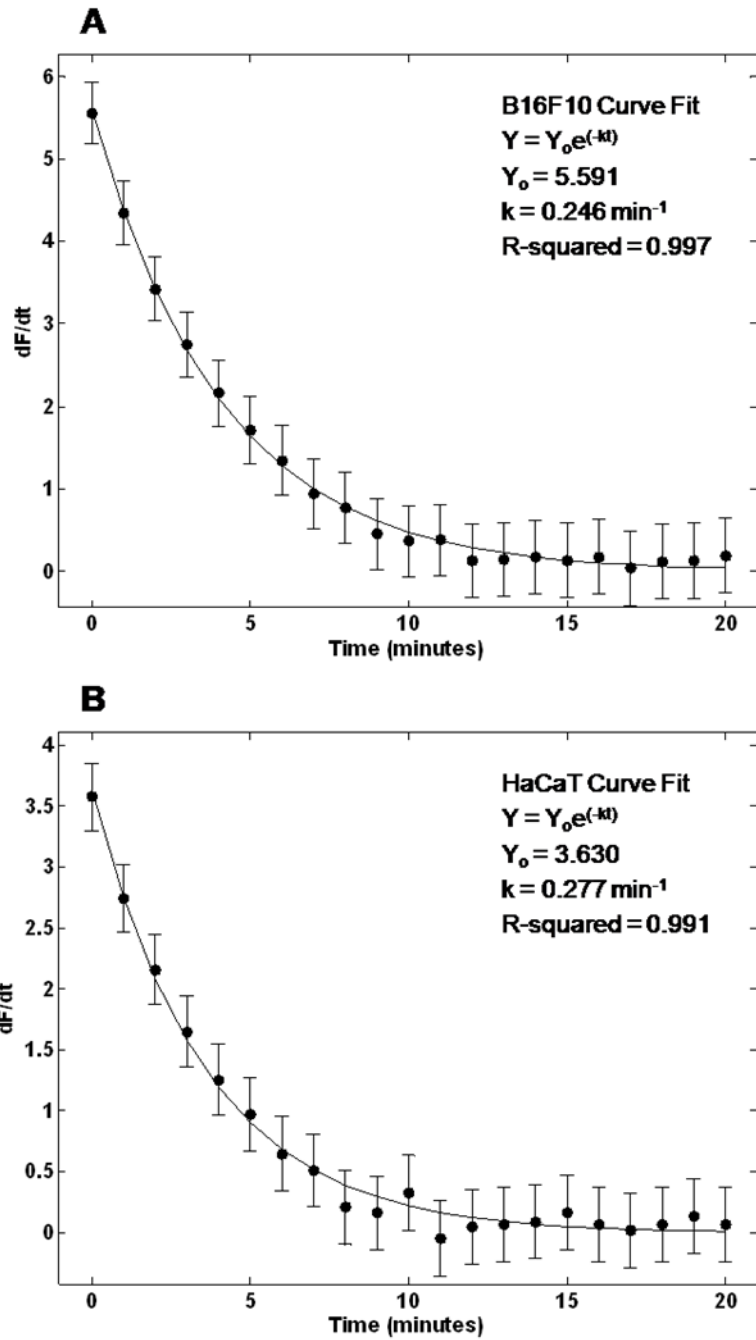
Figure 4.10: Fluorescence measurements differentiated with respect to time after 10 minutes of plasma exposure. These plots display differentiated data for (A) B16F10 and (B) HaCaT cells. Plotted markers indicate the mean and error bars show the standard error of the mean for the data collected. Curves show the fit for a first order kinetic equation.

4.2.6 Conclusions

The results obtained using the plasma discharge are encouraging with regard to plasma mediated molecular delivery. These experiments show a dose-response relationship between exposure time and the delivery of fluorescent tracer molecules, with significant delivery beginning in both HaCaT and B16F10 cells at 5 minutes. Maximum delivery of tracer molecules occurred at 10 minutes of plasma exposure and led to a rise in fluorescence of 62 and 55 percent for HaCaT and B16F10 cells respectively. At the tested plasma exposure levels delivery was attainable without harm to the short term cell viability.

Results from the kinetic experiments offer evidence that plasma exposure and electroporation effect cell membranes similarly. Treatment of cells with either of these modalities causes a temporary increase in the diffusion of exogenous molecules into the cytosol, which is a result of membrane destabilization. In both cases the recovery of membrane integrity and subsequent dye exclusion follows first order kinetics with similar rate constants (0.25 and $0.28 \, \text{min}^{-1}$) for the two cell lines tested. These data were consistent with literature on resealing times for electroporation (Rols and Teissie 1990, Neumann et al. 1998).

The results from these experiments show this non-contact charge-based delivery system is capable of improving the delivery of small molecules, such as cell tracers or drugs. This work provides evidence that ion deposition causes a transient increase in membrane permeability without the deleterious effects of other field driven modalities.

4.3 Delivery of Plasmid DNA to Murine Skin In Vivo

4.3.1 Introduction

After determining the atmospheric plasma delivery system was capable of creating transient membrane destabilization in vitro, the system was tested in vivo to determine the delivery capacity of larger molecules, such as DNA. Successful delivery of DNA in vivo would allow this tool to also be used for gene therapy and DNA vaccine applications. This investigation involved the injection of plasmid DNA encoding luciferase into the dermis of mouse flank skin. After injection the skin was exposed to the noncontact charge-based delivery system for 10 minutes. Expression levels were followed by injecting luciferin and quantifying luminescence over a period of 26 days.

4.3.2 Plasma Treatment

Plasma treatments were performed with an applied potential of +8 kV or -8 kV and a helium flow rate of 15l/min. A portion of the treatments were carried out with a $1.5 \text{G}\Omega$ ring encircling the treatment area. Figure 4.11 shows the relative positions of the plume, animal flank, and high impedance ring during plasma treatment. Operating at these conditions produced a visible glow discharge emanating from the annular electrode that was 3.0cm in length for positive polarity and 2.0cm in length for negative polarity. These distances were used to set the distance between the generator and skin during experiments. Temperature measurements made with an infrared thermometer during the treatments showed no deviation in normal skin temperature throughout plasma exposure.
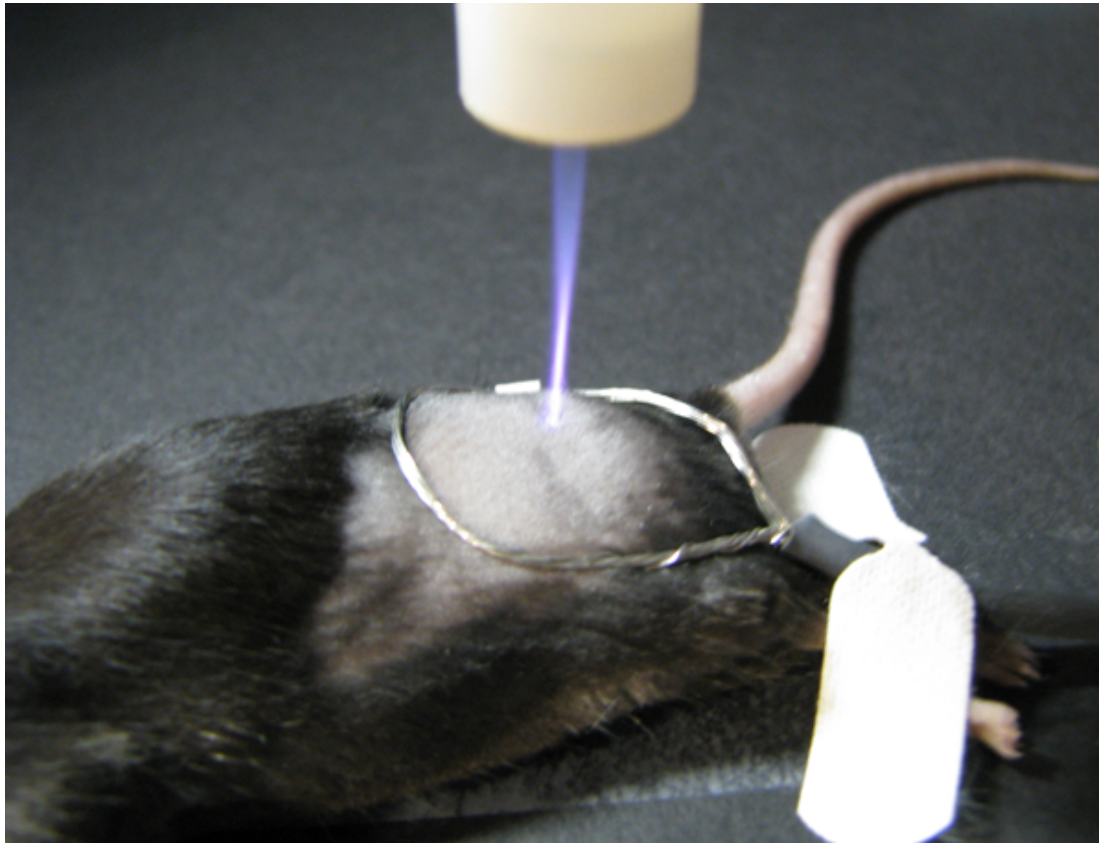
Figure 4.11: Positive polarity plasma treating a mouse flank with the high impedance ring encircling the treatment site.
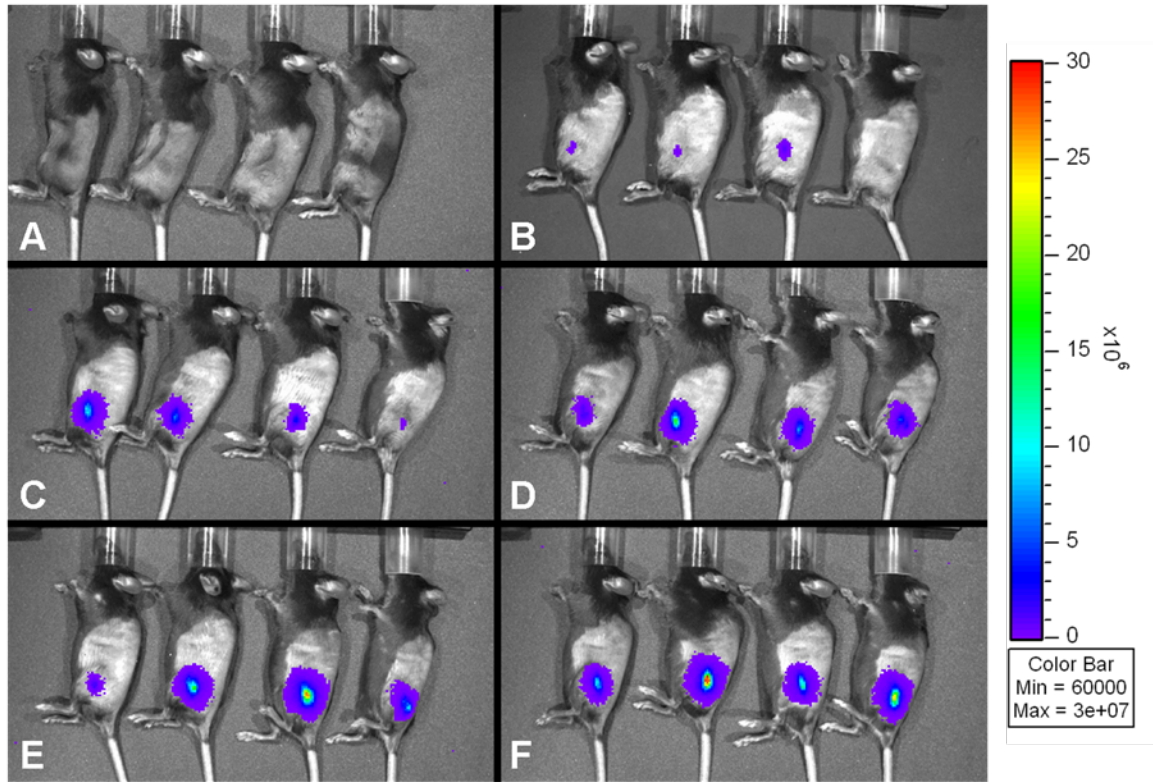
Figure 4.12: Representative Xenogen images demonstrating photon emissions per second acquired on day 2. These images show animals that received (A) no treatment, (B) injection of plasmid only, (C) plasmid with positive plasma treatment, (D) plasmid with positive plasma treatment and high impedance ring, (E) plasmid with negative plasma treatment, and (F) plasmid with negative plasma treatment and high impedance ring.

4.3.3 Molecular Delivery

Figure 4.12 shows Xenogen images of animals from each group two days after treatment. Images A and B in the figure are from animals that received no treatment and injection of plasmid encoding for luciferase, respectively. Note that some luminescence was observed with injection of the plasmid alone. This was anticipated as injection of DNA alone typically results in a low level of expression (Lucas et al. 2001). Image C is from day 2 in the follow up period and represents animals that received plasmid followed by positive plasma treatment for 10 minutes. Image D was taken on the same day from animals that received plasmid and positive plasma treatment with the high impedance ring. Similarly, images E and F were taken on day 2 of animals that received plasmid followed by negative plasma, E, and plasmid and negative plasma treatment that included the high impedance ring, F. Such images suggest that the four treatments involving exposure of the injection site to plasma appeared to have increased expression relative to animals that received only an injection of luciferase encoding plasmid and no subsequent plasma exposure. This increased expression, relative to controls, persisted throughout the 26 day follow-up period.

Mean quantitative luciferase levels for all groups treated with negative polarity plasma are shown in Figure 4.13 for the entire 26 day follow-up period. Similarly, Figure 4.14 shows this same mean data for animals treated with positive polarity plasma to deliver the luciferase encoding plasmid. Day 0 images were taken prior to any treatment, plasmid or plasma, and were used to determine background luminescence levels shown in each figure. For molecular delivery with both negative and positive plasma, maximum expression levels resulted on day 2 and remained nominally at this level until day 18 when luminescence began to decrease.

Mean luciferase level comparisons were made on day 2 relative to the response that resulted from the animals injected with the luciferase encoding plasmid only. These comparisons indicated a 3.8 fold increase (Figure 4.14) when positive plasma was used to treat the
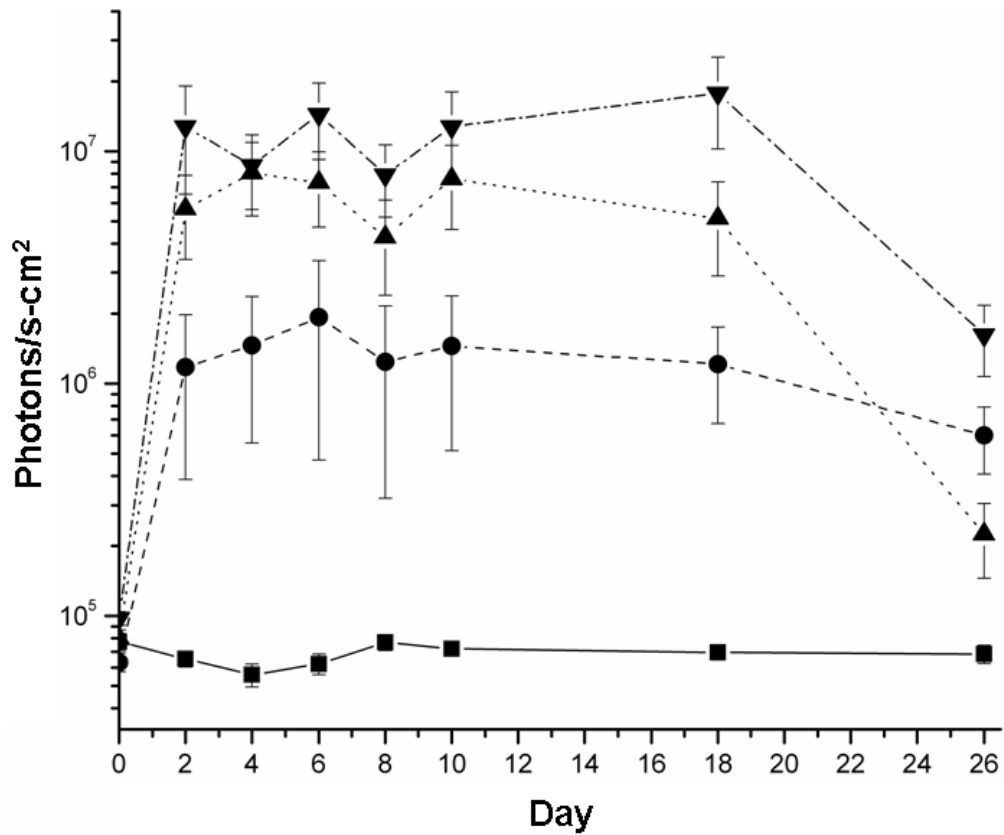
Figure 4.13: Luminescence data collected for all animals exposed to negative polarity plasma. Mean photon flux ($photons/s-cm^2$) and standard error of the mean are shown for animals that received (■) no treatment, (●) injection of plasmid only, (▲) plasmid with negative plasma treatment, and (▼) plasmid with negative plasma treatment and high impedance ring. Each of these groups consisted of 12 animals that were treated 4 at a time in 3 separate, but identical experiments.
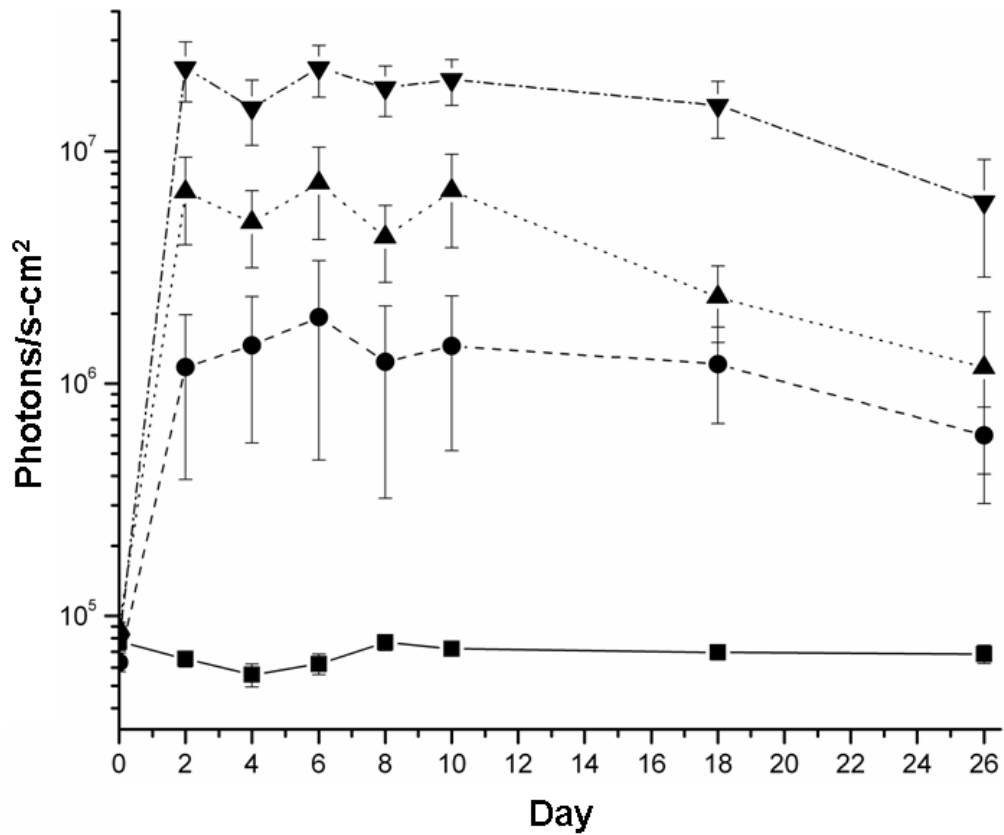
Figure 4.14: Luminescence data collected for all animals exposed to positive polarity plasma. Mean photon flux ($photons/s-cm^2$) and standard error of the mean are shown for animals that received (■) no treatment, (●) injection of plasmid only, (▲) plasmid with positive plasma treatment, and (▼) plasmid with positive plasma treatment and high impedance ring. Each of these groups consisted of 12 animals that were treated 4 at a time in 3 separate, but identical experiments.

plasmid injection site and a 4.5 fold increase when negative plasma (Figure 4.13) was used. These relative levels increased to 8.9 fold when positive plasma and the high impedance ring encircling the treatment site were used together (Figure 4.14). A 9.3 fold increase in response resulted from treating the plasmid injection site with negative plasma combined with a high impedance ring (Figure 4.13).

Statistical analysis was performed between groups using a two sided t-test with a confidence level of 95%. This analysis indicated that animals exposed to negative polarity plasma to facilitate plasmid delivery exhibited a statistically significant higher peak, day 2, expression compared to the plasmid injection only group. Subsequent data points for this treatment group showed statistically insignificant rises over the plasmid injection only control group. Animals treated with negative polarity plasma coupled with the high impedance ring for DNA delivery also showed a statistically significant rise over the plasmid injection only group on day 2; however, these data remained significantly different from the control thorough day 18. This treatment group also had significantly higher luciferase levels on days 2 through 18 when compared to the group that utilized the negative plasma alone.

Treatment with positive polarity plasma also resulted in significant increases in luciferase expression relative to the plasmid injection only group. Animals that were exposed to positive polarity plasma to deliver DNA resulted in significantly higher luciferase levels on days 2 and 4 compared to the injection only control group. Data on the other days from the positive polarity group were not different at a 5% level of significance when compared to control. Animals that had DNA delivered using positive polarity plasma with the high impedance ring showed statistically significant increases over the injection only group for days 2 through 18. Interestingly, luciferase photon flux data resulting from positive polarity delivered plasmid that incorporated the high impedance ring were not statistically different from the results obtained by using positive polarity plasma alone on any of the

Table 4.1: Summary data collected for animals exposed to plasma with and without the high impedance ring. The first data column represent the mean luminescence increase seen on day 2 when compared to control. The next column summarizes the period of time that each condition was found to be statistically significant when compared to control. Significance was established by performing a t-test with a 95% level of confidence.

Treatment	Luminescence Increase	Days of Significance
Positive Plasma	3.8 fold	4
Negative Plasma	4.5 fold	2
Positive Plasma with High Impedance Ring	8.9 fold	18
Negative Plasma with High Impedance Ring	9.3 fold	18

follow up days. This is in contrast to the significant difference that resulted when the mean luciferase level from the negative plasma with the high impedance ring group was compared to the negative plasma only group. This may speak to a difference in the influence of the ring on the net charge density in the region of the injected DNA when positive and negative polarities are used. Data collected from these experiments is summarized in Table 4.1.

4.3.4   Histological Analysis

Exposure of animal skin to plasma created with these generator conditions caused no apparent muscle contractions and no visible damage to the skin, such as burns, redness, swelling, or scaling both immediately after treatment or throughout the follow-up period. Figure 4.15 shows the treatment sites from animals exposed to either positive plasma or negative plasma immediately after treatment and at 24 hours.

Biopsies of the treatment sites confirm these gross observations. The tissue samples collected showed no damage occurring to the dermis or epidermis as a result of exposure. Further none of the characteristic hallmarks of inflammation, such as infiltration of leukocytes or changes in vascularity, were observed immediately after treatment or throughout the 21 day period samples were collected. Figure 4.16 shows representative skin sections collected.
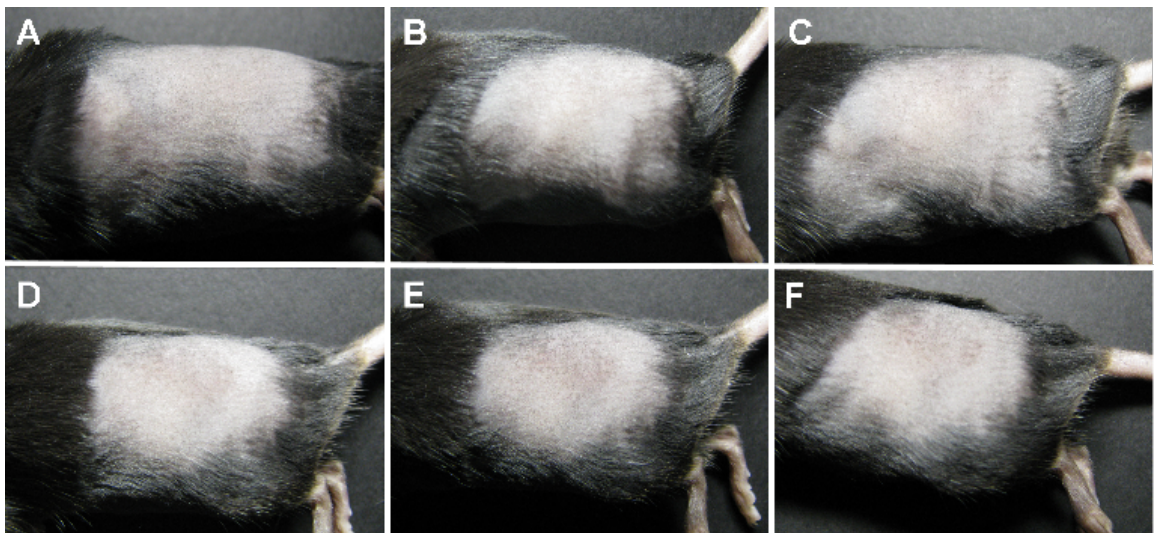
Figure 4.15: Photograph of plasma treatment sites on the flanks of C57Bl/6 mice. These images show animals (A) prior to treatment with positive polarity plasma, (B) immediately following treatment with positive plasma, (C) 24 h after treatment with positive plasma, (D) prior to treatment with negative plasma, (E) immediately after treatment with negative plasma, and (F) 24 h after treatment with negative plasma.
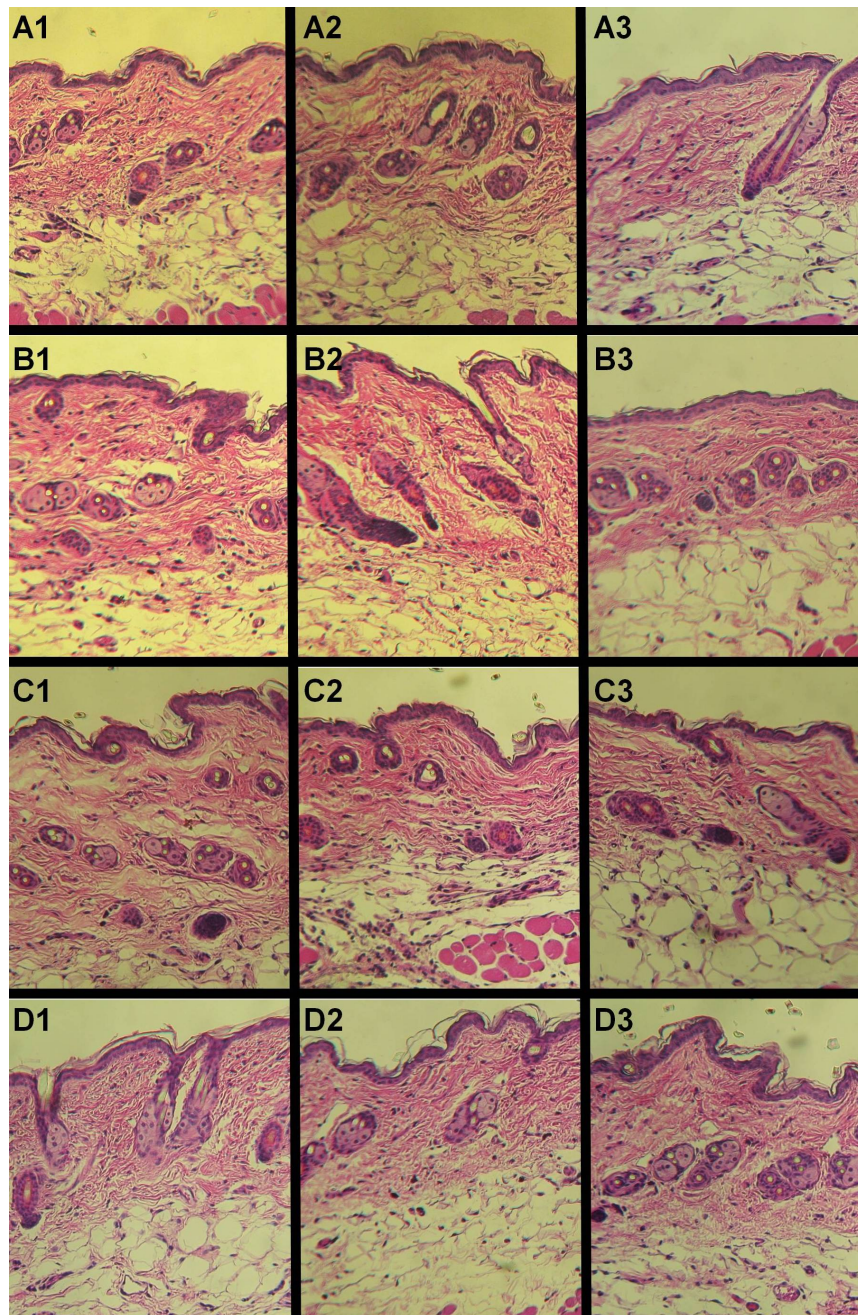
Figure 4.16: Plasma exposed skin sections stained with hematoxylin and eosin and photographed at 20x magnification. Images in row A are from the no treatment group, B are animals only injected with plasmid, C are animals injected with plasmid and exposed to positive plasma, and D are animals injected with plasmid and exposed to negative plasma. Samples in column 1 were collected immediately after treatment, 2 were two days after treatment, and 3 is seven days after treatment.

4.3.5 Conclusions

This study has clearly shown that the deposition of the downstream products of a direct current plasma glow discharge in helium can be used to facilitate the uptake of DNA by cells in murine skin. In contrast to other physical delivery methods available, this method does not appear to cause damage to the skin that often results from the intimate contact of an electrode or applicator with the treatment site which is especially true for electroporation (Mehier-Humbert and Guy 2005). This study demonstrated that non-thermal plasma can achieve significantly higher, as much as 9.3 fold, expression when compared to injection of plasmid DNA alone. Further, similar levels of expression were obtained with either positive or negative potential applied to the high voltage electrode.

One potential mechanism for this delivery method is that charge deposition by the plasma stream may lead to a local electric field in the skin and cause local charge exchange. This could result in a mechanism that is similar to electroporation in that it is generally accepted as a field driven process (Weaver and Chizmadzhev 1996). Additional work with this delivery technology focused on optimizing treatment conditions to determine if greater increases in expression could be obtained.

4.4 Optimization of Plasma Delivery In Vivo

4.4.1 Introduction

After having shown the efficacy of this plasma-based delivery system in vitro and in vivo a more rigorous set of experiments were performed to optimize delivery. These experiments were conducted with the second generation plasma generator, because of its ability to more accurately target the treatment site and provide electrical data concerning the performance of the system. The goal of these optimization experiments was to determine the plasmid dose and plasma exposure time that corresponded to the highest peak and longest duration expression. Due to the extremely large number of experimental variables these goals were addressed individually, where treatment time was first addressed and the results from these experiments were used to optimize the plasmid dose.

4.4.2 Plasma Characterization

Throughout these experiments only slight variations were observed by switching to the second generation system. Data collected from this system allowed monitoring of the electrical characteristics of the plasma generator, as well as electrical data concerning the treatment site. During the plasma treatments discussed in this section the system maintained an average voltage of $7.96\,\text{kV}$ for positive polarity treatments and $-7.92\,\text{kV}$ for negative. While operating at these voltages the high voltage electrode consumed an average current of $17.7\,\mu\text{A}$ for positive and $-15.7\,\mu\text{A}$ for negative polarity. The mean current observed returning to ground through the $1.5\,\text{G}\Omega$ resistor electrode encircling the treatment site was $3.7\,\mu\text{A}$ for positive polarity and $-3.3\,\mu\text{A}$ for negative. Applying Ohm's Law,

$$V = IR \tag{4.2}$$

73

Table 4.2: Electrical characteristics of the generator and return electrode during treatment. All reported vales represents the mean of data points gathered throughout each treatments.

	Positive Polarity	Negative Polarity
Generator Potential	7.96 kV	-7.92 kV
Generator Current	17.7 μA	-15.1 μA
Return Current	3.7 μA	-3.3 μA
Epidermal Potential	5.6 kV	-5.0 kV

where V is the voltage present on the high impedance ring, I is the current flowing through the ring to ground and R is the total resistance present on the ring, allows the voltage present on the ring to be calculated. Essentially this means the treatment site on the animal reaches a potential of $5.6\,$kV for positive treatment and $-5.0\,$kV for negative treatment. A summary of these findings is presented in Table 4.2.

4.4.3   Plasma Dose Response Study

The goal of the first set of delivery experiments was to determine the treatment time that generated the greatest overall plasmid expression. To perform these treatments $100\,\mu$g of luciferase expressing plasmid was injected intradermally in a volume of $50\,\mu$l. Following injection the sites were treated with either positive or negative polarity plasma for 2, 5, 10 or 20 minutes. Expression was followed by quantifying luminescence for 30 days after treatment.

Mean luciferase levels are shown for all groups treated with either polarity plasma in Figure 4.17. Data points expressed at day 0 represent luminescence values prior to treatment. In all groups peak expression occurred on day 2 and remained at the same relative level until day 21.

Mean luciferase level comparisons were made on day 2 relative to the response that resulted from injecting animals with the luciferase encoding plasmid only. Data collected from 2 minutes of plasma exposure revealed a rise of 12.9 fold when positive plasma was used
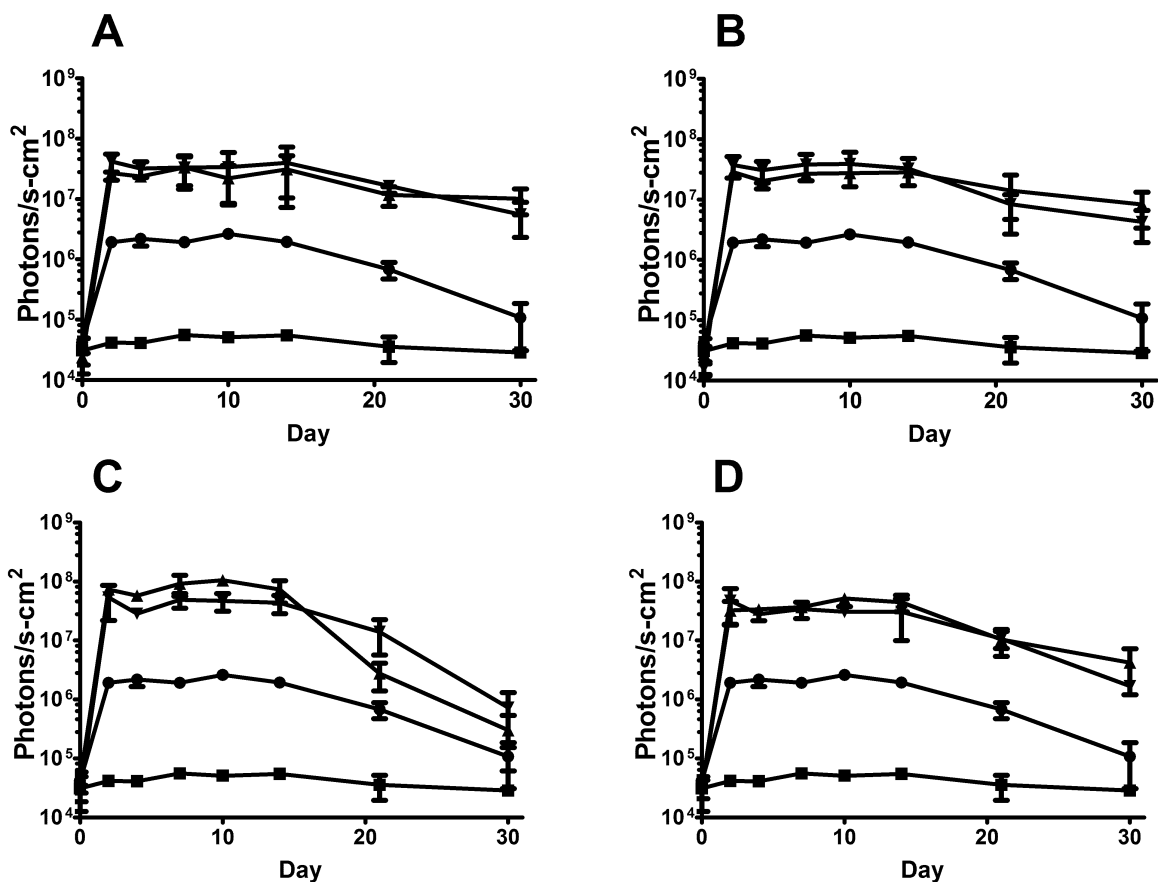
Figure 4.17: Luminescence data collected for animals that were exposed to various plasma treatment times. Mean photon flux ($photons/s-cm^2$) and standard error of the mean are shown for animals that received (■) no treatment, (●) injection of plasmid only, (▲) plasmid with positive plasma treatment, and (▼) plasmid with negative plasma treatment. Data represented in plot A corresponds animals exposed to plasma for 2 minutes, plot B corresponds to 5 minute exposures, plot C corresponds to 10 minute exposures and plot D corresponds to 20 minute exposures. Each of these groups consisted of 12 animals that were treated 4 at a time in 3 separate, but identical experiments.
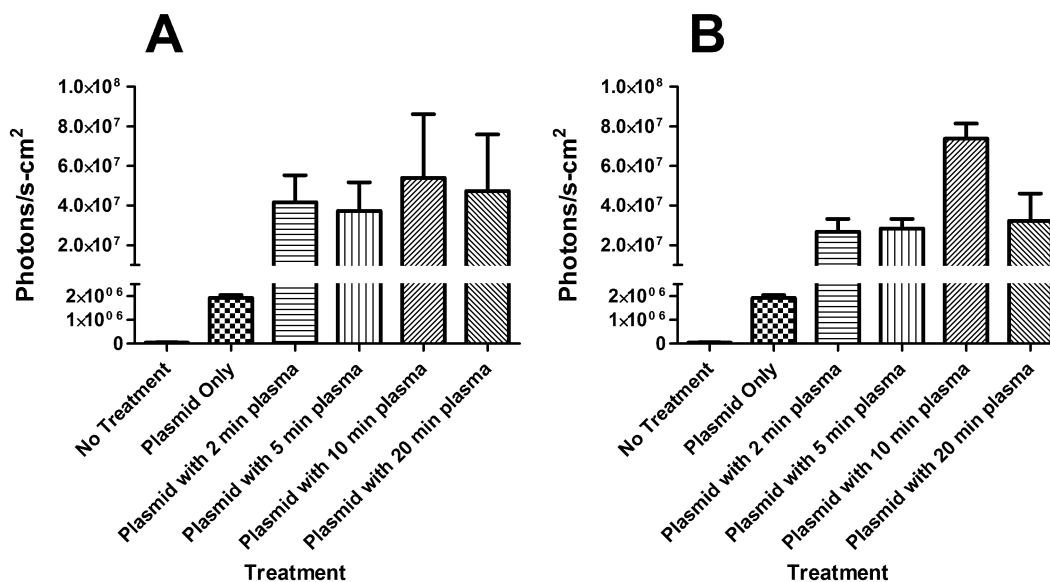
Figure 4.18: Peak luminescence for animals exposed to various plasma treatment times. Luminescence is represented by photon flux ($photons/s-cm^2$) observed on day 2 for animals exposed to either (A) negative or (B) positive polarity plasma. Error bars represent standard error of the mean. A break in the y-axis was provided to allow visualization of the plasmid only group.

to treat the injection site and 20.6 fold when negative plasma was used. Exposure for 5 minutes resulted in an increase of 13.8 fold for positive and 18.4 fold for negative polarity. Exposure for 10 minutes resulted in increases of 37.3 fold for positive and 27.1 fold for negative. Finally, 20 minutes of exposure increased expression by 16.7 fold and 24.5 fold for positive and negative polarity, respectively. Figure 4.18 shows the data collected on day 2 to formulate these comparison values.

Analysis of these data conclude at the 95% confidence level that significant rises exist in all groups exposed to the plasma discharge following plasmid injection when compared to plasmid injection alone. Additional data collected for the 2 minute exposure condition showed significantly higher expression for 7 of the 30 follow up days. Data from the 5 minute exposures showed significantly higher expression for 21 days. Animals exposed to 10 minutes of plasma retained significantly higher expression for 14 days. Finally animals

Table 4.3: Summary of findings for the examined plasma exposure conditions. The first two columns represent the mean increase seen on day 2 when compared to control for positive and negative plasma treatments. The next column summarizes the period of time that each plasma exposure condition was found to be statistically significant when compared to control. Significance was established by performing a t-test with a 95% level of confidence.

	Positive Plasma	Negative Plasma	Period of Significance
2 minutes	12.9 fold	20.6 fold	7 days
5 minutes	13.8 fold	18.4 fold	21 days
10 minutes	37.3 fold	27.1 fold	14 days
20 minutes	16.7 fold	24.5 fold	21 days

exposed to 20 minutes of plasma following injection retained higher expression for 21 days. Table 4.3 summarizes the findings of this section.

4.4.4 Plasmid Dose Response

The goal of the second set of delivery experiments was to determine if a dose-response relationship could be established between the plasmid dose and the amount of expression generated with the most effective plasma treatment time. Performing these experiments involved intradermally injecting either 50, 100 or $200\,\mu$g of plasmid DNA, suspended in $50\,\mu$l of saline, and treating the bolus with the optimum plasma treatment time from the first set of experiments. As a basis for comparison electroporation was performed with the same plasmid doses using a four plate electrode. The electroporation signature selected imparted 8 pulses at a field strength of $100\,\mathrm{V/cm}$ with a duration of $150\,\mathrm{ms}$ each; this pulsing condition was selected as it had already been optimized for this electrode with a similar plasmid construct (Heller et al. 2007).

Mean luminescence values are shown for all groups treated in Figure 4.19. Data points shown at day 0 represent luminescence values prior to performing treatments. As in the first experiments, all groups exhibited their peak expression on day 2.

Figure 4.19: Luminescence data collected for animals injected with various concentrations of plasmid and treated with 10 minutes of plasma. Mean photon flux ($\mathrm{photons/s-cm^2}$) and standard error of the mean are shown for animals that received (■) no treatment, (●) injection of plasmid only, (▲) plasmid with positive plasma treatment, (▼) plasmid with negative plasma treatment and (◆) plasmid with electroporation. Data represented in plot A corresponds animals that received 50 μg of plasmid, plot B corresponds to 100 μg injections and plot C corresponds to 200 μg injections. Each of these groups consisted of 12 animals that were treated 4 at a time in 3 separate, but identical experiments.

Mean luminescence levels were compared on day 2 relative to those animals receiving injection of luciferase encoding plasmid only. Data collected from animals injected with 50 μg of plasmid and treated with positive plasma had an increase of 16.4 fold, negative plasma increased luminescence by 19.4 fold, and electroporation increased luminescence by 25.5 fold. Animals injected with 100 μg of plasmid and treated with positive plasma had an increase of 38.4 fold, negative plasma increased luminescence by 27.6 fold, and electroporation increased luminescence by 42.3 fold. Finally, animals injected with 200 μg of plasmid and treated with positive plasma had an increase of 32.0 fold, negative plasma increased luminescence by 19.1 fold, and electroporation increased luminescence by 66.5 fold. Figure 4.20 shows the data collected on day 2 to formulate these comparison values.
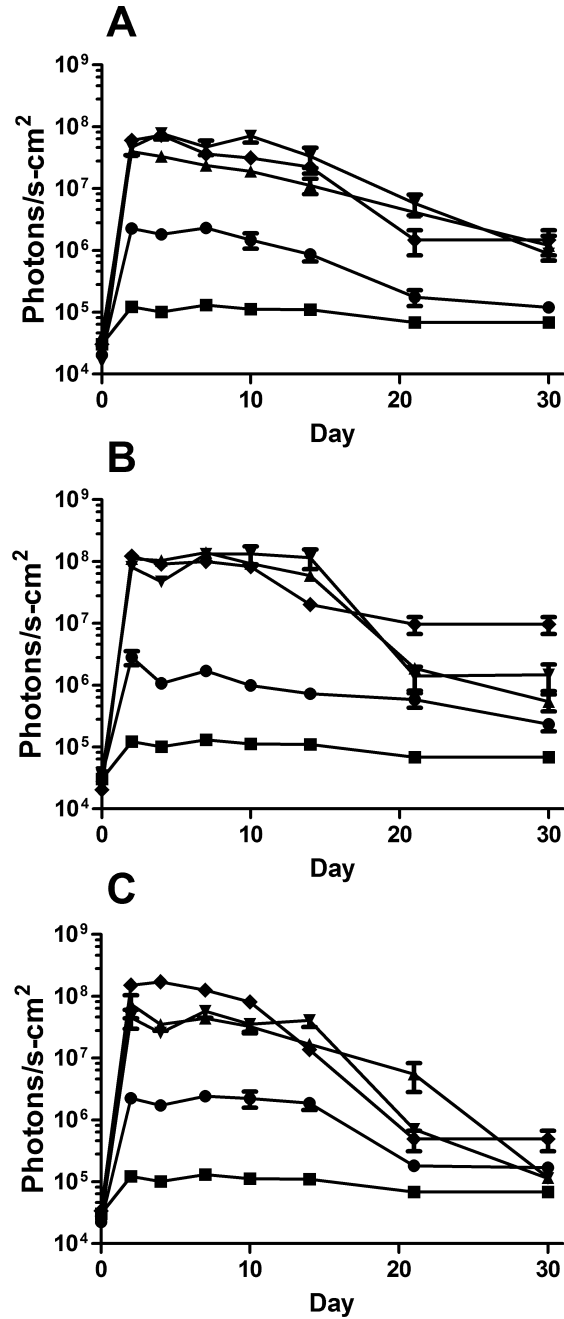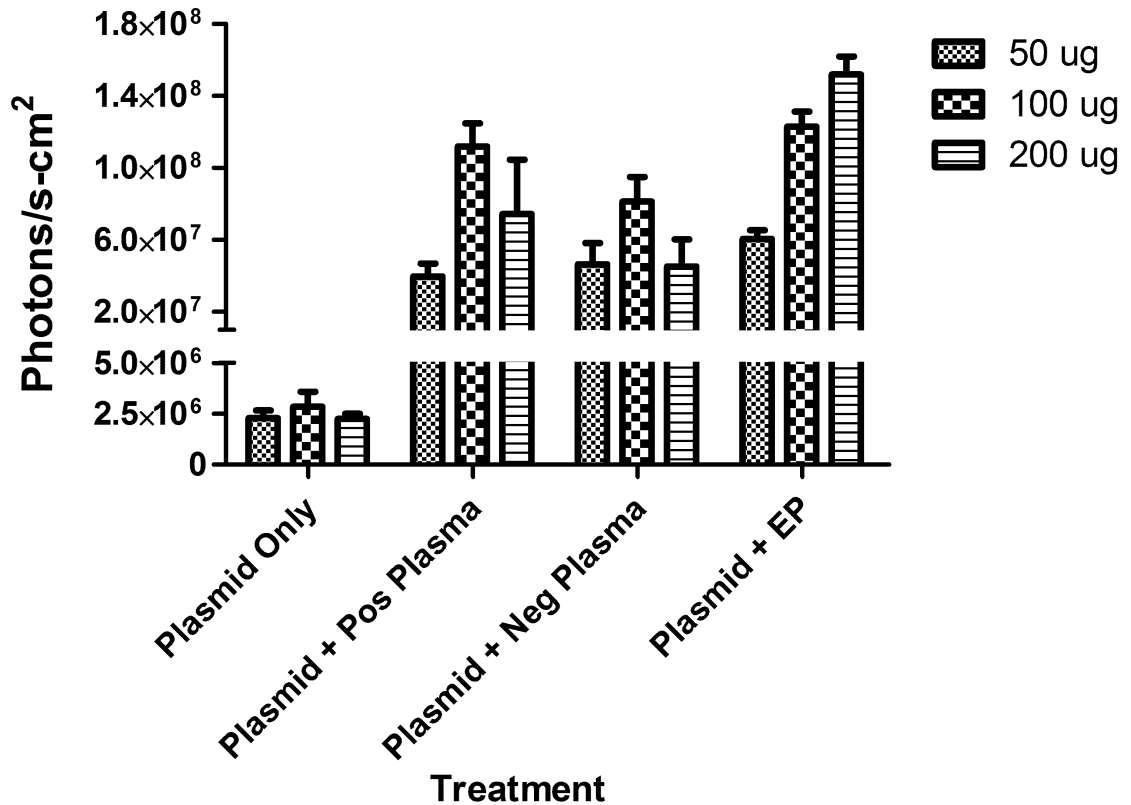
Figure 4.20: Peak luminescence for animals injected with various concentrations of plasmid and treated with 10 minutes of plasma. Luminescence is represented by photon flux ($photons/s-cm^2$) observed on day 2 for animals injected with 50 μg, 100 μg or 200 μg of plasmid prior to exposure to positive plasma, negative plasma or electroporation. Error bars represent standard error of the mean

Analysis of these data at the 95% confidence level showed significant rises over injection alone for each of the treatments carried out following the administration of the plasmid. Additionally, data collected for the $50\,\mu g$ plasmid dose showed significantly higher expression in the plasma treated and electroporated groups for all 30 of the follow-up days. In this group no statistical difference was present between those treated with positive plasma, negative plasma or electroporation. Data collected for the $100\,\mu g$ plasmid dose showed significantly higher expression in the plasma treated groups for 14 days and all 30 days retained statistical significance for electroporation treated groups. At this level no statis-

Table 4.4: Summary of findings for the various injected plasmid amounts. Each column represents the amount of increase observed on day 2 for the specified group compared to the group that received plasmid injection only.

	Positive Plasma	Negative Plasma	Electroporation
50 μg	16.4 fold	19.4 fold	25.5 fold
100 μg	38.4 fold	27.6 fold	42.3 fold
200 μg	32.0 fold	19.1 fold	66.5 fold

tical differences were present between those treated with positive plasma, negative plasma or electroporation for 14 days. However, on days 21 and 30 the animals treated with electroporation had significantly higher means than animals treated with the plasma discharge. Data collected from the highest dose, $200\,\mu\mathrm{g}$, showed significantly higher expression in the plasma treated and electroporated groups for 14 days compared to injection alone. This dose level showed no statistical differences between those treated with positive plasma, negative plasma or electroporation. Table 4.4 summarizes the relative increases seen for each plasmid dose.

4.4.5 Conclusions

This study has shown the second generation technology is also capable of augmenting molecular delivery, and appears to do so in a dose-response fashion. The results obtained by increasing the exposure time indicated as treatment times rise, so too does the luminescence. The first set of experiments show the maximum luminescence occurs with 10 minutes of plasma exposure. Exposing the previously injected flank skin for this amount of time correlated with a rise of 37.3 fold for positive plasma and 27.1 fold for negative plasma, when compared to animals that had only been injected with plasmid. Exposing the tissue beyond 10 minutes does not appear to increase expression, as animals exposed to 20 minutes of plasma had a decrease in luminescence compared to those exposed for 10 minutes. This decrease is likely due to cells dying due to the extended presence of membrane defects.

Proceeding with the optimum 10 minute treatment time from the first set of experiments, the effects of modulating the DNA dose also gave some surprising results. As the dose was escalated from 50 to $100\,\mu g$ a statistically significant increase in luminescence was seen in all groups. However, as the dose was raised from 100 to $200\,\mu g$ the effects became insignificant in the plasma treatment groups. This allowed an optimum DNA dose to be determined, with this system. This $100\,\mu g$ dose coupled with 10 minutes of plasma exposure gave similar results to those found with electroporation.

4.5 Delivery of a DNA Vaccine In Vivo

4.5.1 Introduction

After establishing the delivery capacity of the plasma discharge with luciferase encoding plasmids, the focus of the work shifted to a more biologically relevant protein. In this work, a plasmid was delivered encoding the 120 kilodalton envelope glycoprotein present on the surface of a macrophage tropic HIV. Delivery of the plasmid should invoke an immune response proportional to the extent of delivery. In this study immune responses were ascertained by antibody levels in the serum of mice. Antibody responses obtained by this technique provided the basis for an alternative delivery method for DNA vaccines.

4.5.2 Results

The major goal of this study was to determine if plasma could be used to deliver a DNA vaccine to enhance the induction of antigen specific antibody responses. To perform this vaccination study the JRFLgp120 plasmid was selected due its relatively low immunogenicity when delivered without a forcing function, such as electroporation. Weak immune responses produced by the plasmid only vaccination group allowed the antibody levels caused by the application of plasma to be more easily ascertained. To perform this study $100\,\mu$g of JRFLgp120 plasmid was injected intradermally in a volume of $50\,\mu$l. Following injection the bolus was exposed to positive or negative polarity plasma for 10 minutes, as these conditions generated the greatest luminesence levels in the luciferase work. For comparison other groups were only injected with the plasmid and some were injected and electroporated. Those animals that received electroporation were treated with a four plate electrode that applied a pulsing sequence of 8 rectangular waves at a field strength of $100\,\mathrm{V/cm}$ with a $150\,\mathrm{ms}$ duration. A total of four vaccinations were performed on days 0, 14, 28 and 130.

Figure 4.21: Ratio of optical densities after the third vaccination with $100\,\mu$g JRFLgp120 plasmid. Plots show data from animals that received (A) injection only, (B) injection followed by electroporation, (C) injection followed by 10 minutes of negative plasma and (D) injection followed by 10 minutes of positive plasma. Error bars indication the standard error of the mean.

The data presented in Figure 4.21 was generated from sera samples collected from the different vaccination groups on day 38. This day corresponded to 10 days after the third DNA vaccine was administered. Antigen specific antibody responses from the first two immunizations failed to produce significant antibody responses in any of the treatment groups, when compared to sera collected from naive animals.

These data show the optical density values observed at serial dilutions ranging from 1:64 down to 1:8192. As expected the optical densities tail off by diluting the samples, which

causes a reduction in the number of antibodies available to bind to the gp120 antigen on the ELISA plate. Statistically comparing the data collected at each dilution factor with that of naive animals yields the maximum dilution factor where significant binding is observed, known as the titer. Data collected after three vaccinations with JRFLgp120 showed a titer of 512 for animals that received plasmid only, 512 for plasmid with electroporation, 512 for plasmid with negative plasma and 4096 for plasmid with positive plasma.

Performing another vaccination boosted the responses observed in all groups. The results from the fourth vaccine are summarized in Figure 4.22. Data collected after the fourth vaccine administration with JRFLgp120 gave a titer of 4096 for animals that received plasmid only, 4096 for plasmid with electroporation, 4096 for plasmid with negative plasma and 8192 for plasmid with positive plasma.

Figure 4.23 shows the anti-gp120 geometric mean antibody titers (GMT) for the different vaccination groups after the final vaccination. The GMT values for the plasmid alone, plasmid with electroporation, plasmid with negative plasma and plasmid with positive plasma were 76, 181, 256 and 3444 respectively. A non-parametric Kruskal-Wallis analysis at the 95% confidence level between the different groups indicated the plasmid injection with positive plasma delivery group was significantly higher than the other groups. Also, further analysis indicated that the GMTs of the plasmid alone and plasmid with electroporation were not significantly different. Whereas, plasmid with negative plasma was marginally significantly elevated compared to plasmid injection alone. These results indicate that positive plasma, based on GMT values, was 45 and 19 fold more effective in inducing antigen specific antibodies than the plasmid alone and plasmid with electroporation groups, respectively. This initial study indicated positive plasma was more effective in enhancing induction of humoral immune responses than electroporation, under the electric pulsing conditions utilized in this study.
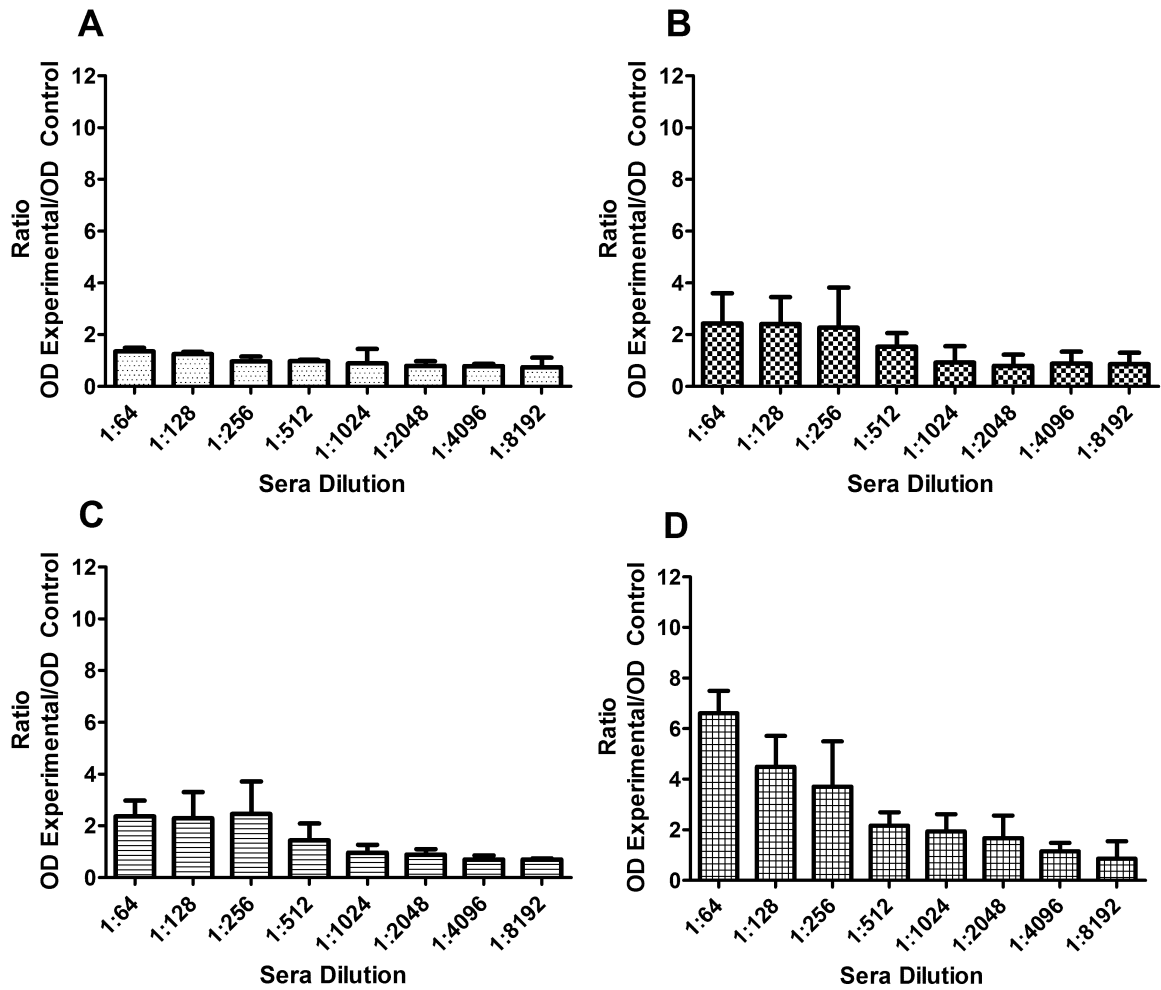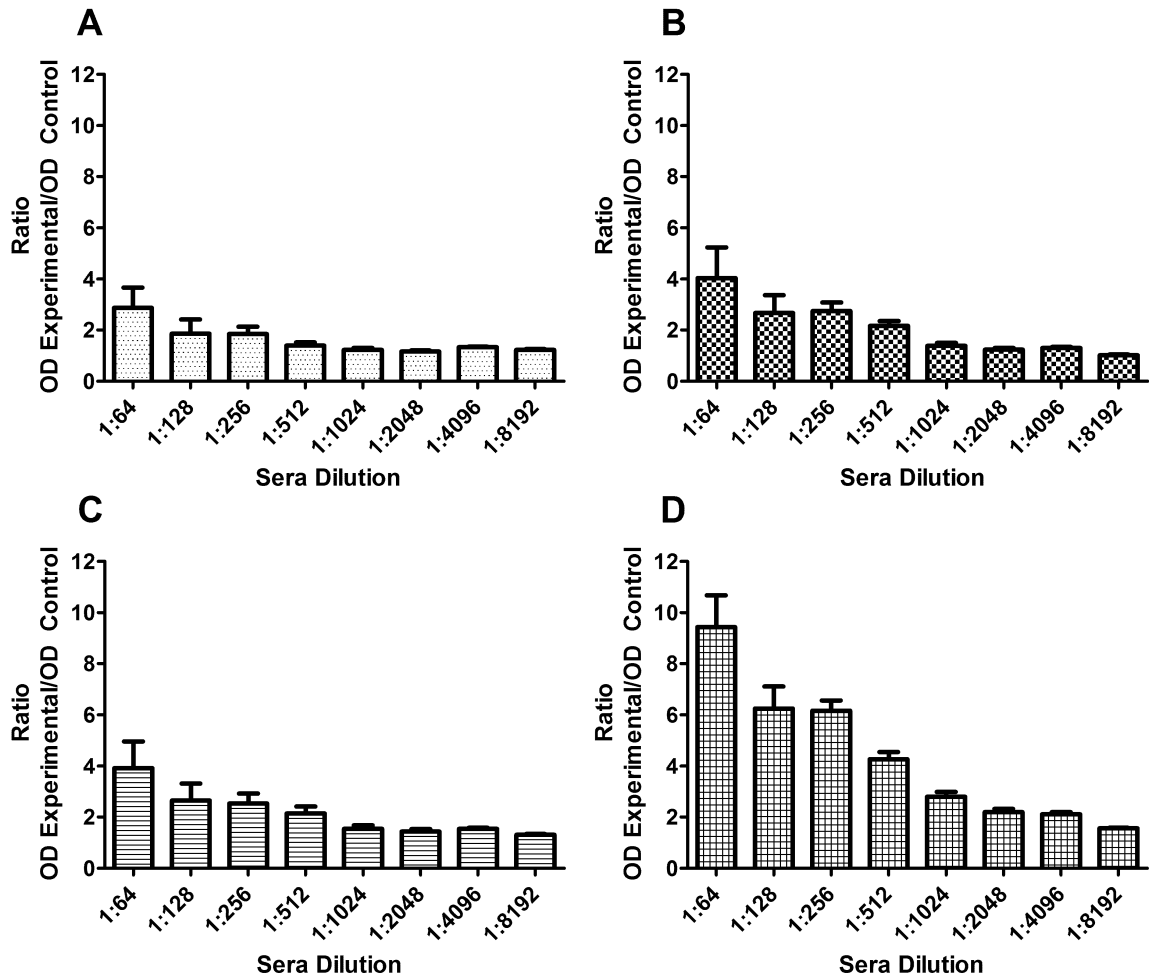
Figure 4.22: Ratio of optical densities after the fourth vaccination with $100\,\mu\mathrm{g}$ JRFLgp120 plasmid. Plots show data from animals that received (A) injection only, (B) injection followed by electroporation, (C) injection followed by 10 minutes of negative plasma and (D) injection followed by 10 minutes of positive plasma. Error bars indication the standard error of the mean.
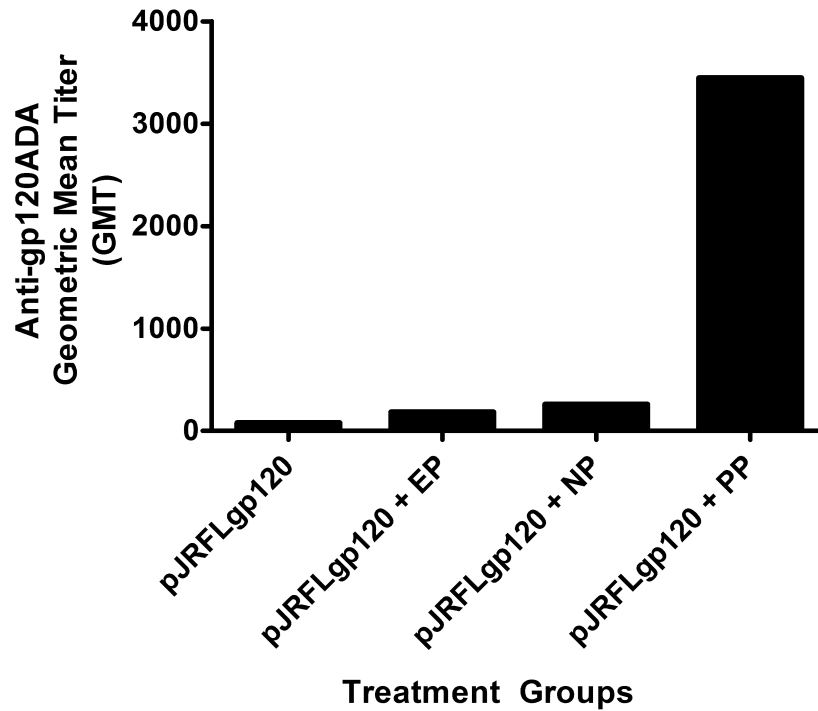
Figure 4.23: Comparison of the antigen specific geometric mean antibody titers among the different vaccination groups following administration of the final vaccine. The treatment conditions shown are: P Only = gp120 plasmid alone; P + PP = gp120 plasmid with positive plasma delivery; P + NP = gp120 plasmid with negative plasma delivery; and P + EP = gp120 plasmid with electroporation delivery. The asterisk indicates statistically elevated GMT values compared to the other groups at the 5% level.

4.5.3 Conclusions

Enhancement of delivery and subsequent expression of plasmid DNA encoding for antigens is thought to be important for the utility and success of plasmid vaccine strategies. A number of methods to enhance delivery have been implemented. Recently, the use of in vivo electroporation has become a popular modality for enhancing the efficacy of DNA vaccines. It has met with some success in enhancing both humoral and cellular immune responses of antigen presenting DNA vaccines (Hirao et al. 2008, Hirao et al. 2010). However, effective non-contact delivery methods may be more useful in terms of clinical utility due to the elimination or attenuation of some of the side effects noted with a contact dependent approach which can include momentary shock and pain. This experiment demonstrates a positive polarity plasma was able to significantly enhance the ability of a gp120 expressing plasmid DNA to induce antigen specific humoral immune responses, relative to the administration of the gp120 expressing plasmid alone. Also, the data indicate that the positive plasma delivery method was more effective than electroporation, under the conditions utilized, in enhancing immunogenicity and presumably expression of antigen by the DNA vaccine.

The results of the study warrant further investigation of the mechanism of enhanced immune responses by this delivery method. As well, it will be useful to determine the ability of this method to enhance antigen specific cellular immune responses. In particular, it will be interesting to determine the reason for the lack of enhancement of immune responses mediated by negative plasma delivery. This is particularly important in light of previous results indicating positive and negative plasma have an equivalent ability to enhance the expression of a luciferase reporter gene. Also, it will be important to determine whether shorter intervals of plasma exposure will be able to mediate the immune response enhancing effect of the 10 minutes exposure. This will be relevant to establish since it is desirable, in terms of potential clinical applicability.

4.6 Transdermal Electric Field Simulation

4.6.1 Introduction

In an attempt to elucidate a plausible mechanism causing the delivery of plasmid DNA in vivo a model was generated. The goal of this model was to analyze the transdermal electric field resulting from the deposition of charge on the epidermal surface of mouse flank skin. Finding an electric field magnitude similar to those encountered with electroporation would supply evidence that these two techniques operate by similar fundamental principles.

To create this model a geometry was first constructed in a finite element software package. The created model contained a two dimensional slice of an animal on top of an electrically insulated heating pad, which sat on an electrically grounded stainless steel operating table. After constructing the model experimentally measured electrical potentials were fit to an equation and placed as a boundary condition on the epidermal surface of the mouse's skin. In this model the operating table served as the reference ground in the system. The resulting electric fields were calculated by Laplace's equation.

4.6.2 Surface Potentials

Prior to creating a model, steady state surface potentials were evaluated on mouse skin during normal plasma treatment. Measurements made at 5 mm intervals yielded the result in Figure 4.24. These data points were fit with an exponential equation,

$$V = A \exp(-Bx) + C, \tag{4.3}$$

which provided the voltage, V, at any distance from the treatment site, x. Evaluating the fitting variables for positive plasma gave values of 5.936 for A, 36.160 for B and -0.145

for *C* and correlated to an r-squared value of 0.985. Fitting the negative plasma potentials yielded a value of -5.583 for *A*, 46.7 for *B* and 0.259 for *C*, which correlated to an r-squared of 0.983.

4.6.3   Resulting Electric Field

Supplying these equations as boundary conditions in the models allowed electric fields to be obtained in the finite element model. As would be expected the model showed the greatest field strength occurs in the skin below the treatment site. At this point 7300 V/cm was present for positive polarity plasma and 8000 V/cm for negative plasma. Figure 4.25 shows the typical results obtained with this electrostatic model for the case of positive polarity plasma.

4.6.4   Conclusions

The results yielded by this model indicate the presence of a high magnitude electric field across the skin. Field strengths of 7300 V/cm for positive polarity plasma and 8000 V/cm for negative plasma are consistent with those found in the literature to induce the phenomena called electroporation. A major difference in these two techniques is the duration of exposure to the field. One factor accounting for this differential is the time required for deposited charges to accumulate over the entire epidermal surface of the animal being treated with the discharge. Which is unlike electroporation where a pair of electrodes in direct contact with the tissue generate an electric field by the application of high energy pulses. Another major difference in these techniques is the passage of current through the treatment site that occurs with electroporation, which does not occur with plasma exposure. The presence of strong ionic currents in the tissue likely enhances the delivery process, making it occur at much faster rates. However, this results in transient pain and damage to the treatment site.
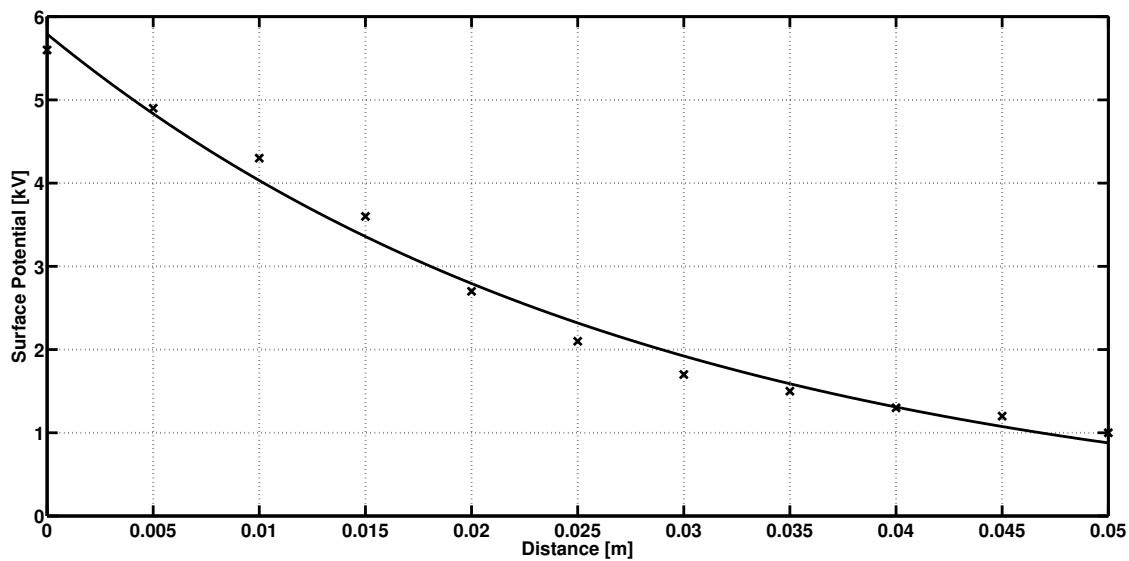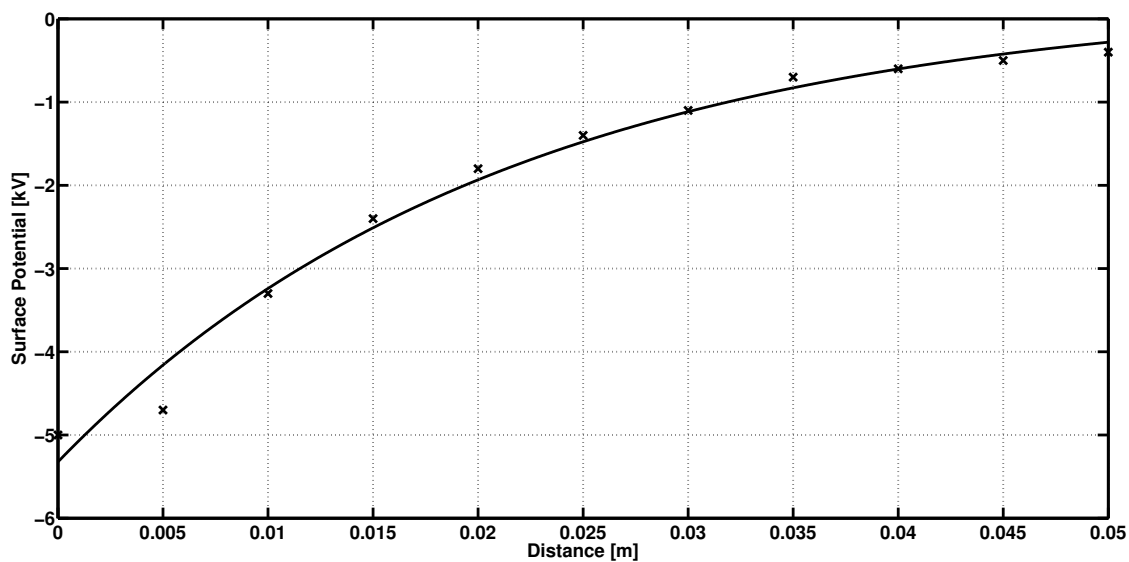
Figure 4.24: Potential data collected on the epidermal surface of animals treated with (a) positive and (b) negative plasma. Graphs display experimental data points (x) and exponential curve fits.
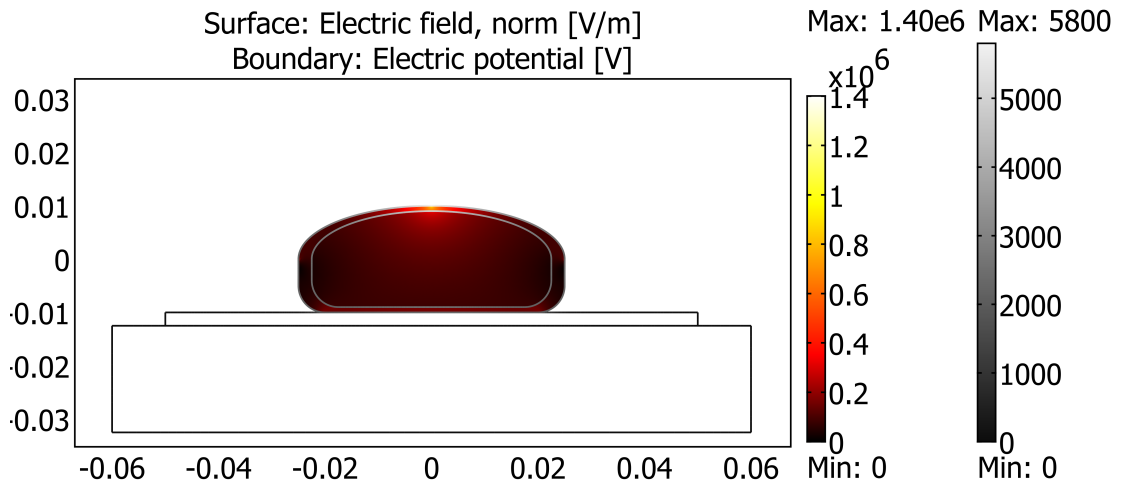
Figure 4.25: Electrostatic model showing the cross section of a mouse during treatment with positive polarity plasma. Electric field intensities are represented by the thermal scale and electric potentials on the boundaries are represented by the black and white scale. All subdomains other than the mouse were suppressed.

Field strengths of these magnitudes are also likely to cause electro-kinetic diffusion of the injected DNA in the tissue. This phenomena occurs due to the net negative charge carried by DNA and the presence of an electric field across the tissue. In the case of positive plasma exposure DNA should move in the direction of the more positively charged epidermis, which would result in expression of plasmid DNA in the papillary dermis and possibly the basal cells of the epidermis. Conversely, exposure to negative plasma should cause a migration of DNA deeper into the tissue, resulting in expression in the reticular dermis and hypodermis. The location of DNA being expressed would change the nature of the response in the skin.

To determine the effects plasma exposure has on skin it will be necessary to develop a more detailed model. The presented model offers a simplistic representation of the skin. Separating these layers will require electrically characterizing each individual layer and rebuilding the model to reflect the permittivity and resistance associated with each layer.

CHAPTER V: DISCUSSION AND FUTURE DIRECTIONS

5.1   Discussion

Current research has shown great potential for DNA-based drugs in the future of medicine. A significant drawback to these therapies and vaccines is their reliance on the concomitant application of a forcing function to aid in the uptake of exogenous DNA molecules. Of the physical methods employed to augment delivery, electric fields are the most developed and clinically relevant. While electric field application is an efficient way to produce thera- peutic protein levels, current contact dependent methodologies generate tissue damage and transient pain. An alternative means of applying these fields is through the deposition of charge from an ionized gas source.

The source developed for these experiments relies on a static electric field to impart energy to gas molecules. In this system helium gas is exposed to the greatest electric field strength as it flows out of the generator. A transfer of energy caused by collisions between ambi- ent charged molecules and helium gas creates a 1s2p–1s3s transition in helium. Energy transfer from further collisions in the gas phase and photon emissions from helium causes excitement of species present in the ambient air, which creates spectroscopic emissions for O, OH, N_2 and N_2^+. While the majority of these emissions occur in the ultraviolet range, the total irradiance for negative polarity is $28\,\mu\mathrm{W/cm^2}$ and positive polarity $30\,\mu\mathrm{W/cm^2}$. This level of irradiance is comparable to that generated by fluorescent lighting.

All treatments performed with this generator utilized a potential of about $8\,\mathrm{kV}$, irrespec- tive of the polarity, on the high voltage electrode. Operating at this potential consumed on

the order of $10\,\mu A$, so the generator operated at approximately $80\,mW$. When operating at these parameters a stable afterglow $2\,cm$ in length was measured for negative polarity and $3\,cm$ for positive polarity. Temperature measurements made in the gas volume and on treated surfaces showed no variation due to exposure to the discharge. It can be inferred from these measurements that only a small fraction of the gas is being excited by the generator; therefore, a non local thermal equilibrium discharge is created.

Exposure of the discharge to cells in vitro was successful in proving a capacity for mediating molecular delivery of small molecules existed. It was also apparent that a dose-response relationship existed between exposure to plasma and rise in fluorescence. Maximum delivery of tracer molecules was attained at 10 minutes of plasma exposure and led to a fluorescence increase of 62 and 55 percent for HaCaT and B16F10 cells respectively. These results were achieved without adversely affecting short term cell viability.

Kinetic experiments performed in vitro offered some evidence that plasma exposure and electroporation affect cell membranes similarly. Treatment of cells with either of these modalities will cause a temporary increase in the diffusion of exogenous molecules into the cytosol, which results from a destabilization of the cell membrane. In both cases the recovery of membrane integrity and subsequent dye exclusion followed first order kinetics with similar rate constants as electroporation, 0.25 and $0.28\,\text{minutes}^{-1}$ for the two cell lines tested. These data were consistent with literature on resealing times for electroporation (Rols and Teissie 1990, Neumann et al. 1998).

Experiments conducted in animal models support the findings of plasmas being a useful tool for molecular delivery. Results obtained by modulating the treatment time show as plasma exposure increases, so too does the amount of expression. The maximum expression in these experiments was found to occur at 10 minutes of plasma exposure, and was correlated with a rise in luminescence of 37.3 fold for positive polarity and 27.1 fold for negative polarity. Increasing the exposure time beyond 10 minutes was found to be inef-

fective, which is likely due to cells becoming nonviable due to the extended presence of membrane defects. Delivery of plasmids obtained with 10 minutes of plasma exposure was determined to be similar to that obtained by electroporation, which produced a rise in luminescence of 42.3 fold.

As 10 minutes was found to give the optimum expression of luciferase plasmid, a second set of experiments was performed to determine the effects of modulating the DNA dose. As the dose was escalated in these experiments from 50 to $100\,\mu g$ a statistically significant increase in luminescence was observed, but increasing the dose above $100\,\mu g$ caused no significant change in luminescence. Based on this data it was determined that $100\,\mu g$ at 10 minutes of exposure generated the optimum results.

Following the success of delivering luciferase encoding DNA a more biologically relevant plasmid was tested using a $100\,\mu g$ DNA injection followed by exposure to plasma for 10 minutes. The plasmid delivered in these experiments encoded for gp120, which is a surface antigen of HIV. After performing a treatment regimen that consisted of an initial vaccination and three booster vaccinations, significant antigen specific antibody responses were measured in the serum. Of the treatments performed positive plasma exposure generated the greatest antibody response, which correlated to a geometric mean titer of 3444. Negative plasma and electroporation conditions generated geometric mean titers of 256 and 181 respectively.

The reason positive polarity plasma generated a greater immune response than negative polarity is currently unknown. A possible explanation could be due to electrokinetic diffusion of the DNA in the tissue during treatment. Exposure to negative polarity plasma could have pushed the DNA into the subcutaneous fat tissue and positive polarity could have pulled the DNA up into the upper layers of the dermis and possibly the epidermis where there are a larger number of immune cells present.

The results obtained from these experiments give validity to plasma-based methods for

molecular delivery. These experiments show plasma exposure is capable of destabilizing cell membranes in a similar fashion as electroporation, which allows for the uptake of exogenous molecules. This destabilization phenomena is transient in nature and is attainable without deleterious effects to cell viability. Unlike electroporation, delivery performed by the plasma method does not cause tissue damage nor does it induce inflammatory responses.

5.2   Future Direction

This research has produced an effective charge-based system for molecular delivery, which served the purpose of a first generation technology. As such there is significant room to improve upon the technology and findings generated in this research. A first step in moving the technology forward is repeating the vaccine experiment with a larger group of animals. This experiment was performed with groups of four animals per treatment, which creates a situation with low statistical power. Repeating these experiments will also help to answer the question concerning the effects of polarity on delivery.

Another future endeavor with this technology should focus on determining the mechanism responsible for delivery. If it turns out this is a purely voltage driven phenomena experiments should be performed with higher voltage and lower treatment times. If the phenomena is related to current, experiments should be performed with higher current. This must be improved as 10 minutes of treatment is going to dissuade all but the most motivated of patient populations. Also long treatments will not be well received by scientist or physicians.

Improving the knowledge base concerning the mechanism should also increase the ability to make a new generation device. To make the device more accepted a modular device not requiring a desktop computer, large power supply, flow meter and electronic components should be sought after. Currently the generator and controlling equipment takes up the better part of an operating table, which would be cumbersome for a physician to work with on a regular basis.

Future research with this device should also test the delivery capacity attainable in tumor models. Past research in this area with the corona based system failed to produce significant delivery, it was hypothesized that this was due to a failure to treat deeper into tissue. This should be investigated to determine if there is a depth limit to the current technol-

ogy. Research in this area should involve the delivery of chemotherapeutic agents and immunomodulatory genes.

Finally, research should be performed to determine if it is possible for the high voltage generated by the plasma system to push drugs and genes into the tissue, similar to iontophoresis. Performing research in this area would allow treatments to be performed entirely needle-free. Successful transport into the skin and transfection of the cells would revolutionize contact independent methods of drugs and gene delivery.

REFERENCES

Aiuti, A., Cattaneo, F., Galimberti, S., Benninghoff, U., Cassani, B., Callegaro, L., Scaramuzza, S., Andolfi, G., Mirolo, M., Brigida, I., Tabucchi, A. and Carlucci, F.: 2009, Gene therapy for immunodeficiency due to adenosine deaminase deficiency, *The New England Journal of Medicine* 360, 447–458.

Barajas, M., Mazzolini, G., Genove, G., Bilbao, R., Narvaiza, I., Schmitz, V., Sangro, B., Melero, I., Qian, C. and Prieto, J.: 2001, Gene therapy of orthotopic hepatocellular carcinoma in rats using adenovirus coding for interleukin 12., *Hepatology* 33, 52–61.

Best, S., Peng, S., Juang, C., Hung, C., Hannaman, D. and Saundersa, J.: 2009, Administration of hpv dna vaccine via electroporation elicits the strongest cd8+ t cell immune responses compared to intramuscular injection and intradermal gene gun delivery, *Vaccine* 27, 5450–5459.

Boyer, J. D., Kutzler, M. A., Chattergoon, M. A., Calarota, S. A., Pavlakis, G., Sekaly, R., MacGregor, R. R. and Weiner, D.: 2003, Engineering dna vaccination as an approach to hiv immune therapy, *Clinical and Applied Immunology Reviews* 3, 183–197.

Broderick, K., Shen, X., Soderholm, J., Lin, F., McCoy, J., Khan, A., Yan, J., Morrow, M., Patel, A., Kobinger, G., Kemmerrer, S., Weiner, D. and Sardesai, N.: 2010, Prototype development and preclinical immunogenicity analysis of a novel minimally invasive electroporation device, *Gene Therapy* pp. 1–8.

Capecchi, M.: 1980, High efficiency transformation by direct microinjection of dna into cultured mammalian cells, *Cell* 22(2), 479–488.

Caruso, M., Pham-Nguyen, K., Kwong, Y., Xu, B., Kosai, K., Finegold, M., Woo, S. and Chen, S.: 1996, Adenovirus-mediated interleukin-12 gene therapy for metastatic colon carcinoma., *Proceedings of the National Academy of Sciences* 93, 11302–11306.

Chalberg, T. W., Vankov, A., Molnar, F. E., Butterwick, A. F., Huie, P., Calos, M. P. and Palanker, D. V.: 2006, Gene transfer to rabbit retina with electron avalanche transfection, *Investigative Ophthalmology and Visual Science* 47, 4083–4090.

Connolly, R., Rey, J., Jaroszeski, M., Hoff, A., Gilbert, R. and Llewellyn, J.: 2009, Effectiveness of non-penetrating electroporation applicators to function as impedance spectroscopy electrodes, *IEEE Transactions on Dielectrics and Electrical Insulation* 16, 1348–1355.

Conrads, H. and Schmidt, M.: 2000, Plasma generation and plasma sources., *Plasma Sources Science and Technology* 9, 441–454.

Daud, A. I., DeConti, R. C., Andrews, S., Urbas, P., Riker, A. I., Sondak, V. K., Munster, P. N., Sullivan, D. M., Ugen, K. E., Messina, J. L. and Heller, R.: 2008, Phase i trial of interleukin-12 plasmid electroporation in patients with metastatic melanoma, *Journal of Clinical Oncology* 26(36), 5896–5903.

Davalos, R., Rubinsky, B. and Otten, D.: 2002, A feasibility study for electrical impedance tomography as a means to monitor tissue electroporation for molecular medicine, *IEEE Transactions on Biomedical Engineering* 49, 400–403.

Dean, D.: 2010, Dna electrotransfer to the skin: a highly translatable approach to treat peripheral artery disease, *Gene Therapy* 17, 691.

Denet, A.-R., Vanbever, R. and Preat, V.: 2004, Skin electroporation for transdermal and topical delivery, *Advanced Drug Delivery Reviews* 56, 659– 674.

El-Aneed, A.: 2004, Current strategies in cancer gene therapy, *European Journal of Pharmacology* 498, 1–8.

Emery, D. W.: 2004, Gene therapy for genetic diseases: On the horizon, *Clinical and Applied Immunology Reviews* 4, 411–422.

Fischer, A. and Cavazzana-Calvo, M.: 2008, Gene therapy of inherited diseases, *The Lancet* 371(9629), 2044–2047.

Gaforio, J., Serrano, M., Ortega, E., Algarra, I. and Alvarez de Cienfuegos, G.: 2002, Use of sytox green dye in the flow cytometric analysis of bacterial phagocytosis, *Cytometry* 48, 93–96.

Greenleaf, W. J., Bolander, M. E., Sarkar, G., Goldring, M. B. and Greenleaf, J. F.: 1998, Artificial cavitation nuclei significantly enhance acoustically induced cell transfection, *Ultrasound in Medicine & Biology* 24(4), 587–595.

Grossin, L., Gaborit, N., Mir, L., Netter, P. and Gillet, P.: 2003, Gene therapy in cartilage using electroporation, *Joint Bone Spine* 70(6), 480–482.

Guo, Z. S., Li, Q., Bartlett, D. L., Yang, J. Y. and Fang, B.: 2008, Gene transfer: the challenge of regulated gene expression, *Trends in Molecular Medicine* .

Gurunathan, S., Wu, C.-Y. and Freidag, Brenda L.and Seder, R. A.: 2000, Dna vaccines: a key for inducing long-term cellular immunity., *Current Opinion in Immunology* 12, 442–447.

Haar, G. t.: 2007, Therapeutic applications of ultrasound, *Progress in Biophysics and Molecular Biology* 93, 111–129.

Hassan, M., Buldakov, M., Ogawa, R., Zhao, Q., Furusawa, Y., Kudo, N., Kondo, T. and Riesz, P.: 2010, Modulation control over ultrasound-mediated gene delivery: Evaluating the importance of standing waves, *Journal of Controlled Release* 141, 70–76.

Heller, L. C., Jaroszeski, M. J., Coppola, D., McCray, A. N., Hickey, J. and Heller, R.: 2007, Optimization of cutaneous electrically mediated plasmid dna delivery using novel electrode, *Gene Therapy* 14(275-280).

Heller, R., Cruz, Y., Heller, L., Gilbert, R. and Jaroszeski, M.: 2010, Electrically mediated delivery of plasmid dna to the skin, using a multielectrode array, *Human Gene Therapy* 21, 357–362.

Heller, R., Jaroszeski, M., Atkin, A., Moradpour, D., Gilbert, R., Wands, J. and Nicolau, C.: 1996, In vivo gene electroinjection and expression in rat liver, *FEBS Letters* 389, 225–228.

Herzog, R., Hagstrom, J., Kung, S., Tai, S., Wilson, J. and Fisher, K.: 1997, Stable gene transfer and expression of human blood coagulation factor ix after intramuscular injection of recombinant adeno-associated virus., *Proceedings of the National Academy of Sciences* 94, 5804–5809.

Herzog, R., Yang, E., Couto, L., Hagstrom, J., Elwell, D. and Fields, P.: 1999, Long-term correction of canine hemophilia b by gene transfer of blood coagulation factor ix mediated by adeno-associated viral vector., *Nature Medicine* 5, 56–63.

Hirao, L. A., Wu, L., Khan, A. S., Satishchandran, A., Draghia-Akli, R. and Weiner, D. B.: 2008, Intradermal/subcutaneous immunization by electroporation improves plasmid vaccine delivery and potency in pigs and rhesus macaques, *Vaccine* 26(3), 440–448.

Hirao, L., Wu, L., Satishchandran, A., Khan, A., Draghia-Akli, R., Finnefrock, A., Bett, A., Betts, M., Casimiro, D., Sardesai, N., Kim, J., Shiver, J. and Weiner, D.: 2010, Comparative analysis of immune responses induced by vaccination with siv antigens by recombinant ad5 vector or plasmid dna in rhesus macaques., *Molecular Therapy* 18, 1568–1576.

Kang, J. G., Kim, H. S., Ahn, S. W. and Uhm, H. S.: 2002, Development of the rf plasma source at atmospheric pressure, *Surface and Coatings Technology* 171(1-3), 144–148.

Karra, D. and Dahm, R.: 2010, Transfection techniques for neuronal cells, *The Journal of Neuroscience* 30, 6171–6177.

Klein, T., Wolf, E., Wu, R. and Sanford, J.: 1987, High-velocity microprojectiles for delivering nucleic acids into living cells, *Nature 327* 327, 70–73.

Kunieda, T. and Kubo, T.: 2004, In vivo gene transfer into the adult honeybee brain by using electroporation, *Biochemical and Biophysical Research Communications* 318(1), 25–31.

Laroussi, M.: 2000, Biological decontamination by nonthermal plasmas, *IEEE Transactions on Plasma Science* 28(1), 184–188.

Laroussi, M. and Lu, X.: 2005, Room-temperature atmospheric pressure plasma plume for biomedical applications, *Applied Physics Letters* 87(11), 113902.

Li, S., Xia, X., Zhang, X. and Suen, J.: 2002, Regression of tumors by ifn-alpha electroporation gene therapy and analysis of the responsible genes by cdna array., *Gene Therapy* 9, 390–397.

Livingston, B., Little, S., Luxembourg, A., Ellefsen, B. and Hannaman, D.: 2010, Comparative performance of a licensed anthrax vaccine versus electroporation based delivery of a pa encoding dna vaccine in rhesus macaques, *Vaccine* 28, 1056–1061.

Lohr, F., Lo, D., Zaharoff, D., Hu, K., Zhang, X., Li, Y., Zhao, Y., Dewhirst, M., Yuan, F. and Li, C.: 2001, Effective tumor therapy with plasmid-encoded cytokines combined with in vivo electroporation, *Cancer Research* 61, 3281–3284.

Loudon, P., Yager, E., Lynch, D., Amithi Narendran, A., Stagnar, C., Franchini, A., Fuller, J., White, P., Nyuandi, J., Wiley, C., Murphey-Corb, M. and Fuller, D.: 2010, Gm-csf increases mucosal and systemic immunogenicity of an h1n1 influenza dna vaccine administered into the epidermis of non-human primates, *Public Library of Science* 5, 1–14.

Lucas, M., Heller, L., Coppola, D. and Heller, R.: 2002, Il-12 plasmid delivery by in vivo electroporation for the successful treatment of established subcutaneous b16.f10 melanoma., *Molecular Therapy* 6, 668–675.

Lucas, M. L., Jaroszeski, M. J., Gilbert, R. and Heller, R.: 2001, In vivo electroporation using an exponentially enhanced pulse: A new waveform, *DNA and Cell Biology* 20, 183–188.

MacGregor, R. R., Boyer, J. D., Ugen, K. E., Lacy, K. E., Gluckman, S. J., Bagarazzi, M. L., Chattergoon, M. A., Baine, Y., Higgins, T. J., Ciccarelli, R. B., Coney, L. R., Ginsberg, R. S. and Weiner, D. B.: 1998, First human trial of a dna-based vaccine for treatment of human immunodeficiency virus type 1 infection: Safety and host response, *The Journal of Infectious Diseases* 178, 92–100.

Mancini, D. and Farr, M.: 2010, Gene therapy for heart failure: An investigational treatment that is coming of age, *Revista Espanola de CardiologÃa* 63, 137–140.

Matthews, K., Mills, G., Horsfall, W., Hack, N., Skorecki, K. and Keating, A.: 1993, Bead transfection: rapid and efficient gene transfer into marrow stromal and other adherent mammalian cells, *Experimental Hematology* 21(5), 697–702.

Mehier-Humbert, S. and Guy, R. H.: 2005, Physical methods for gene transfer: Improving the kinetics of gene delivery into cells, *Advanced Drug Delivery Reviews* 57, 733–753.

Moreau, M., Orange, N. and Feuilloley, M.: 2008, Non-thermal plasma technologies: New tools for bio-decontamination, *Biotechnology Advances* 26, 610–617.

Morrow, M. and Weiner, D.: 2010, Dna drugs come of age, *Scientific American* 303, 48–53.

Nathwani, A., Davidoff, A., Hanawa, H., Hu, Y., Hoffer, F. and Nikanorov, A.: 2002, Sustained high-level expression of human factor ix (hfix) after liver-targeted delivery of recombinant adeno-associated virus encoding the hfix gene in rhesus macaques., *Blood* 100, 1662–1669.

Neumann, E., Toensing, K., Kakorin, S., Budde, P. and Frey, J.: 1998, Mechanism of electroporative dye uptake by mouse b cells, *Biophysical Journal* 74, 98–108.

Niidome, T. and Huang, L.: 2002, Gene therapy progress and prospects: Nonviral vectors, *Gene Therapy* 9(24).

NIST atomic spectra database [electronic resource]: 1995. (U.S.) Version 3. Title from home page last updated Sept. 2007 (viewed on Oct. 19, 2007).

O'Brien, J. A., Holt, M., Whiteside, G., Lummis, S. C. R. and Hastings, M. H.: 2001, Modifications to the hand-held gene gun: improvements for in vitro biolistic transfection of organotypic neuronal tissue, *Journal of Neuroscience Methods* 112(1), 57–64.

Ogawa, Y., Morikawa, N., Ohkubo-Suzuki, A., Miyoshi, S., Arakawa, H., Kita, Y. and Nishimura, S.: 2005, An epoch-making application of discharge plasma phenomenon to gene-transfer, *Biotechnology and Bioengineering* 92(7), 865–870.

Prausnitz, M. R.: 1996, The effects of electric current applied to skin: A review for transdermal drug delivery, *Advanced Drug Delivery Reviews* 18, 395–425.

Ramachandran, N., Jaroszeski, M. J. and Hoff, A. M.: 2008, Molecular delivery to cells facilitated by corona ion deposition, *IEEE Transactions on NanoBioscience* 7(3), 233–239.

Ries, L., Kosary, C., Hankey, B., Miller, B., Clegg, L. and Edwards, B. (eds): 1999, *SEER Cancer Statistics Review, 1973-1996*, National Cancer Institute. Bethesda, MD.

Rols, M. and Teissie, J.: 1990, Electropermeabilization of mammalian cells. quantitative analysis of the phenomenon, *Biophysical Journal* 58(5), 1089–1098.

Saudemont, A., Buffenoir, G., Denys, A., Desreumaux, P., Jouy, N., H. D., Bauters, F., Fenaux, P. and Quesnel, B.: 2002, Gene transfer of cd154 and il12 cdna induces an anti-leukemic immunity in a murine model of acute leukemia., *Leukemia* 16, 1637–1644.

Sboros, V.: 2008, Response of contrast agents to ultrasound, *Advanced Drug Delivery Reviews* 60(10), 1117–1136.

Shi, F., Rakhmilevich, A., Heise, C., Oshikawa, K., Sondel, P., Yang, N. and Mahvi, D. .: 2002, Intratumoral injection of interleukin-12 plasmid dna, either naked or in complex with cationic lipid, results in similar tumor regression in a murine model., *Molecular Cancer Therapeutics* 1, 949– 957.

Titomirov, A., Sukharev, S. and Kistanova, E.: 1991, In vivo electroporation and stable transformation fo skin cells of newborn mice by plasmid dna., *Biochem. Biophys. Acta* 1088, 131–134.

Ugen, K. E., Goedert, J. J., Boyer, J., Refaeli, Y., Frank, I., Williams, W. V., Willoughby, A., Landesman, S., Mendez, H. and Rubinstein, A.: 1992, Vertical transmission of human immunodeficiency virus (hiv) infection. reactivity of maternal sera with glycoprotein 120 and 41 peptides from hiv type 1., *The Journal of Clinical Investigation* 89, 1923–1930.

Verma, I. M. and Somia, N.: 1997, Gene therapy - promises, problems and prospects, *Nature* 389.

Vleugels, M., Shama, G., Deng, X. T., Greenacre, E., Brocklehurst, T. and Kong, M. G.: 2005, Atmospheric plasma inactivation of biofilm-forming bacteria for food safety control, *IEEE Transactions on Plasma Science* 33(2), 824–828.

Weaver, J. C. and Chizmadzhev, Y. A.: 1996, Theory of electroporation: A review, *Bioelectrochemistry and Bioenergetics* 41, 135–160.

Weiss, J., Subleski, J., Wigginton, J. and Wiltrout, R.: 2007, Immunotherapy of cancer by il-12-based cytokine combinations., *Expert Opinion on Biological Therapy* 7, 1705–1721.

Weissinger, F., Reimer, P., Waessa, T., Buchhofer, S., Schertlin, T., Kunzmann, V. and Wilhelm, M.: 2003, Gene transfer in purified human hematopoietic peripheral-blood stem cells by means of electroporation without prestimulation, *Journal of Laboratory and Clinical Medicine* 141(2), 138–149.

Wigginton, J. M., Park, J. W., Gruys, M. E., Young, H. A., Jorcyk, C. L., Back, T. C., Brunda, M. J., Strieter||, R. M., Ward, J., Green, J. E. and Wiltrout, R. H.: 2001, Complete regression of established spontaneous mammary carcinoma and the therapeutic prevention of genetically programmed neoplastic transition by il-12/pulse il-2: Induction of local t cell infiltration, fas/fas ligand gene expression, and mammary epithelial apoptosis, *The Journal of Immunology* 166, 1156–1168.

Yamashita, Y., Shimada, M., Hasegawa, H., Minagawa, R., Rikimaru, T., Hamatsu, T., Tanaka, S., Shirabe, K., Miyazaki, J. and Sugimachi, K.: 2001, Electroporation-mediated interleukin-12 gene therapy for hepatocellular carcinoma in the mice model, *Cancer Research* 61, 1005–1012.

Yuan, T.-F.: 2008, Vaccination by muscle electroporation: The injury helps, *Vaccine* 26(33), 4105–4106.

Zhang, L., Conejo-Garcia, J. R., Katsaros, D., Gimotty, P. A. andMassobrio, M., Regnani, G., Makrigiannakis, A., Gray, H., Schlienger, K., Liebman, M. N., Rubin, S. C. and Coukos, G.: 2003, Intratumoral t cells, recurrence, and survival in epithelial ovarian cancer, *New England Journal of Medicine* 348, 203–221.

ABOUT THE AUTHOR

Richard Connolly began his college education in 2001 at the University of South Florida. During his time as an undergraduate student he performed basic research in the field of biomedical engineering. In 2004 membership to the Tau Beta Pi and Omega Chi Epsilon honor societies was granted. He was awarded a bachelors of science degree in chemical engineering with honors in 2005.

Research performed during his undergraduate degree motivated him to pursue higher education in biomedical engineering. During his time as a graduate student he was awarded fellowships from the National Science Foundation's Integrative Graduate Education and Research Traineeship program and the Florida Center of Excellence for Biomolecular Identification and Targeted Therapeutics program. In 2007 he received a masters of science degree in biomedical engineering. This document constitutes the research component necessary to obtain the doctorate degree in biomedical engineering.